Application of triazolylidene metal complexes of Fe, Ni and Cu: synthesis, characterization and applications in oxidation catalysis

A thesis submitted to the University of KwaZulu-Natal in fulfillment of the requirements for the degree of Doctor of Philosophy in Chemistry

Siyabonga Gift Mncube

January 2018

Exploration of triazolylidene metal complexes of Fe, Ni and Cu: synthesis, characterization and applications in oxidation catalysis
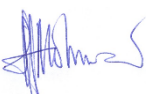
By

Siyabonga Gift Mncube
University of KwaZulu-Natal

Dissertation submitted in fulfilment of the academic requirements for the degree of Doctor of Philosophy to School of Chemistry and Physics, the College of Agriculture, Engineering and Science, University of KwaZulu-Natal, Westville Campus, Durban, South Africa

This thesis was written in chapters which are set as discrete research papers, with an overall Introduction and conclusion. One of the chapters has already been published.

As the candidate's supervisor, I have approved this thesis for submission:
Supervisor:

Signed: …Name … Muhammad D. Bala …Date: 04-Jan. 2018..

ABSTRACT

N-heterocyclic carbene (NHC) metal complexes have great potentials as useful catalysts. This has over the years helped to generate large interest from researchers worldwide on their synthesis, reactions and applications. In this PhD thesis, the synthesis of metal (Fe, Ni and Cu) complexes bearing functionalized triazolylidene NHC ligands is presented. The synthesis and characterization of the complexes by NMR, IR, MS, EA and single crystal X-ray (sc-XRD) analysis is described in full detail. The molecular and electronic structures of some of the complexes were further analyzed by density functional theory (DFT) calculations aimed at gaining some insight into their structural and physical properties. In all cases, the experimental (NMR, IR, sc-XRD) were in good agreement with theoretical data from the DFT studies.

When utilized as catalysts for oxidation catalysis at mild reaction conditions, all the metal complexes were found to be effective catalyst precursors for the oxy-functionalization of alkanes and alcohols in the presence of simple oxidants. Half-sandwich nickel complexes showed activity for catalytic oxidation of *n*-octane, yielding a range of oxygenated products. Catalyst **2.3c** with small *N*-substituents showed the highest catalytic activity of up to 15% total conversion to products. *N*-fuctionalized *trans*-$Cl_2Ni(mNHC)_2$ showed good catalytic activities of circa 15% and 19% for cyclohexane and *n*-octane respectively. Furthermore, the *in-situ* generated Cu-triazolylidene complexes exhibited the highest catalytic activity (up to 22%) with H_2O_2 as the most productive oxidant. oxidation of toluene resulted in a mixture of oxygenated products (total conversion up to 11 %) with benzaldehyde (PhCHO, 62 %) and benzyl alcohol ($PhCH_2OH$, 29%) as the main products. Finally, the synthesis and full-characterization of a new 2-bromo-1,2,3-triazolium dibromoiodate ionic salt is reported. It was isolated in an effort to produce a copper *N*-heterocyclic carbene complex from the ligand. Interesting intermolecular Br…Br halogen bonds between bromine atoms of the triazolium and dibromoiodate moieties was shown.

DECLARATIONS: 1 – PLAGIARISM

I, …………………………………….………………………., declare that:

i.   the research reported in this dissertation, except where otherwise indicated or acknowledged, is my original work;

ii.   this dissertation has not been submitted in full or in part for any degree or examination to any other university;

iii.   this dissertation does not contain other persons' data, pictures, graphs or other information, unless specifically acknowledged as being sourced from other persons;

iv.   this dissertation does not contain other persons' writing, unless specifically acknowledged as being sourced from other researchers. Where other written sources have been quoted, then:

    a.   their words have been re-written but the general information attributed to them has been referenced; where their exact words have been used, their writing has been placed inside quotation marks, and referenced;

v.   where I have used material for which publications followed, I have indicated in detail my role in the work;

vi.   (vi) this dissertation is primarily a collection of material, prepared by myself, published as journal articles or presented as a poster and oral presentations at conferences. In some cases, additional material has been included;

vii.   (vii) this dissertation does not contain text, graphics or tables copied and pasted from the Internet, unless specifically acknowledged, and the source being detailed in the dissertation and in the References sections.

Signed:………………………………….

Date: January 2018

DECLARATION 2 – PUBLICATIONS

DETAILS OF CONTRIBUTION TO PUBLICATIONS that form part and/or include research presented in this thesis (include publications in preparation, submitted, *in press* and published)

Publication 1:
Mncube, S.G.; Bala, M.D. **Application of 1,2,3-triazolylidene nickel complexes for the catalytic oxidation of *n*-octane** *Mol. Catal.*, 2017. dio: /10.1016/j.mcat.2017.03.005

Publication 2:
Mncube, S.G.; Bala, M.D. **Highly symmetric Ni(II) complexes of mesoionic carbene ligands utilized in catalytic oxidation reactions.** Manuscript submitted to *Molecular Catalysis (2017).*

Publication 3:
Mncube S. G., Zamisa S. J., Ajayi T. J. and Bala M. D. **Trihalide-based 1,2,3-triazolium ionic liquid: Synthesis, X-ray crystallography and DFT studies**. Manuscript to be submitted to *Acta Crystallographica, Section C.*

Publication 4:
Mncube, S.G.; Bala, M.D. **Homogeneous oxidation reactions catalyzed by *in situ* generated Cu-mesoionic triazolylidene complexes.** Manuscript in preparation.

Publication 5
Mncube, S.G.; Bala, M.D. **Selective alkane oxidation catalyzed by piano-stool iron-triazolylidene complexes** Manuscript in preparation.

CONFERENCE PRESENTATIONS

1. Mncube, S.G.; Bala, M.D.: **Application of 1,2,3-triazolylidene nickel complexes for the catalytic oxidation of *n*-octane** (paper presented at catalysis society of South Africa (CATSA) conference 13-16th November **2015**, Cape town, South Africa)

2. Mncube, S.G.; Bala, M.D.**: Application of 1,2,3-triazolylidene nickel complexes for the catalytic oxidation of *n*-octane**. (paper presented at South African Chemical (SACI) November **2015**, Durban, South Africa)

3. Mncube, S.G.; Bala, M.D. **Application of 1,2,3-triazolylidene nickel complexes for the catalytic oxidation of alkanes** (paper presented at University of KwaZulu-Natal postgraduate colloquium **2015**, UKZN Pietermaritzburg Campus)

4. Mncube, S.G.; Bala, M.D. **Triazolium-based nickel carbene complexes and their application as paraffin oxidation catalysis** (paper presented at International Conference on Organometallic Chemistry (ICOMC) 17-22nd July **2016**, Melbourne, Australia.).

5. Mncube, S.G; Bala, M.D. **Triazolium-based nickel carbene complexes and their application as paraffin oxidation catalysis.** (Catalysis Society of South Africa (CATSA) conference 6-9th Nov. 2016, Champagne Sports Resort (Central Drakensberg), South Africa.

6. Mncube, S.G.; Bala, M.D. **Application of 1,2,3-triazolylidene nickel complexes for the catalytic oxidation of alkanes** (paper presented at the University of KwaZulu-Natal postgraduate colloquium **2016**, Howard Collage Campus)

DEDICATION

**This work is dedicated to my late grandmother
(Mashoba)**

ACKNOWLEDGEMENTS

LIST OF FIGURES

LIST OF TABLES

List of Schemes

List of Abbreviation

Å	Angstrom unit, 10^{-10} m
A/K	alcohol/ ketone ratio
cm^{-1}	wavenumber
Cp	cyclopentadiene or cyclopentadienyl
DMF	$N,N´$-dimethylformamide, Me_2NCHO
DMSO	dimethyl sulfoxide
DTA	differential thermal analysis
EI MS	electron impact mass spectrometry
en	ethane-1,2-diamine
Et	ethyl
ES MS	electrospray mass spectrometry
FT	Fourier Transform
GC-MS	gas chromatography-mass chromatography
Hz	Hertz
HRMS	high resolution mass spectrometry
J	coupling constant, Hz
M	metal
m/z	mass-to-charge ratio
OAc	acetate $–O_2CCH_3$
PPh_3	triphenylphosphine
Ph	phenyl,$-C_6H_5$
ppm	parts per million
py	pyridine
TGA	thermogravimetric analysis
THF	tetrahydrofuran, C_4H_8O
TON	turnover number

TABLE OF CONTENTS

Foreword

The development of highly active and selective catalyst systems still remains a challenge to the scientific research community. In particular for oxidation catalysis, the adoption of a biomimetic approach to catalyst development (organometallic approach) is thus far the closest to producing a practical system, mainly due to recent developments in catalyst design based on oxidation-resistant ligands and mild organic oxidants. However, these systems still suffer from various drawbacks, including inadequate catalyst stability, poor recycling and low selectivity. In the past, ligands were used to largely control the catalyst performance by changing its steric and electronic properties, while the ligand largely plays a "spectator" role. However, recent approaches deviate from this concept, whereby, ligands are designed to be more active and play much more prominent roles in directing catalyst activity and selectivity. Based on this concept, the main research objective of this thesis is to develop new oxidation catalysts that are selective for a variety of substrates, exhibiting good conversions, which are also cheap and environmentally friendly. In the best cases, the catalysts should be stable and work under mild reaction conditions. Inspired by recent advances, we became interested in using triazolylidene (a useful subclass of the popular N-heterocyclic carbenes (NHCs)) as ligands in metal complexes for catalytic applications. The unique features of these ligands will be considered in details in the following chapters.

In particular, the project aims are in two parts:

Firstly, well established methods are applied to the synthesis of triazole compounds and their triazolium salts using well established methods. The synthesised 1,3,4-trisubstituted-1,2,3-triazolium salts are then complexed to first row transition metal centres (Fe, Ni and Cu). The earth-abundant first-row transition metals, such as Fe, Ni, and Cu have turned out to be significantly more attractive, because of their conspicuous advantages, including been low price, low poisonous, and unique catalytic characteristics.

The obtained triazolylidene metal complexes are then tested as homogeneous catalysts for the oxidation of mainly alkanes in the presence of mild oxidants to yield oxygenated products. The effects of various reaction conditions, substrate scope, various selectivity features, and the nature of the active catalytic species will be studied in detail.

CHAPTER 1

Introduction

1.1   Carbenes

A carbene is a neutral divalent compound containing a carbon atom with six electrons in its valence shell.[1, 2] Carbenes can exist either as singlet or triplet variants depending on the electronic structure. A singlet carbene is defined by one sp^2 hybridized lone-pair in while the triplet variant has two unpaired electrons; in the hybridized sp^2 orbital and other contained in an unhybridized p orbital (see Figure 1.1).

singlet   **triplet**

Figure 1.1: Representative orbital structures of singlet and triplet carbenes.

Singlet and triplet carbenes display divergent reactivity, thereby generate different metal complexes. There are three types of carbenes: Fischer, Schrock and *N*-heterocyclic carbenes. This thesis will mainly focus on *N*-heterocyclic carbenes and their properties, synthesis and applications.

1.2   N-Heterocyclic carbenes

N-heterocyclic carbenes (NHCs) are heterocyclic carbenes with at least one carbene carbon and one nitrogen atom in a ring structure. The lone pair of the nitrogen atom(s) stabilise the carbene

moiety, making this type of carbene more stable than the traditional carbenes (Figure 1.2). This phenomenon has been determined by X-ray diffraction studies, showing that the N-C$_{carbene}$ bond is shorter than usual N-C single bonds.[3] The cyclic nature of NHCs favour the singlet state by forcing the carbene carbon into bent sp^2 arrangement.[4]
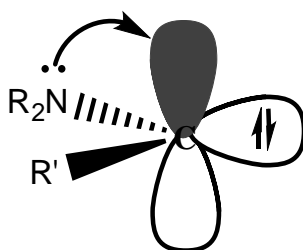
Figure 1.2**: Stabilisation of carbene by lone pairs of an adjacent nitrogen atom.[3]

Although NHCs were investigated as early as the 1960s, the first isolation of a stable NHC by Arduengo and co-workers[5] accelerated widespread research interest in their synthesis and applications. 1,3-diadamantylimidazol-2-ylidene (**1.1**, Figure 1.3), also known as Arduengo's carbene (IAd), contains an sp^2-hybridized C^2 carbon in a singlet ground-state electronic configuration with the σ molecular orbital filled with two electrons in antiparallel spin orientation at the highest energy and an unoccupied p-orbital at the lowest energy.[4] This carbene was found to be stable in the absence of air and moisture.

1.1
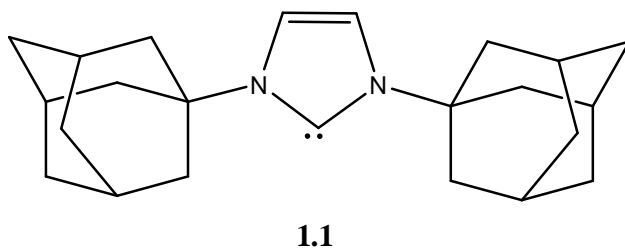
Figure 1.3: Structure of Arduengo's carbene (IAd).

1.3   Types of N-heterocyclic carbenes

The structures of the most commonly encountered classes of NHCs are shown in Figure 1.4. These NHCs have characteristic adjacent nitrogen atoms which stabilise the carbene moiety by an inductive effect. NHC species vary vastly in size, substituent patterns, and degrees of heteroatom stabilization which have great influences on electronic and steric properties.

The most common NHC used are the five-membered ring type.[4, 6] Furthermore, a number of 5-membered ring (**1.6**) NHCs with modified backbones (extended ring size)[7-10] including some acyclic[11, 12] and 6-7 membered[13, 14] ring ones, which are less common are known. These will not be discussed further in this thesis.

(**1.1**) imidazolylidene

(**1.2**) imidazolinylidene

(**1.3**) thiazolylidene, X= S
oxazoylidene, X= O

(**1.4**) 4,5-dibromoimidazolinylidene

(**1.5**) triazolylidene

(**1.6**) benzimidazolylidene

(**1.7**) dihydroperimidinylidene

(**1.8**) tetrahydrodiazepinylidene
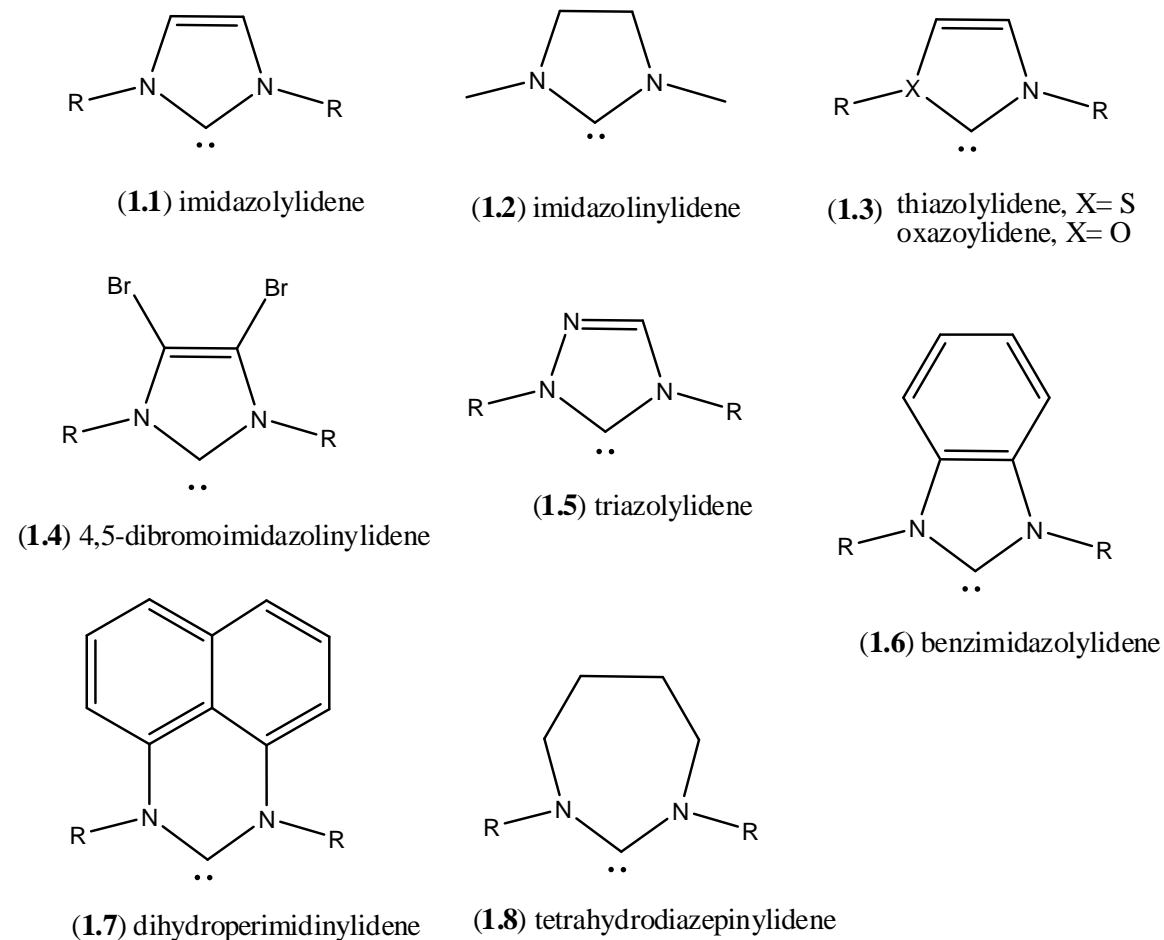
Figure 1.4: Commonly encountered NHC compounds.

3

In the family of NHC compounds, Arduengo's carbene type (**1.1**, IAd) still dominate the area. This is due to the fact that they are relatively easy to prepare, functionalised and handled.[15] However, the electron donating ability of these carbenes have led to a wide range of modified heterocycles by the displacement of one or both carbene-stabilising heteroatoms to more remote positions within the heterocyclic ring.[16] In this way, "new" set of NHC compounds with 'abnormal' σ-donating modes different to the traditional IAd-type compounds have been reported. This NHC subfamily were then termed abnormal and mesoionic N-heterocyclic carbenes (*m*NHCs). This thesis will focus specifically on the mesoionic 1,2,3-triazol-5-ylidenes (**1.11**, Figure 1.5). This carbene (**1.11**) has attracted considerable attention due to the fact that it is readily synthesized using the well-established modular and functional group tolerant "click" chemistry.[16, 17]

(**1.9**) pyrazolin-4-ylidenes   (**1.10**) imidazol-4-ylidenes   (**1.11**) 1,2,3-triazol-5-ylidenes
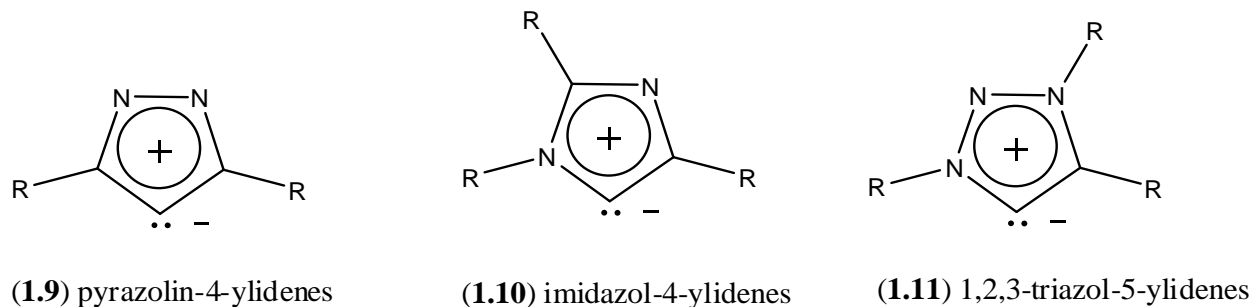
Figure 1.5: Mesoionic N-heterocyclic carbenes.

1.4 NHCs as ligands in metal complexes

Following the first examples of NHC-metal (NHC-M) complexes reported by Wanzlick[18] and Öfele[19] in 1968, NHCs as ligands have become very prominent in organometallic chemistry due to their ability to form stable covalent metal-ligand bonds (M-$C_{carbene}$) and also offer structural versatility and variability with an almost endless possibility to modify the wingtip nitrogen atom substituents. Studies on the bonding nature of these compounds to metal centres has been reported and reviewed by a number of research groups.[20, 21] According to molecular orbital calculations by Frenking and co-workers, σ-donation contribute about 80% of the overall M-NHC bond energy, which makes the π-back-bonding from the metal and π-donation from the carbene p-orbital negligible.[22] However, the amount of π-back donation from the metal is

dependent upon the particular metal and carbene in question.[23] Experimental data have also confirmed the M-NHC bond length to be longer than double and there is rotation around the M-NHC bond. Consequently, the M-NHC coordination is generally drawn as a single rather than double bond with π-donation from the carbene *p*-orbital restricted and delocalised within the NHC ring.[4]

1.12   **1.13**

NHC-[M] = 44-54 Kcal/mol

NHC-[M] = 25-37 Kcal/mol
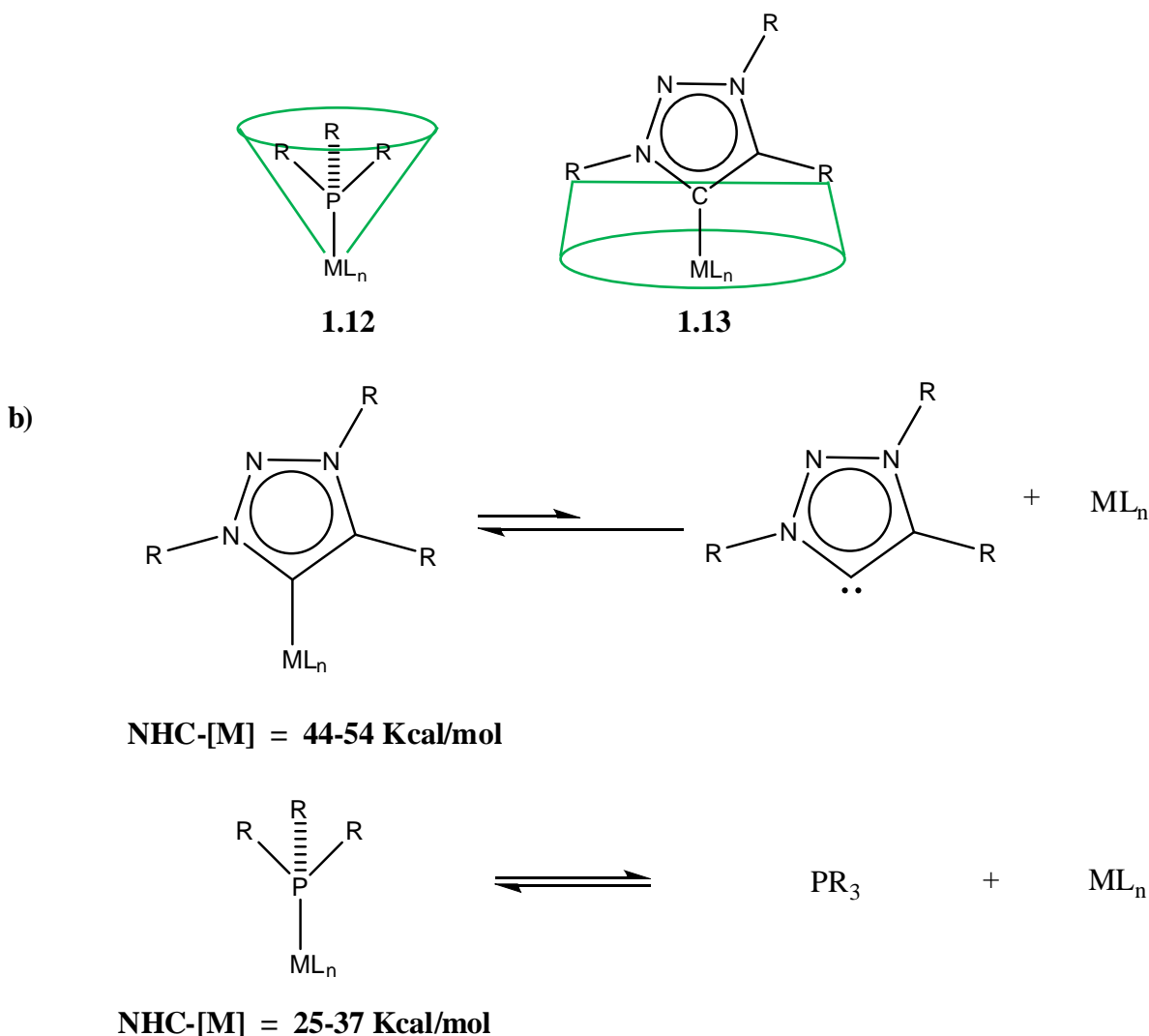
Figure 1.6: Comparison between the steric (a) and stability (b) properties of phosphine and NHC metal complexes.

The coordination and steric characteristics of NHCs (strong σ-donor and weak π-acceptor) can be regarded as similar to the well-known phosphines. However, there are some advantages which favour the NHC over a phosphine.[24] In the phosphine ligands, the substituents are pointing away

(in a cone-shape spatial arrangement) from the metal center, while most NHCs are pointing towards (in an umbrella-shape) the metal center giving the *N*-heterocyclic carbene ligands a larger impact on the metal center (Figure 1.6a). Furthermore, changing the *N*-substituents and heterocyclic size have been shown to have direct influence on the steric properties around the carbene moiety and also the metal centre. Thereby, quite a large number of structurally diverse NHC analogues can be prepared and studied.[4]

NHCs are more electron donating than phosphines, thereby stronger NHC-M bonds are formed which is reflected by greater bond dissociation energies than M-PR$_3$ (Figure 1.6b). Therefore, the equilibrium between the MHC-M complex and free NHC carbene lies far more on the side of the complex than in the case for phosphines (Figure 1.6b). With these attractive features, NHCs and their transition metal complexes are generally considered to be more stable than the phosphines equivalents.[25]

1.5   Synthesis of NHC-metal complexes

Due to the growing number of application of metal-NHC complexes, a variety of methods have been reported for their synthesis. However, the most widely used synthetic methods are based on three pathways (Scheme 1.1);

i.   **Deprotonation**: preparation of a free carbene followed by its reaction with a suitable metal precursor. This is the oldest and most common route for the synthesis of NHC-metal complexes.[2, 5, 26] The free carbene is obtained by reaction of azolium salts with a strong base in a suitable solvent under inert conditions. The free carbene is then either isolated or reacted with a suitable metal precursor to give the corresponding NHC-metal complex. Milder bases have also been employed, although they require heating in order to generate the free carbene.[27, 28]

ii.   **Direct metalation**: reaction of the azolium salt with a suitable basic transition metal complex. In some cases, the use of a strong base is not an option.[23] In such cases, an alternative milder option has been reported. Such methods involve the use of basic metal

precursors which *in-situ* deprotonate azolium salts generating free carbenes followed by binding of the metal to form NHC-metal complexes. Abernethy and co-workers, reported the *in-situ* synthesis of the diamagnetic complex [Ni(η_5-C$_5$H$_5$) (Cl)(IAd)] by reaction of nickelocene with IAd in refluxing THF in high yield. More recently, copper(I) oxide (Cu$_2$O) has been employed as a reactant for the direct synthesis of mono NHC copper complexes.[29]

iii. **Transmetalation**: transfer of NHC ligands from one metal to another. Alternatively, another recent but widely used route is transmetalation, which involves the transfer of ligands from one metal to another. Following the first report of a NHC silver complex by Arduengo and co-workers[30], the first silver carbene transfer using imidazolium salt and Ag$_2$O for the synthesis of a number of gold and palladium NHC complexes was reported by Wang and Lin[31]. This synthetic method involves the reaction of an azolium salt with silver(I) oxide to produce the corresponding mono- or *bis*-NHC silver complex. The resulting silver complex is then either isolated or used *in-situ* in subsequent reactions with metals of choice to form the related M-NHC complex.[32]
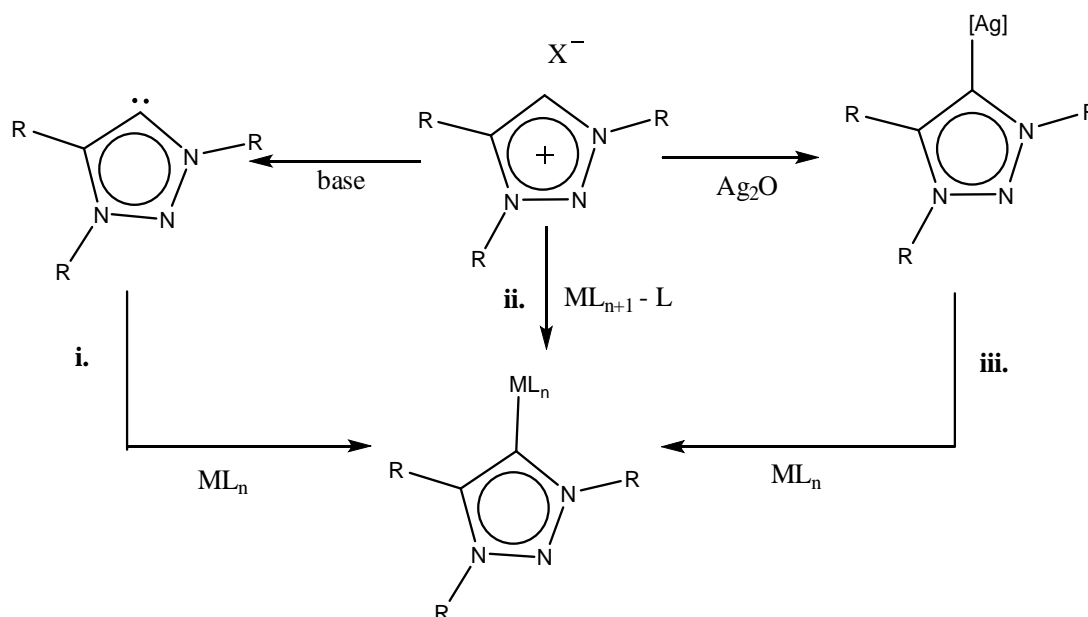
Scheme 1.1: Main synthetic strategies for the formation of NHC-complexes.

7

1.6　Application of *N*-Heterocyclic carbene metal complexes in catalysis

The potential of NHC ligands as useful ligands in catalytic reactions stems from work by Herrmann and co-workers in 1995 after they reported synthesis and catalytic potential of a *bis*–NHC palladium diiodido complex (Figure 1.7).[33] NHC complexes of various transition metals are have created a large diversity of catalysts with different reactivity. In the family of NHC ligands, the imidazolin-2-ylidene based metal complexes have been widely studied and still dominate the area.
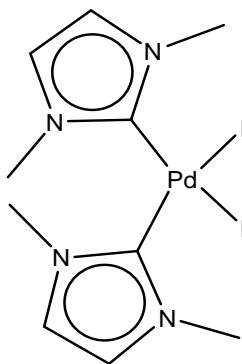
1.14

Figure 1.7: *bis*–NHC palladium diiodido complex.

The use of 1,2,3-triazolylidene ligands in metal complexes have consistently been gaining significant attention in recent years. Much of the success of 1,2,3-triazolylidene ligands in in catalysis can be attributed to the combined benefits of increased catalyst stability, and consequent lower rates of catalyst decomposition. Triazolylidene metal complexes have been reported to be active catalyst precursors for a variety of processes including "click" chemistry, cross coupling, olefin metathesis, cyclisation and oxidation processes.
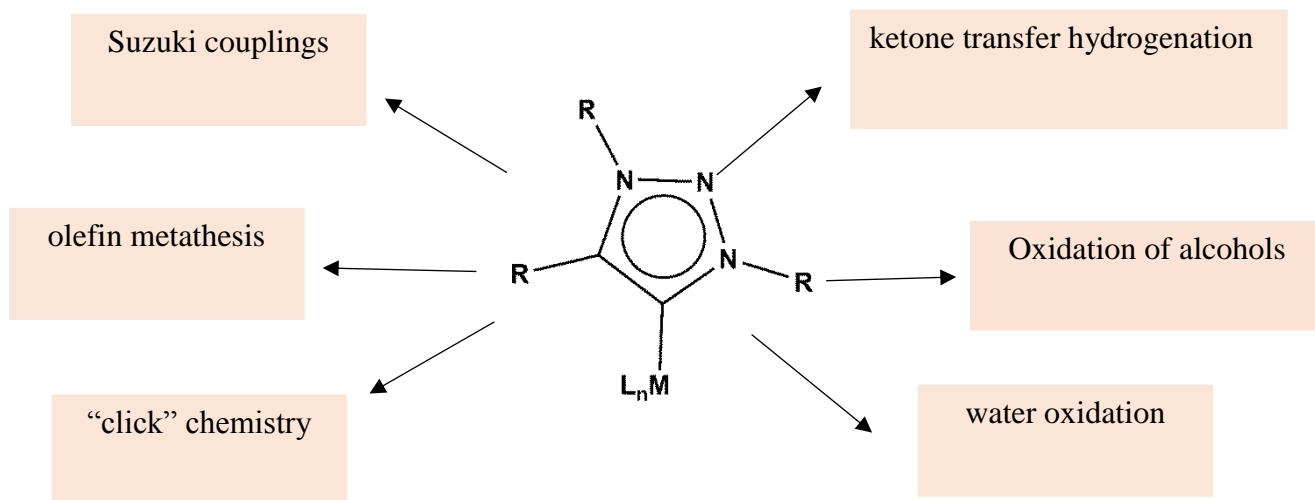
Figure 1.8: Representative applications of triazolylidene ligands coordinated to transition metals.

1.6.1 Suzuki coupling

The first report in application of triazolylidene metal complexes as pre-catalysts stems from work by Sankararaman and co-workers[34] in 2009. They found that chiral palladium complex was catalytically active for a range of standard Suzuki couplings to form biaryl complexes (with yield up to 96%, (Scheme 1.2). The authors believed that the strong donor properties of the triazolylidene ligand increased the electron density around palladium (compared to phosphines and IAd-type imidazolylidenes) which was expected to promote the oxidative addition of aryl bromide to the Pd(0) intermediate, often a limiting factor in aryl chloride conversion. However, sterically more demanding substrates were found to be poorly converted. The authors suggest that sterically demanding boronic acids **1.16** result in deborylation instead of Suzuki coupling.
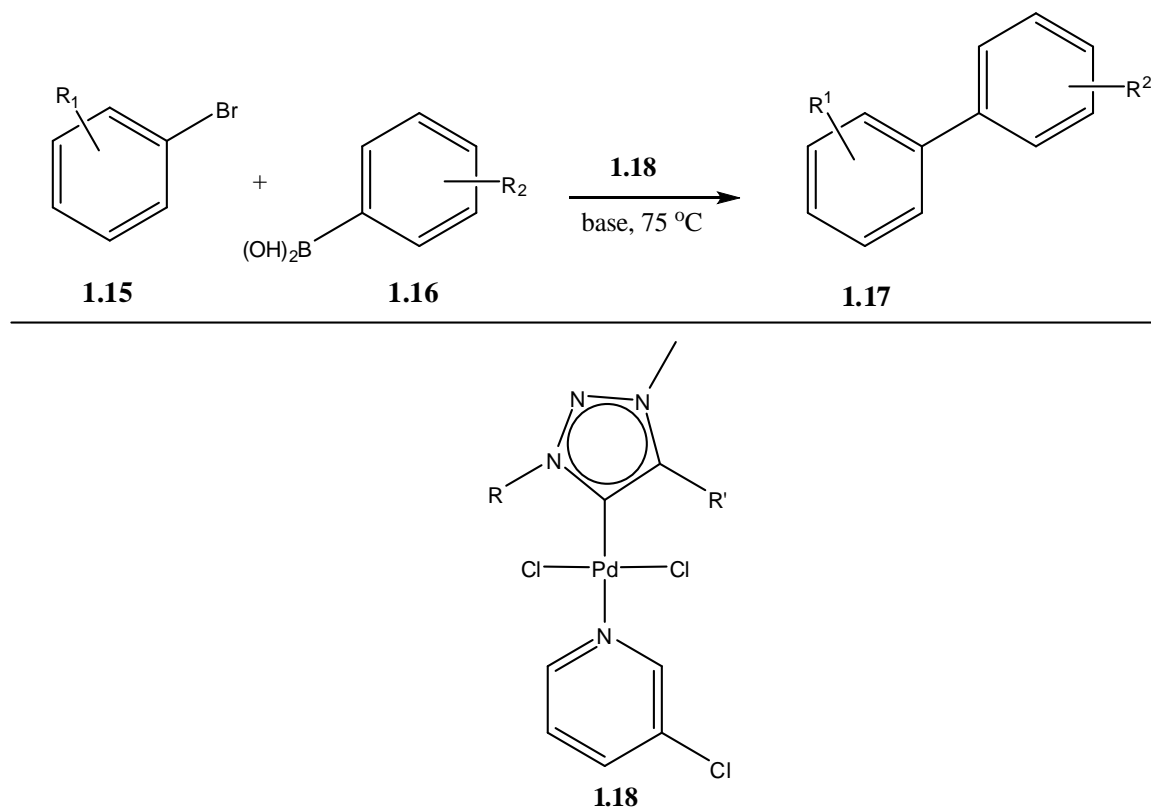
Scheme 1.2: Suzuki couplings catalysed by the Pd-1,2,3-triazolylidene complexes.

1.6.2 Olefin metathesis

The groups of Grubbs and Bertrand reported triazolylidene ruthenium complexes as active room-temperature pre-catalysts for the ring-opening metathesis polymerization of cyclic olefins and for ring-closing olefin metathesis reactions (Scheme 1.3).[35] Even though the complexes were found to be unstable in solution, higher activities were observed in ring opening metathesis polymerisation for this NHC complex than the original bis(phosphine) compound. The presence of bulky groups at the triazolylidene position N1 and C4 induced a slightly slower catalytic activity. Kinetic and computational studies revealed that the sterics of **1.19** play a significant role in the catalytic initiation step.[36]

1.19
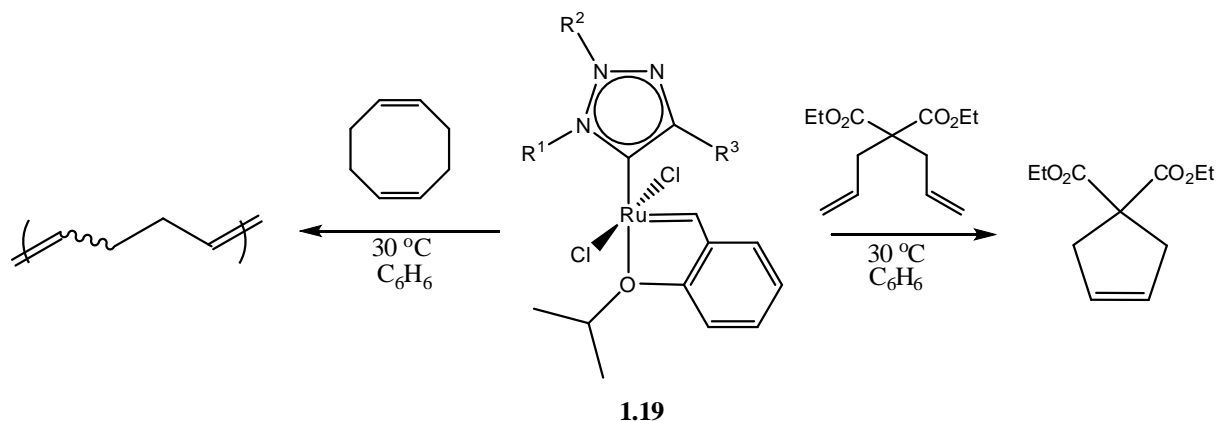
Scheme 1.3: Ring opening and ring closing metathesis using Bertrand and Grubbs' 1,3,4-triaryl-1,2,3-triazol-5-ylidene containing ruthenium catalysts **1.19**.

Similar observations were noted with ring closing metathesis, complex **1.19** with bulky (R^1 and R^3) substituents around the carbene moiety was found to be inactive. Meanwhile, complexes with bulkier substituents proved to be stable and active. Furthermore, high catalytic activity induced upon addition of a strong acid such as trifluoroacetic acid (TFA) or HCl.[37] This observation is of importance for further development of olefin metathesis catalysts.

1.6.3   Copper-catalyzed alkyne–azide coupling

Considering the popularity of copper in "click" chemistry, it is not surprising that many triazolylidene copper complexes have been investigated as catalyst precursors for these reactions. Fukuzawa and co-workers reported the application of new triazolylidene copper complexes as catalyst precursors for the azide-alkyne cycloaddition reaction (CuAAC).[38] The trz-copper complexes were found to be the most efficient surpassing even well-known 2-imidazolylidene copper analogues[39].
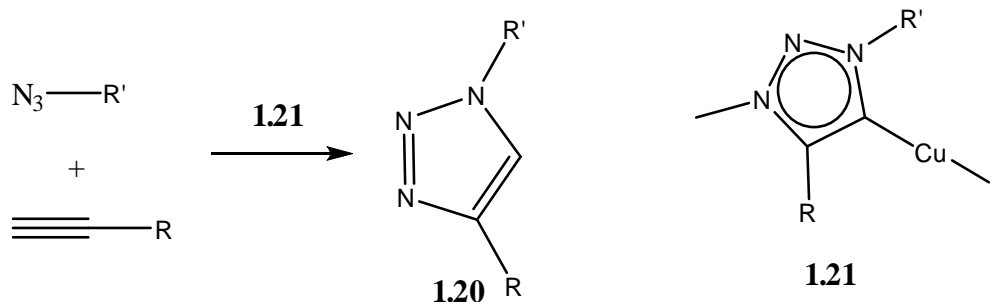
Scheme 1.4: Cu(trz)-catalysed cycloaddition of alkynes and azides.

The coupling of sterically bulky alkynes with bulky proceeds faster with higher yields compared to 2-imidazolylidene copper analogues which gave lower yields.

1.6.4 Water oxidation

Albrecht and co-workers reported the use of triazolylidene iridium complexes as water-oxidation catalysts.[40] The water-soluble catalyst led to efficient O_2 evolution from water in the presence of $(NH_4)_2[Ce(NO_3)_6]$ (CAN) as a sacrificial oxidant. Variation of triazolylidene substituents was shown to have direct effects on activity and have allowed for catalyst optimisation.
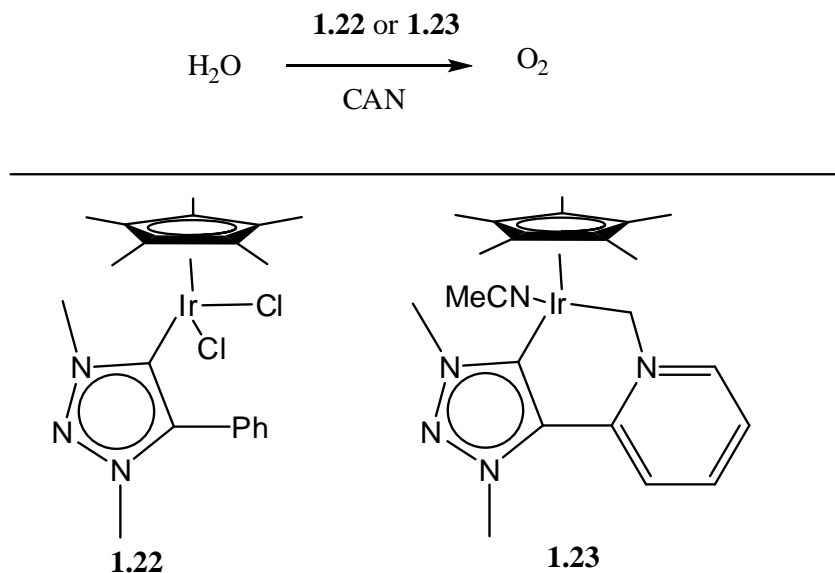
Scheme 1.5: Ir(trz)-catalysed water oxidation

After full optimisation reactions, the turnover frequencies (TOF) and turnover numbers (TON) were substantially higher than those of the best ruthenium based water-oxidation catalysts known to date. In addition, within 5 days the TON had reached nearly 10000, the largest number reported to date for water oxidation.

1.6.5   Oxidation of alcohols

Recently, Albrecht and co-workers have reported a series of Ru^{II}(cymene) complexes bearing 1,3,4-trisubstituted-1,2,3-triazol-5-ylidene ligands and applied them to the oxidation of alcohols and ketone transfer hydrogenation.[41] In both catalytic reactions, the mono-cationic complexes (**1.24**) containing chloride cymene spectator ligands performed better than the phosphines ruthenium complexes (**1.25**).
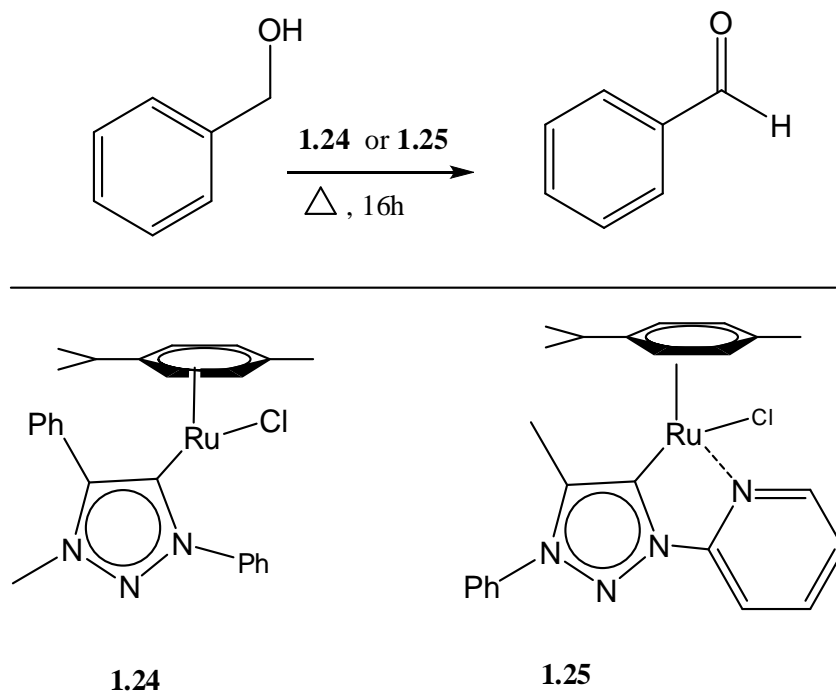
Scheme 1.6: Oxidation of benzyl alcohol with triazolylidene ruthenium complexes.

The donor functionality of **1.25** had a further profound impact on catalytic activity. These results highlight the potential of donor groups on the triazolylidene ligand for catalytic applications and provide an attractive strategy for further catalyst improvement to mediate such redox transformations.[41] Kinetic, computational and electrochemical analysis provided evidence that the 1,2,3-triazolylidene MIC ligands are directly involved in the catalytic process.

The discussions thus far indicate that triazolylidene metal complexes are catalytically active for a variety of known reactions, mostly surpassing the reactivity of metal complexes bearing traditional ligands such as the phosphines. Also the strong σ donor properties, make these ligands suitable for applications in unique catalytic reactions than conventional NHC ligands. Furthermore, the ease of variation of the triazolylidene ligand framework was shown to have direct implications on activity.

1.7   Alkane or Paraffins: beneficiation

In this section, a short introduction to the oxidation of alkanes is given, focusing on the advantages and challenges encountered in catalytic oxidation of paraffins in general.

Alkanes are compounds that consist only of hydrogen and carbon atoms. They are major constituents of natural gas and petroleum and due to the relatively inertness nature of the alkane C−H bond they are very stable and unreactive.[42] The field of alkane activation still remains a challenge to chemists, biochemists and engineers because of its inertness, however the field is not only of academic challenge but also of considerable interest to chemical industries globally.[43] Alkanes derived from natural gas, such as methane, are available in very large amounts at remote locations as permanent gas that are economically challenging to transport. Therefore conversion of these natural gas into transportable liquids such as methanol would make viable economic sense. Currently, alkanes derived from both petroleum and natural gas are converted to energy, fuel and chemicals at high temperatures and/or via multi-steps reactions leading to inefficient, environmentally and economically unviable results.[44]

1.8 Catalytic oxidation of paraffins

The main challenge for organometallic approaches to this transformation remains to produce stable and highly active catalysts. Most organometallic catalysts are extremely sensitive to stoichiometric oxidants typically required for these reactions.[45] Out of the three broad approaches to catalysis namely, homogeneous, heterogeneous, and bio-catalysis, the homogeneous soluble metal complexes have been reported to be the more useful catalysts for CH bond activation. Homogeneous oxidation catalysts, however, suffer from various drawbacks including low selectivity simultaneous activation of different competing alkane CH bonds and the difficulty in recycling relatively expensive metal catalysts.

Initial success in alkane oxidation via transition metal catalysis was achieved as early as 1894 by Fenton[46], although the catalyst proved to have very low selectivity to the required alcohol product. The classic Shilov system, discovered in 1969 is perhaps the most important of all alkane oxidation catalysts after "Fenton Chemistry". Shilov and co-workers discovered a system that was capable of oxidising alkanes to alcohol in water using Pt(II) salt.[47-48] The system followed a unique mechanism accounting for the increased selectivity and yield.[47-49] However the primary issue with the Shilov system is the irreversible decomposition of the expensive Pt(II) salt to insoluble polymeric Pt salts such (PtCl$_2$)n. Also, the system gives large quantities of functionalised product (RX) instead of oxidised alkanes (ROH).

1.9 Biomimetic in oxidation catalysis

Enzymes are the most efficient oxidation catalysts found in nature, hence, a variety of enzymes have been reported as efficient and selective catalysts for n-alkane oxidation reactions under physiological conditions.[50] These enzymes (mostly monooxygenases) are capable of catalysing the incorporation of a single atom from molecular oxygen into an organic substrate (Scheme 1.6).

$$R\text{-}H \quad + \quad NADH \ + \ H^+ \ + \ O_2 \quad \xrightarrow{\text{enzyme}} \quad ROH \ + \ NAD^+ \ + \ H_2O$$
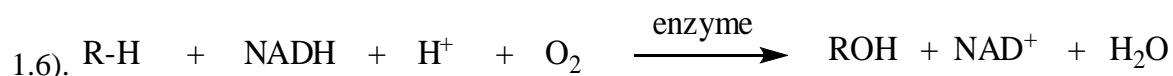
Scheme 1.7: Enzyme catalysed oxidation of an alkane R-H.

In practice, this approach seems to be applicable only to small scale conversions, and not for large scale bioprocesses for n-alkane transformations. However, recent research has been focused on further understanding the mechanisms of the biological systems[51], so as to guide the design of synthetic catalysts by mimicking their function, efficiency and selectivity. Inspired by nature, a variety of metal complexes have been reported to mimic the structure of well-established cytochrome P450 enzyme. Biomimetic catalysis has been extensively reviewed.[52-55]

1.10 Aim and Objectives

The main research objective of this thesis is to develop new oxidation catalysts that are selective for a variety of substrates, exhibiting good conversions, which are also cheap and environmentally friendly. In the best cases, the catalysts should be stable and work under mild reaction conditions. Inspired by recent advances, we became interested in using triazolylidene (a useful subclass of the popular N-heterocyclic carbenes (NHCs)) as ligands in metal complexes for catalytic applications.

1.10 Thesis outline

This thesis is written in chapters with each chapter addressing a specific subsection of the overall aims of the study:

- Chapter 1- general introduction of NHC ligands and their applications in catalysis.
- Chapter 2- focuses on synthesis of related triazolylidene (trz) nickel(II) complexes [NiCpI(trz)], full characterisation of the NiCpI(trz) complexes by standard spectroscopic techniques and single-crystal X-ray crystallography as discussed in detail and application in catalytic oxidation of *n*-octane under mild reaction condition.
- Chapter 3- addresses the synthesis of trans-dihalido-bis(trz) nickel complexes [*trans*Ni(trz)$_2$I$_2$] and their catalytic application in oxidation of alkanes.
- Chapter 4- focuses on the synthesis of triazolylidene copper complexes, characterisation and application for the *in-situ* catalytic oxidation of alkanes.
- Chapter 5- report synthesis and application of triazolylidene (trz) iron(II) complexes [FeCpI(trz)] as catalysts for oxidation of alkanes under mild reaction conditions
- Chapter 6- describe the synthesis, characterisation, X-ray structures and computational studies of novel triazolylidene-bromo dibromoiodate salt.
- Chapter 7- draws conclusions and provides a summary of the work presented.

1.11 References

1.   A. J. Arduengo III, H. V. R. Dias, R. L. Harlow and M. Kline, *J. Am. Chem. Soc.*, 1992, **114**, 5530-5534.

2.   F. Glorius, *Top. Organomet. Chem*, 2007, **21**, 1-20.

3.   D. Bourissou, O. Guerret, F. P. Gabbaï and G. Bertrand, *Chem. Rev.*, 2000, **100**, 39-92.

4.   M. N. Hopkinson, C. Richter, M. Schedler and F. Glorius, *Nature*, 2014, **510**, 485-496.

5.   A. J. Arduengo III, R. L. Harlow, M. Kline and . *J. Am. Chem. Soc.*, 1991, **113**, 361–363.

6.   W. A. Herrmann, *Angew. Chem. Int. Ed.*, 2002, **41**, 1290-1309.

7.   J. Nasielski, N. Hadei, G. Achonduh, E. A. B. Kantchev, C. J. O'Brien, A. Lough and M. G. Organ, *Chem.–Eur. J.*, 2010, **16**, 10844–10853.

8.   A. S. K. Hashmi, C. Lothschütz, K. Graf, T. Häffner, A. Schuster and F. Rominger, *Adv. Synth. Catal.*, 2011, **353**, 1407–1412.

9.   M. Iglesias, D. J. Beetstra, J. C. Knight, L.-L. Ooi, A. Stasch, S. Coles, L. Male, M. B. Hursthouse, K. J. Cavell, A. Dervisi and I. A. Fallis, *Organometallics*, 2008, **27**, 3279–3289.

10.   M. Iglesias, D. J. Beetstra, B. Kariuki, K. J. Cavell, A. Dervisi and I. A. Fallis, *Eur. J. Inorg. Chem.*, 2009, **2009**, 1913–1919.

11.   A. Igau, H. Grutzmacher, A. Baceirdo and G. Bertrand, *J. Am. Chem. Soc.* , 1988, **10**, 6463-6466.

12.   L. M. Slaughter, *ACS Catal.*, 2012, **2**, 1802–1816.

13.   R. W. Alder, M. E. Blake, C. Bortolotti, S. Bufali, C. P. Butts, E. Linehan, J. M. Oliva, G. Orpen and M. Quayle, *J. Chem. Commun.*, 1999, **131**, 241-242.

14.   M. Iglesias, D. J Beetstra, A. Stasch, P. N. Horton, M. B. Hursthouse, S. J. Coles, K. J. Cavell, A. Dervisi and I. A. Fallis, *Organometallics*, 2007, **26**, 4800-4809.

15.   F. E. Hahn and M. C. Jahnke, *Angew. Chem. Int. Ed.*, 2008, **47**, 3122-3172.

16.   J. D. Crowley, A.-L. Lee and K. J. Kilpin, *Aust. J. Chem.* , 2011, **64**, 1118-1132.

17.   H. C. Kolb, M. G. Finn and K. B. Sharpless, *Angew. Chem. Int. Ed.*, 2004, **40**, 2-5.

18.   H.-W. Wanzlick and H.-J. Schonherr, *Angew. Chem. Int. Edn Engl.*, 1968, **7**, 141–142.

19.   K. Ofele, *J. Organomet. Chem.* 1968, **12**, 42–P43.

20.   S. Diéz-González and S. P. Nolan, *Coord. Chem. Rev.*, 2007, **251**, 874-883.

21. H. Jacobsen, A. Correa, A. Poater, C. Costabile and L. Cavallo, *Coord. Chem. Rev.*, 2009, **253**, 687–703.

22. D. Nemcsok, K. Wichmann and G. Frenking, *Organometallics*, 2004, **23**, 3640–3646.

23. Garrison and Youngs, *Chem. Rev.*, 2005, **105**, 3978-4008.

24. J. Crabtree, *Organomet. Chem.* 2005, **690**, 5451-5457.

25. C. M. Crudden and D. P. Allen, *Coord. Chem. Rev.*, 2004, **248**, 2247–2273.

26. Lin and Vasam, *Coord. Chem. Rev.* 2007, **251**, 642-670.

27. C. J. O'Brien, E. A. B. Kantchev, C. Valente, N. Hadei, G. A. Chass, A. Lough, A. C. Hopkinson and M. G. Organ, *Chem.-Eur. J.*, 2006, **12**, 4743-4748.

28. A. Collado, A. Gomez-Suarez, A. R. Martin, A. M. Z. Slawin and S. P. Nolan, *Chem. Commun.*, 2013, **49**, 5541-5543.

29. J. Chun, H. S. Lee, G. Jung, S. W. Lee, H. J. Kim and S. U. Son, *Organometallics*, 2010, **29** 1518–1521.

30. A. J. Arduengo III, H. V. R. Dias, J. C. Calabrese and F. Davidson, *Organometallics*, 1993, **12**, 3405–3409.

31. H. M. J. Wang and I. J. B. Lin, *Organometallics*, 1998, **17**, 972–975.

32. J.A. Mataa, M. Poyatos and E. Peris, *Coord. Chem Rev.*, 2007, **251**, 841-859.

33. W. A. Herrmann, M. Elison, J. Fischer, C. Köcher and G. R. J. Artus, *Angew. Chem., Int. Ed. Engl.*, 1995, **34**, 2371–2374.

34. T. Karthikeyan and S. Sankararaman, *Tetrahedron Lett.*, 2009, **50**, 5834-5837.

35. J. Bouffard, B. K. Keitz, R. Tonner, G. Guisado-Barrios, G. Frenking, R. H. Grubbs and G. Bertrand, *Organometallics*, 2011, **30**, 6017-6021.

36. T. M. Trnka, J. P. Morgan, M. S. Sanford, T. E. Wilhelm, M. Scholl, T.-L. Choi, S. Ding, M. W. Day and R. H. Grubbs, *J. Am. Chem. Soc.*, 2003, **125**, 2546-2558.

37. B. K. Keitz, J. Bouffard, G. Bertrand and R. H. Grubbs, *J. Am. Chem. Soc.*, 2011, **133**, 8498-8501.

38. T. Nakamura, T. Terashima, K. Ogata and S.-i. Fukuzawa, *Org. Lett.*, 2011, **13**, 620–623.

39. S. Dıéz-González, A. Correa, L. Cavallo and S. P. Nolan, *Chemistry*, 2006, **12**, 7558-7564.

40.	R. Lalrempuia, N. D. McDaniel, H. Mueller-Bunz, S. Bernhard and M. Albrecht, *Angew. Chem. Int. Ed.*, 2010, **49**, 9765–9768.

41.	M. Delgado-Rebollo, D. Canseco-Gonzalez, M. Hollering, H. Mueller-Bunz and M. Albrecht, *Dalton Trans.*, 2014, **43**, 4462–4473.

42.	A. Sivaramakrishna, P. Suman, E. V. Goud, S. Janardan, C. Sravani, C. S. Yadav and H. S. Clayton, *Res. Rev. Mat. Sci. Chem.*, 2012, **1**, 75–103.

43.	E. Peris and R. H. Crabtree, *C. R. Chim.* 2003, **6**, 33–37.

44.	R. A. Periana, G. Bhalla, W. J. Tenn III, K. J. H. Young, X. Yang Liu, O. Mironov, C. J. Jones and V. R. Ziatdinov, *J. Mol. Catalysis A: Chemical* 2004, **220**, 7–25.

45.	A. Sivaramakrishna, P. Suman, E. V. Goud, S. Janardan, C. Sravani, T. Sandeep, K. Vijayakrishna and H. S. Clayton, *J. Coord. Chem.* 2013, **66**, 2091–2109.

46.	H. S. H. Fenton, *J. Chem. Soc.,Trans.*, 1894, **65**, 899-910.

47.	A. E. Shilov, *Riedel, Dordrecht,*, 1984, 245–249.

48.	A. E. Shilov and A. A. Shteinman, *Kinet. Katal.*, 1973, **14**, 117-120.

49.	N. F. Gol'dshleger, V. V. Eskova, A. E. Shilov and A. A. Shteinman, *Russ. J. Phys. Chem.*, 1972, **46**, 785–789.

50.	D. A. Kopp and S. J. Lippard, *Curr. Opin. Chem. Biol.*, 2002, **38**, 568–576.

51.	F. Ogliaro, N. Harris, S. Cohen, M. Filatov, S. P. d. Visser and S. S. Shaik, *J. Am. Chem. Soc.*, 2000, **122**, 8977-8989.

52.	T. C. Bruice, *Acc. Chem. Res.*, 1991, **24**, 243-249.

53.	B. Meunier, *Chem. Rev.*, 1992, **92**, 1411-1456.

54.	J. T. Groves, *J. Chem. Educ.*, 1985, **65**, 928-931.

55.	J. T. Groves, *J. Porphyrins Phthalocyanines*, 2000, **4**, 350-352.

CHAPTER 2

Half-sandwich trigonal planar Ni(II) complexes of 1,2,3-traizolylidene ligands utilized as catalysts for the oxidation of *n*-octane

2.1   General introduction

N-heterocyclic carbenes (NHC) have become one of the most popular supporting ligands in organometallic chemistry and homogeneous catalysis, due mainly to unique binding properties that make them superior to related two-electron donor ligands such as the ubiquitous phosphines.[1-3] The Arduengo-type imidazol-2-ylidenes dominate NHC chemistry because they are comparatively easy to prepare from readily available and affordable starting materials and have better stability than most phosphines.[4, 5] However, limitations in their donating ability to transition metals, especially to highly reactive base metals (Fe, Co, Ni) has led to moves toward other heterocyclic azolium scaffolds that include triazolylidenes or so-called mesoionic carbene (*m*NHC) ligands.[6]

This is related to the fact that 1,2,3-triazolylidenes are strong σ-donors that stabilise and provide access to highly reactive metal centres especially during catalysis.[7] [8]. In addition, the ease with which substituents around the triazole moiety may be fine-tuned to yield a myriad of ancillary *m*NHC ligands that display a wide variety of requisite properties has also added to the intense interest in the use of their metal complexes in catalysis.[9, 10] In spite of all the interest, the isolation of metal-NHC complexes is non-trivial, and there are many synthetic techniques available for their preparation, of which the earliest and most utilised involves the preparation of "free" carbenes[11] that are subsequently reacted with metal precursors. However, concerns on the relative stability of "free" carbene ligands have resulted in the development of *in situ* approaches as alternative methods. Thus, the direct substitution of a labile basic metal bound ligand by a *m*NHC has been used as an effective strategy for the synthesis of triazolylidene transition metal complexes.[12] An example of this route developed by Cowley and co-workers [13] is the direct reaction of nickelocene with azolium salts to yield NHC-nickel complexes. Later, Albrecht and co-workers[14] adapted the method to the synthesis of *m*NHC-Ni complexes used in catalysis. In general, base metal complexes of this nature have demonstrated catalytic activity in a variety of

reactions that include cross-coupling reactions[15, 16], hydroarylation of alkynes[17] and enantioselective cyclopentane synthesis[18]. In much broader terms, NHC-metal complexes have been utilised in cross coupling reactions[6, 19, 20] and ring-closing metathesis[21] to mention just a few of their numerous applications. However, due to the relative inertness of saturated paraffin hydrocarbon C_{sp}^{3}–H bonds, the area of alkane oxidation has remained a challenge that is relatively unexplored[15, 16]. Hence, as a continuation of our contributions [22-24] to the subject of paraffin oxidation using non-precious base metal complexes, we herein present the first use of *m*NHC-Ni complexes prepared via the direct (ligand substitution) route for the oxidation of *n*-octane under mild reaction conditions.

2.2 Results and discussion

2.2.1 Synthesis of triazolium nickel complexes

All the neutral triazoles and their corresponding salts were synthesized by reported methods via the well-established CuAAC 'click' protocols.[25, 26] For the synthesis of the metal complexes, we adapted the method of Cowley and co-workers[13] developed for imidazolium ligand precursors to suit the triazolium compounds reported here. Hence, a series of the triazolium salts were treated with nickelocene in THF under reflux, a rapid colour change from deep green to reddish-violet was observed and noted as the first signs of ligand coordination and reaction between the carbene and the nickel centre. In this manner, the various synthesised ligand precursor salts **2.2(a-d)** were all successfully coordinated to nickel (**2.3(a-d)**, Scheme 2.1). The aim of this is to study the effects of both steric and electronic variations on the catalytic activity of the prepared metal complexes (*vide infra*).
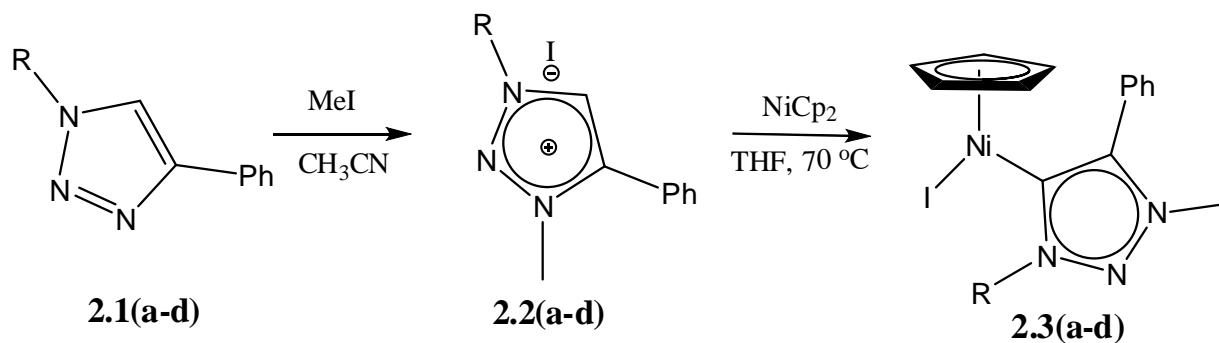
a R' = phenyl, **b** R' = ethyl propionate , **c** R' = propyl, **d** R' = benzyl,

Scheme 2.1: Synthesis of nickel complexes **2.3(a-d)**.

The complexes were isolated from THF in good to excellent yields as violet crystalline solids, a clear improvement over earlier methods[27] that reported comparatively lower product yields when the reactions were conducted in dioxane. All the complexes were characterised by spectroscopic analysis and the solid-state structures of **2.3c** and **2.3d** were further analysed by single crystal X-ray diffraction.

The compounds were all stable in air and only soluble in polar solvents, and ^{1}H-NMR spectroscopic analysis of their solutions in CDCl$_3$ showed disappearance of the distinct characteristic triazolium C-5 proton that normally resonates around 9-10 ppm for uncoupled triazolium salts, suggesting successful deprotonation and ligand complexation to the Ni(II) centre. It should be noted that due to residual unreacted nickelocene, we initially encountered complications in assigning some NMR peaks due to abnormal chemical shifts, line broadening, and unusual signal integrations. This is similarly observed and documented in the literature[27, 28], where some ^{1}H-NMR peaks assigned to the triazolium portion of the complexes were not fully resolved or became more complicated than expected. Following further purification and recrystallization, pure Ni-NHC complexes **2.3(a-d)** were confirmed.

From the NMR data, the presence of an intense singlet peak at circa 5 ppm signifies the presence of one η^5-bonded cyclopentadienyl ligand. The NMR peak positions of the substituents on the bonded triazolium ligands were observed to in general have shifted slightly downfields when compared to the chemical shifts of corresponding uncoordinated salts (e.g. **2.3b** vs **2.2b**, supporting information). The complexes were also characterised by ^{13}C NMR spectroscopy in

which all the spectra indicated the presence of bonded triazolium ligands and a sharp peak resonating at circa 90 ppm assigned to the bonded Cp ligand clearly indicates formation of proposed half-sandwich complexes **2.3(a-d)** from nickelocene and the respective ligands. Observations from paraffin activation studies indicates that the incorporation of hydrophobic regions in the choice of ligand substituents is often favourable to catalytic efficiency of the complex in terms of alkane conversion to oxygenated products.[24] Hence, we attempted to extend the R substituent group (Scheme 2.1) to longer straight alkyl chains beyond propyl, but under the current reaction conditions, we only isolated traces of *trans*-ligated *bis*-carbene complexes which we believe resulted from the decomposition (double substitution or second carbene insertion) of the targeted half-sandwich complexes[27].

Violet single crystals of **2.3c** and **2.3d** suitable for X-ray diffraction studies were obtained from the slow diffusion of hexane into concentrated solutions of the complexes in dichloromethane. The molecular structures of **2.3c** and **2.3d** showing the connectivity of atoms in the complexes with important bond lengths and angles highlighted are shown in Figures 2.1 and 2.2 respectively.
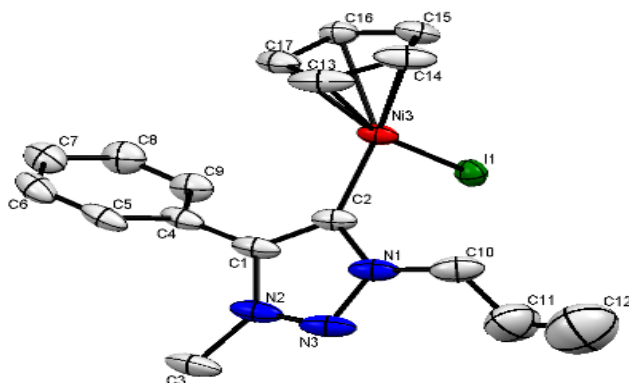
Figure 2.1: ORTEP plot of complex **2.3c** with thermal ellipsoids drawn at the 50% probability level and hydrogen atoms omitted for clarity. Selected bond lengths (Å) and angles (°): Ni-I(1) = 2.4951(5); Ni-C$_{carbene}$ = 1.881(3); Ni-Cp$_{centroid}$ = 1.750(4); C(2)-Ni-I = 97.49(9); C(2)-Ni-Cp$_{centroid}$ = 131.28(6); I-Ni-Cp$_{centroid}$ = 131.18(4).

Complex **2.3c** crystallised in the monoclinic *P21/c* space group while **2.3d** crystallised in the orthorhombic *Pna21*. With the cyclopentadienyl ring represented by a centroid, both complexes

showed trigonal-planar coordination of the three ligands around each nickel(II) centre. Also, both structures clearly show the 1,3,4-distribution of substituents around each 1,2,3-triazolium ligand coordinated to the metal in a $C_{carbene}$-Ni fashion. The half-sandwich geometry incorporates the centroid of the cyclopentadienyl ligand as the mid-point between its five carbon atoms.
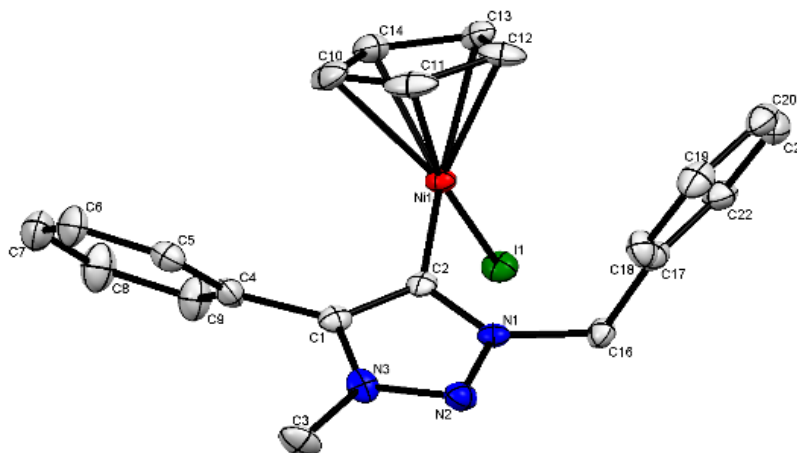
Figure 2.2: ORTEP plot of complex **2.3d** with thermal ellipsoids drawn at the 50% probability level and hydrogen atoms omitted for clarity. Selected bond lengths (Å) and angles (°): Ni-I(1) = 2.5130(7); Ni-$C_{carbene}$ = 1.872(5); Ni-Cp$_{centroid}$ = 1.753(6); C(2)-Ni-I = 100.1(2); C(2)-Ni-Cp$_{centroid}$ = 127.25(4); I-Ni-Cp$_{centroid}$ = 132.72(7).

Major bond lengths and angles of both complexes are standard and no deviations of significance were observed in comparison with related compounds reported in the literature. This attests to the open nature of the coordination environment around the metal centre that allows for extensive ligand variability.[27, 29, 30]

2.2.2 Application of compounds 2.3(a-d) as catalysts for the oxidation of *n*-octane

To test the efficiency of the prepared nickel complexes for the oxidation of *n*-octane we conducted a set of reactions aimed at studying any structure-activity relationships based on the chemical compositions of the catalysts. All experiments were conducted under similar conditions and initial results are presented in Table 2.1. Our main interest in paraffin oxidation research is

the activation and functionalisation of readily available medium to light straight chain alkanes such as *n*-octane to value-added oxygenated products (octanols and octanones) under mild reaction conditions, which we aim to achieve using very common oxidants.

The chemical inertness of the saturated alkane C-H bond limits the range of oxidants amenable to its activation and functionalisation. From a viewpoint of cost and environmental awareness, air and molecular oxygen (O_2) are the ideal oxidants, but the enthalpy requirement for their utilisation is inaccessible via the mild conditions utilised in this study. Hence, hydrogen peroxide (H_2O_2) and tertiary-butyl hydroperoxide (TBHP) are the more commonly encountered in homogeneous alkane oxidation because the former is relatively cheap and only produce H_2O as by-product while the latter is more stable to decomposition by metal ions and its by-product hardly interferes with GC data analysis of the products. The H_2O_2 and TBHP oxidation of *n*-octane with the catalysts **2.3(a-d)** produced a mixture of isomeric 2-, 3- and 4- octanones and octanols as the major products (Scheme 2.2). The minor products (1-octanol, octanal and octanoic acid) all resulted from primary carbon (C1) activation and no cracking of the substrate was observed under the mild temperature conditions of 80 °C.
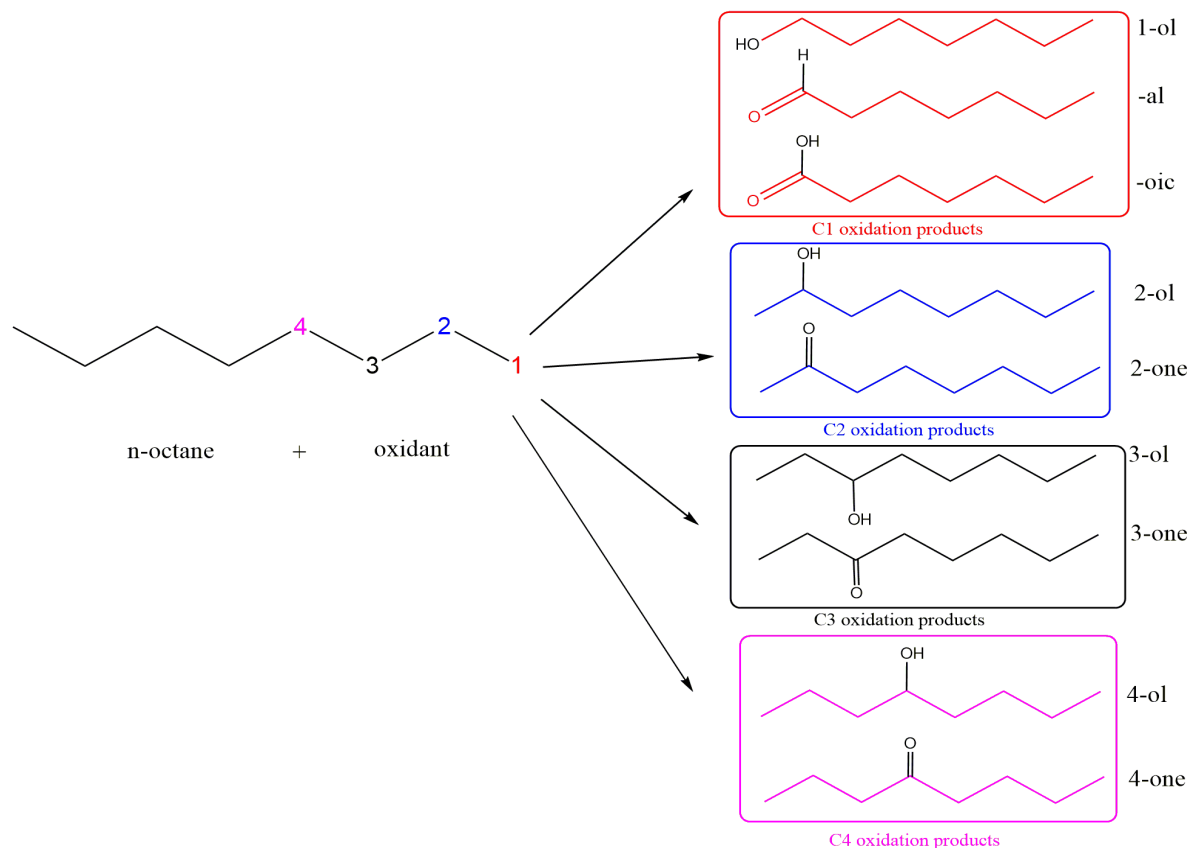
Scheme 2.2: Product distribution in the oxidation of *n*-octane.

Table 2.1 shows the results of the catalytic testing beginning with a blank study (entry 1) in the absence of any metal additive, for which only 2% of mainly isomeric ketones was observed and no alcohols, products of C(1) activation or cracking were observed. Conversely, the addition of catalysts **2.3(a-d)** resulted in low to moderate conversions (4-15%) to oxygenated products in which production of ketones dominated over that of the alcohols with ratios of total alcohols/ketones (A/K) < 1. TBHP is a commonly utilised oxidant and in some cases preferred over H_2O_2 due to the greater stability of its active hydroperoxo species in catalysis when compared to H_2O_2 which easily decomposes to water and oxygen.

Table 2.1: Peroxide promoted catalytic oxidation of *n*-octane based on catalysts **2.3(a-d)**[a]

Entry	Catalyst	Conversion (%)	Product distribution (%)				A/K ratio [b]
			ketones (4-;3-;2-)	alcohols (4-;3-;2-;1-)	aldehyde	acid	
1	Blank	2	100 (37; 21;42)	0	0	0	0.00
2	2.3a	10	63 (17:14:32)	26 (9;3;12;2)	7	4	0.41
3	2.3a-TBHP	4	39 (12;06;21)	57 (15;11;26;5)	4	0	1.46
4	2.3a-AcOH	7	54 (25;16;31)	19 (7;3;9;0)	2	7	0.35
5	2.3b	8	70 (22;12;36)	22 (5;4;13;0)	3	5	0.31
6	2.3c	15	64 (20;21;23)	28 (7;8;11;2)	5	3	0.44
7	2.3d	12	67 (21;16;30)	19 (6;3;9;1)	1	9	0.28

[a] Conditions for all reactions: solvent (MeCN) = 5 mL; *n*-octane = 0.84 M; oxidant (H_2O_2 or TBHP) = 14 mole equivalent; catalyst = 0.1 mol% (except entry 1 = none added); 80 °C; 24 hr. [b] A/K = relative ratio of total alcohol to total ketone products.

As indicated by the results (entry 3), the adoption of TBHP has resulted in an improvement in selectivity to the alcohols (A/K >1.4), but the total conversion to oxygenated products was very low (4%) for further utilisation in the current study, hence the remainder of the reactions were conducted using H_2O_2 as the oxidant. This is an advantage for the current system since in comparison; H_2O_2 is considered a relatively 'greener' and environmentally benign oxidant.

When an acid is added to oxidation reaction mixtures utilising H_2O_2 as the oxidant, a marked improvement in catalytic performance is usually observed. This improvement in catalytic performance of the acidified peroxide system has been attributed to stabilisation of the oxidant by the acid which slows down its decomposition to water and oxygen. Hence, we added acetic

acid as a promoter to the reaction mixture (entry 4) and except for the early signs of catalyst decomposition no appreciable improvement in catalytic efficiency was recorded. In fact, for the current Ni catalysed reactions, the acetic acid may have accelerated the oxidation reaction, however during the course of the reaction we observed changes in the colour of the solution that may be attributed to catalyst decomposition which consequently led to overall reduction in its activity to only 7% total conversion to products compared to 10% conversion for the non-acidified system (entry 2).In continuation, entries 5-7 respectively represent results for the variations in catalyst structure and molecular composition, mainly the effects of ring substituents of the triazolium ligand on the catalysis using the complexes **2.3(b-d)**. Systematic and gradual changes in electronic and steric influences of ligands around a metal ion are often invoked as tools in catalyst design for fine-tuning the catalytic efficiency of the metal with an overall aim of optimisation and improvement in efficiency. The results may be summarised thus:

- All the tested catalysts were active for the peroxide oxidation of *n*-octane with the ketones as the major product group (> 50% total conversion to 2-, 3- and 4-one).This indicates that the catalysts are more selective to the activation and functionalization of internal methylene carbons.[31] See below for further discussion on product selectivity.Clearly, complex **2.3c** is the most active catalyst at a total conversion to products of 15%. We believe that the relatively higher activity of **2.3c** is due to the sterically less hindered propyl N-substituent which is also chemically more compatible with the substrate.

- Differences in electronic influence arising from variation in the composition of the ligands also play some role in determining the magnitude of catalytic activity of the tested complexes. For instance, the stark activity difference between **2.3a** and **2.3c** may be rationalised based on electronic differences of the ligands. Complex **2.3a** contains a set of phenyl groups as triazolium ring substituents, while **2.3c** is *N*-substituted with an electron donating propyl group. Hence, the delocalised aromatic electrons in **2.3a** rendered the ligand less nucleophilic with a negative influence on the metal centre and its catalytic activity.

- In the oxidation of straight-chain *n*-alkanes, preferential functionalisation of the terminal C(1) carbon atoms is much desired over the functionalisation of internal carbons C(2, 3,

etc.). This is best illustrated in biological systems where the hydrophobic region of enzymes was reported to be involved in the ready uptake, correct orientation and subsequent functionalization (hydroxylation) of C-H containing compounds selectively to primary alcohols and acids[31].

- For the present set of complexes, analysis of products due to C(1) activation showed that catalyst **2.3c** exhibited the highest production of terminal oxidation products (octanal, 1-octanol and octanoic acid) in comparison to the other catalysts tested. It also showed higher selectivity towards the formation of alcohol products (with TBHP its A/K = 1.46) relative to the other catalysts. We believe that the presence of the hydrophobic alkyl chain substituent in the catalyst structure also contributed to the correct orientation of the *n*-octane chain for the preferential C(1) activation in **2.3c**.

- However, in homogeneous solutions, due to numerous factors (nature of catalyst, solvent system, oxidants, etc.) straight-chain *n*-alkanes may adopt varying and continuously altering conformations[32, 33] thus leading to poor selectivity and a mix-product stream. As illustrated in Scheme 2.2 for the functionalisation of *n*-octane with an atom of oxygen, depending on the position of attack and extent of oxidation, a total of nine oxygenated products are statistically possible. Hence, the concept of the regioselectivity parameter has become a useful tool for expressing the efficiency and selectivity of catalysts.

The regioselectivity parameter for *n*-octane (C1:C2:C3:C4) is the relative reactivity at carbon positions 1, 2, 3, 4 respectively along its backbone and is used to analyse selectivity to the diversity of possible products in the oxidation reaction data. It represents the relative reactivity of the internal methylene (CH_2) hydrogen atoms normalised to the terminal methyl (CH_3) hydrogen atoms. Irrespective of type, the products are grouped together based on the position of the inserted oxygen, with normalisation carried out by dividing the total selectivity at each carbon by the number of hydrogens at that position (three for the terminal CH_3 and two for each unique internal CH_2). As a reference, the reactivity at the terminal carbon 1 is set to one. For this study, the selectivity parameter expressing total reactivity at each carbon atom is presented in Table 2.2. Also presented is the oxidation data for related systems for *n*-octane oxidation and for a full analysis and discussion on some of the systems presented in Table 2.2. In general, the data in

Table 2.2 strengthens our initial observation that products of internal carbon oxidation (2-, 3- and 4-one & -ol, Scheme 2.2) especially the ketones predominate in the oxidation of n-octane.

It is also clear that the terminal C(1) position is the least productive. It is worth noting that the accumulation of ketones in the oxidation reaction of alkanes has been shown to occur as a secondary process from the over-oxidation of alcohol products.[23, 35, 38]

Minimising interaction between the initial alcohol products and the catalyst (oxidant) improves the A/K ratio and overall selectivity to alcohols. Hence, a possible explanation in favour of **2.3c** is that the presence of the short chain (hydrophobic) propyl group maximised the interaction between the substrate alkane and the catalyst to initially produce alcohols as the primary products while curtailing over-oxidation of the alcohols. In comparison, it is also obvious that the regioselectivity parameters for the oxidation of *n*-octane with H_2O_2 catalysed by our catalysts are comparable to those reported previously[23, 33, 34] suggesting that (i) our systems have followed similar mechanisms to those reported by Shul'pin and co-workers[35, 39] and (ii) the conformations of *n*-octane have favoured oxidation of internal carbons especially C(2). This is because in all the systems listed in Table 2.2, functionalisation at the C(2) position is the most favoured oxidation site as reflected by the regioselectivity parameters.

Table 2.2: Site efficiency in the oxidation of *n*-octane by various catalyst systems.

System	C1:C2:C3:C4[a]	Reference
2.3a	1.0 : 5.1 : 2.0 : 3.0	This work
2.3b	1.0 : 9.1 : 3.0 : 5.0	This work
2.3c	1.0 : 5.2 : 4.4 : 4.1	This work
2.3d	1.0 : 5.3 : 2.6 : 3.6	This work
Co[L]$^{2+}$/TBHP[b]	1.0 : 4.1: 3.3: 3.0	[23]
[L$_2$Mn$_2$O$_3$](PF$_6$)$_2$/H$_2$O$_2$[c]	1.0: 29.2: 25.5: 24.4	[34]
[L$_2$Mn$_2$O$_3$](PF$_6$)$_2$/H$_2$O$_2$[d]	1.0: 6.8: 5.9: 5.1	[34]
[O-Cu$_4${N(CH$_2$CH$_2$O)$_3$}$_4$(BOH)$_4$][BF$_4$]$_2$/H$_2$O$_2$[e]	1.0: 5.1: 5.2: 4.3	[35]
[O-Cu$_4${N(CH$_2$CH$_2$O)$_3$}$_4$(BOH)$_4$][BF$_4$]$_2$/TBHP[f]	1: 10: 6: 6	[35]
NaVO$_3$–H$_2$SO$_4$/H$_2$O$_2$[g]	1: 10.1: 10.7: 8.4	[36]
Al(NO$_3$)$_3$/H$_2$O$_2$[h]	1: 5.6: 5.6: 5.0	[37]

[a] Selectivity parameter C1:C2:C3:C4 is the normalized reactivity at carbon positions 1,2,3 and 4 respectively of the octane backbone with the reactivity at C(1) set 3 to 1. Conditions for this study are the same as in Table 1. [b] L= *bis*-tridentate-SNS-pyridine. MeCN, 80 °C, 24 hrs. [c] L=1,4,7-trimethyl-1,4,7-triazacyclononane. MeCN, 50 °C, 60 min. [d] L=1,4,7-trimethyl-1,4,7-triazacyclononane. UV irradiated, MeCN, 50 °C, 60 min. [e] CF$_3$COOH, MeCN, 50 °C. [f] MeCN, 50 °C. [g] MeCN, 50 °C. [h] MeCN, 70 °C.

2.2.3   Effects of variations in reaction conditions

At the onset, it is necessary to establish the optimum catalyst concentration based on the most active complex from the preliminary trial runs, i.e. complex **2.3c**. The molar concentration of the catalyst was varied between 0.05, 0.1, 0.2 and 0.5 mol%. Each run was monitored over a 24 hrs period at the solvent reflux temperature of 80 °C. The results showed that as the catalyst concentration was doubled from 0.05 to 0.1 mol%, total conversion to oxygenated products also doubled (7 to 15%), which also happens to correspond to the highest turnover (TON = 150) recorded for the current catalyst system. However, as we ramped up the catalyst concentration to 0.5 mol%, no measurable increase in *n*-octane conversion was observed, except that the TON massively decreased. Hence all further optimisation studies were conducted at a 0.1% molar concentration of the most active catalyst **2.3c**.

Reaction temperature is a very important variable in most catalytic processes including paraffin oxidation reactions where it is often observed that catalytic productivity is temperature dependent. Figure 2.3 presents the results of our investigation into the influence of reaction temperature on the current catalyst systems. Reactions were conducted in 5 mL MeCN using 0.84 M *n*-octane and 16 mole equivalent of the oxidant H_2O_2 and 0.1 mol% concentration of catalyst **2.3c** for a period of 24 hrs. The reaction temperature was gradually increased from 40 °C to the reflux temperature of the solvent (80 °C). It is important to note that earlier trial runs at room temperature indicated that no reaction occurred under all circumstances. Figure 2.3 shows that our results followed established trends in which total conversion of the substrate to the major oxidation products (octanones and secondary octanols) increased with increase in temperature.
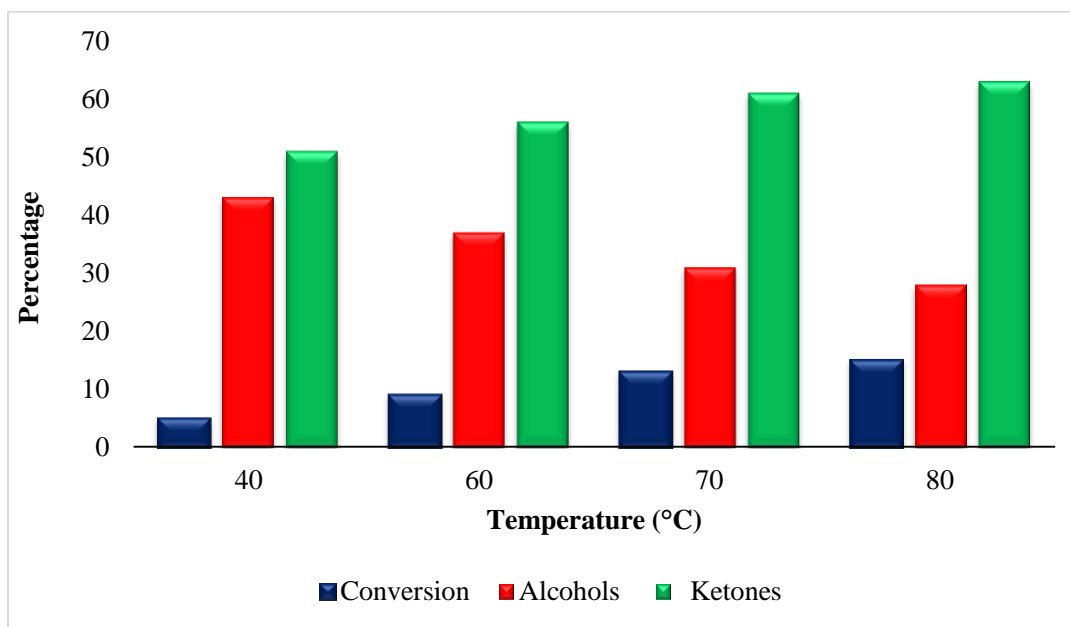
Figure 2.3: Effect of temperature on selectivity to major products in the oxidation of *n*-octane with catalyst **2.3c.**

The test was conducted up to 80 °C in order to work within limits that ensure catalyst stability, controlled reflux of the solvent (acetonitrile) and well below the boiling point of the substrate *n*-octane.[22, 23] Depending on the temperature used, different concentrations of isomeric alcohols and ketones were observed. At 40 °C comparable amounts of isomeric ketones and alcohols were

obtained, however, the concentration of the alcohols gradually dropped with increase in temperature. Along the octane backbone, carbon position C(2) is the more reactive since it gave the highest combined concentration of products (2-ol and 2-one) while carbon C(1) is the least reactive. Also, products (formaldehyde and formic acid) associated with oxidation of the solvent acetonitrile were not observed in this study.

To determine the optimum reaction time, we conducted a set of reactions under reflux monitored at six hourly intervals (6, 12, 24 and 36 hrs). Other reaction conditions are similar to those presented above. The results showed that in the first 6 hr, isomeric alcohols and ketones are the major products, however, after 24 hrs the concentration of alcohols has diminished significantly. Slow accumulation of ketones was also observed within the first 12 hrs, but after 24 hrs the rate of their formation was faster. This is most likely due to further oxidation of the alcohols by H_2O_2 to afford the corresponding ketones leading to a reduction in the molar concentrations of the alcohols relative to the ketones (reduction in A/K ratio). Hence all the optimised catalytic tests reported here were conducted over 24 hrs reaction period. It is well established that in catalytic processes under an oxidising environment, alcohol products (which are easier to oxidise than the substrate alkane) often react further to yield corresponding ketones or acids.[38]

Further, we also studied the effect of variation in the relative quantity of the oxidant H_2O_2 to the substrate. This was varied from 1:1 to 1:28 (mole/mole) and the results (Figure 2.4) indicate that the yield of products increased with increase in the relative ratio of substrate to oxidant up to a maxima at 1:16. The proportion of the alcohol products (lower A/K ratio) was observed to drastically drop beyond this ratio, hence all other reactions were conducted with the relative amount of oxidant capped at 1:16.
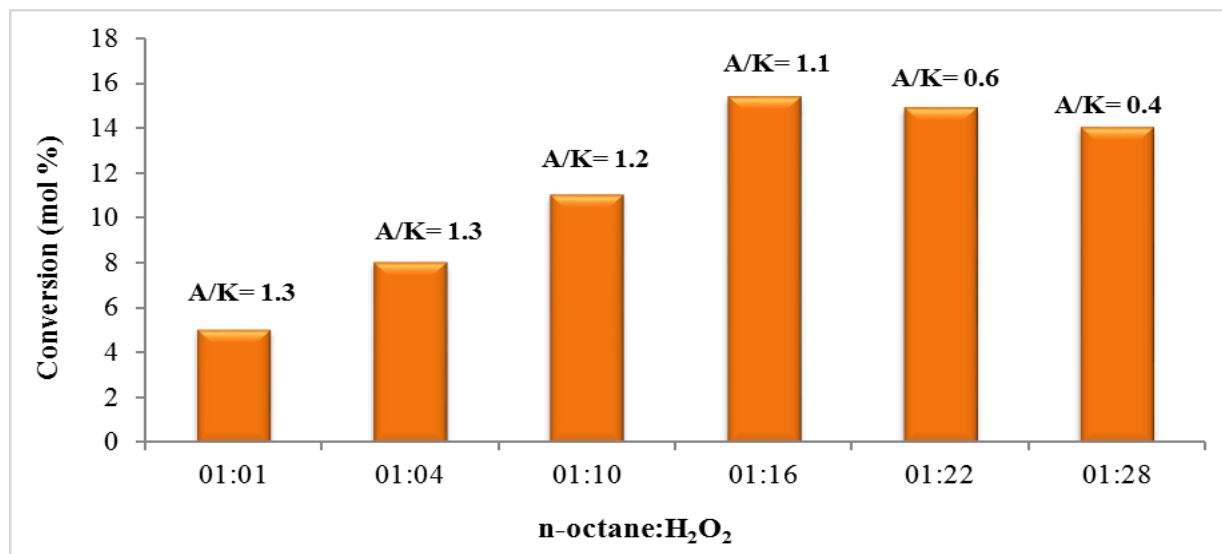
Figure 2.4: Effects of variation in oxidant quantities on the oxidation of *n*-octane catalysed by complex **2.3c**.

Catalyst stability in an oxidising environment (without *n*-octane) was studied using time dependent UV-vis spectroscopy to detect any spectral changes due to structural transformations of the catalyst. The most active complex **2.3c** was used as a representative catalyst under similar conditions as the catalytic runs. The result is presented in Figure 2.5, where no sign of change was observed within the first 60 min (top spectrum). However, after 4 hr (middle spectrum), the solution gradually changed from bright red to reddish-brown, and the UV-vis spectrum showed a drop in intensity of absorbance (λ_{max} = 357 nm) which might be due to the onset of catalyst decomposition[27] or the formation of active intermediates[40]. From the product distribution profiles (Table 2.2), it is obvious that the most obvious active intermediates for this oxidation reaction are metal-oxo and -peroxo species[33, 38], hence octyl hydroperoxide was the major product prior to its reduction by PPh$_3$. Also, these results agree with our earlier observations that no oxygenated products (or very negligible) were observed during the early stages of the reaction.

It is also interesting to note that a measurable intensity of absorbance in the UV-vis spectrum persisted up to 16 hr of reaction time (bottom spectrum), most probably indicating the availability of the active specie albeit at a diminished concentration, this is accompanied by a further change in colour of the solution to a light brown hue. After 48 hrs, the solution colour has

completely changed into light brownish colour with a greenish paste-like precipitate (most probably nickel oxide).
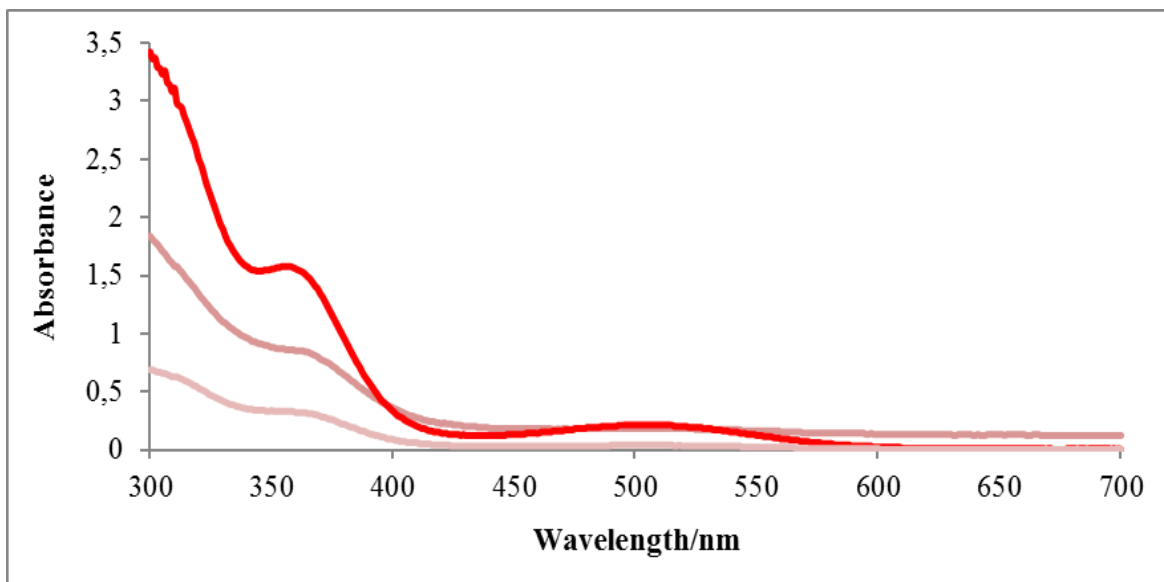
Figure 2.5: Time dependent UV-vis spectral changes following the addition of H_2O_2 to a solution of **2.3c** in acetonitrile at 80 °C. Top (60 min), mid (4 hr), bottom (16 hr).

In summary, it is obvious from all the data presented that a fine balance exists between product distribution (selectivity) and substrate conversion. This balance hinges on both the time of reaction and the relative amount of the oxidant. Shorter reaction times yielded more alcohol products albeit at low substrate conversions which is also supported by the use of relatively low quantity of the oxidant (up to 1:16). The catalyst is also shown to gradually transform in an oxidising environment, but remain relatively stable up to a period of 16 hrs.

2.3   Conclusions

1,2,3-triazolium-based nickel carbene complexes **2.3(a-d)** were synthesised by modification of reported synthetic methods. The crystal structures of two new Cp-Ni-NHC complexes were reported and discussed. All the complexes were applied for the catalytic oxidation of *n*-octane in the presence of oxidants under mild reaction conditions. All complexes were found to be active as catalysts and at the optimum reaction conditions, ketones were observed as the major product

group. Overall, the catalyst system with a hydrophobic alkyl chain substituent (**2.3c**) in the catalyst structure yielded the highest substrate conversion of 15 mol% at a turnover of 150.

2.4   Experimental

Toluene and THF were dried over sodium wire and benzophenone, dichloromethane (DCM) was dried over phosphorous pentoxide. All solvents were freshly distilled before used. High purity nitrogen gas was purchased from Afrox. Glassware was oven dried at 110 °C. Triazoles **2.1(a-d)** and their corresponding salts **2.2(a-d)** were synthesised as described in published literature and all their characterisation data are consistent with the literature reports[25, 26, 41]. Amongst the catalysts, only complex **2.3(a-d)** was previously reported by Albrecht and co-workers[27], for which we also obtained similar spectroscopic, analysis and single crystal XRD data. All NMR experiments were done using a 400 MHz Bruker Ultrashield spectrometer and samples were dissolved in deuterated solvents. Chemical shifts (δ) in ppm were reported with respect to tetramethylsilane (TMS) as internal standard. The following abbreviations were used to describe peak splitting patterns when appropriate: br = broad, s = singlet, d = doublet, t = triplet, q = quartet, m = multiplet. Infrared spectra (FTIR) were recorded on a Perkin Elmer FT-IR 1600

2.4.1   General procedure for synthesis of complexes 2.3(a-d)

(**2.3a**) Reddish powder (0.78 g, 73%). Crystals suitable for X-ray crystallography were grown by layering hexane on dichloromethane. ^{1}H-NMR (CDCl$_3$ 400 MHz) δ 7.17-7.54 (bm, Ar), 4.81 (s, Cp), 2.92 (s, N-CH$_3$), ^{13}C-NMR (CDCl$_3$, 400 MHz):148.5, 130.7, 129.9, 129.8, 129.7, 129.1, 128.7, 128.4, 128.3, 128.0, 125.8, 120.5, 117.7, 91.8, 37.9.IR vmax (cm^{-1}): 3054 (m) 2922 (m), 2853 (m), 1695 (m), 1593 (m), 1400(m), 1042 (m), 917(m), 756 (s), 607 (s), 513 (m). HRMS (ESI) m/z for C$_{20}$H$_{18}$N$_3$Ni [M-I]: calculated: 358.0854, found: 358.0866.

(**2.3b**) Reddish solid product (0.71 g, 66%). ^{1}H-NMR (CDCl$_3$ 400 MHz) : δ 7.26-7.92 (bm, Ar), 5.21 (s, Cp), 4.33 (s, CH$_2$), 4.29 (s, N-CH$_3$), 1.13-1.33 (m, 5H, CH$_2$ +CH$_3$); ^{13}C NMR (CDCl$_3$ 400 MHz): δ 166.2, 148.2, 130.3, 129.1, 128.8, 125.8, 120.9, 96.0, 62.4, 50.39, 22.6, 11.4. IR

ν_{max} (cm^{-1}): 3429 (b), 2929(m), 2360 (m), 1730 (b), 1616 (m), 1464 (m), 1370 (m), 1213 (b), 1025(s), 765(s), 695 (s), 502(m). HRMS (ESI) m/z for $C_{18}H_{20}N_3NiIO_2$ [M]: calculated: 497.0954, found: 497.0934.

(**2.3c**) Reddish crystalline product (0.49 g, 63%). Crystals suitable for X-ray crystallography were grown by layering hexane on dichloromethane. ^{1}H-NMR (CDCl$_3$ 400 MHz) : δ 7.66-7.83 (bm, Ar), 5.15 (s, Cp), 4.35 (s, N-CH$_3$), 4.70 (m, CH$_2$), 2.14-2.19 (m, CH$_2$), 1.11 (s, CH$_3$).^{13}C-NMR (CDCl$_3$, 400 MHz) : δ 148.0, 130.5, 129.8, 129.7, 128.8, 128.6, 91.5, 57.7, 37.1, 23.3, 11.3. IR vmax (cm^{-1}): 3439(m), 3350(m), 2987 (m), 1608 (s), 1579 (m), 1483 (s), 1464 (s), 1433 (s), 1345 (s), 1227 (m), 1073 (s), 1045 (m), 765 (s), 691 (s), 508 (s). HRMS (ESI) m/z for $C_{17}H_{20}N_3Ni$ [M-I]: calculated: 324.1011, found: 324.1071.

(**2.3d**) Reddish solid product (0.50 g, 63%).Crystals suitable for X-ray crystallography were grown by layering hexane on dichloromethane.^{1}H-NMR (CDCl$_3$ 400 MHz) : δ 7.26-8.19 (bm, Ar), 4.82(s, Cp), 4.35(s, N-CH$_3$), 4.02 (s, CH$_2$) ; ^{13}C-NMR (CDCl$_3$ 400 MHz) : δ 130.7, 129.9, 129.8 , 128.9, 128.8, 125.8, 125.4, 120.5, 91.8, 61.4, 37.5. 1. IR vmax (cm^{-1}): 3433(b), 2927 (m), 1695 (s), 1622 (m), 1450 (s), 1338 (s), 1073(s), 780 (m), 727 (s), 694(m), 698 (s). HRMS (ESI) m/z for $C_{21}H_{20}N_3Ni$ [M-I]: calculated: 372.1011, found: 372.0851.

2.4.2   Oxidation reaction of *n*-octane with compounds 2.3(a-d) as catalysts

The oxidants H$_2$O$_2$ (30%) and TBHP (70%) were respectively purchased from Sigma-Aldrich and DLD Scientific and used as supplied. The reagents utilised for the calibration of the GC: 1-octanol (99%), 2-octanol (97%), 3-octanol (98%), 4-octanone (99%), octanal (99%) and octanoic acid (99%) were obtained from Sigma-Aldrich, 2-octanone (98%), 3-octanone (97%), 4-octanol (98%) and *n*-octane (99%) were sourced from Fluka, and pentanoic acid (98%) from Merck. When required, double distilled water was used.

A typical oxidation reaction was carried out in a 2-neck round bottom flask fitted with an efficient reflux condenser operating under an atmosphere of nitrogen as follows: the catalyst (as indicated) and substrate were dissolved in dry solvent acetonitrile (CH$_3$CN), then an aqueous solution of H$_2$O$_2$ (or TBHP) was added and stirred vigorously at indicated temperature and time.

Except for studies on the optimisation of temperature and time, all the reactions were conducted at 80 °C and 24 hr respectively. The product was analysed by GC after the required time period, an aliquot of sample was removed using a Pasteur pipette and filtered through a cotton wool plug, after which 0.5 μL of the aliquot was injected into the GC for analysis and quantification. In all samples, excess solid triphenylphosphine (PPh$_3$) was added in order to capture alkyl hydroperoxides (if present) which are known to gradually decompose into corresponding ketones (aldehydes) and alcohols in the hot injector and columns.[42, 43] Total conversion was calculated as total moles of product/initial moles of substrate while selectivity was calculated as moles of product/total moles of product and both were expressed as a percentage. 2,4,6-trichlorobenzene was used as the internal standard and all experiments were conducted in an Agilent Technology 6820 GC System equipped with a flame ionization detector (FID) and an Agilent DB-Wax column with a length of 30 meters, inner diameter of 0.25 mm and a thickness of 0.25 mm.

2.4.3   X-ray structure determination

Single crystals were selected and glued onto the tip of a glass fibre, mounted in a stream of cold nitrogen at 173 K and centred in the X-ray beam using a video camera. Intensity data were collected on a Bruker APEX II CCD area detector diffractometer with graphite monochromated Mo Kα radiation (50 kV, 30 mA) using the APEX 2 data collection software. The collection method involved ω-scans of width 0.5° and 512 × 512 bit data frames. Data reduction was carried out using the program SAINT+ while face indexed and multi-scan absorption corrections were made using SADABS. The structures were solved by direct methods using SHELXS.[44] Non-hydrogen atoms were first refined isotropically followed by anisotropic refinement by full matrix least-squares calculations based on F^2 using SHELXS. Hydrogen atoms were first located in the difference map then positioned geometrically and allowed to ride on their respective parent atoms. Diagrams were generated using SHELXTL, PLATON[45] and ORTEP-3[46]. Crystallographic data for the structures in this article have been deposited with the Cambridge Crystallographic Data Centre, CCDC 1457104-1457105 for **2.3(c-d)** respectively. These data can be obtained free of charge at http://www.ccdc.cam.ac.uk/conts/retrieving.html (or from the

Cambridge Crystallographic Data Centre, 12 Union Road Cambridge CB2 1EZ, UK; Fax: +44-1223/336-033; E-mail: deposit@ccdc.cam.ac.uk).

2.5 References

1. Glorius, *Top. Organomet. Chem*, 2007, **21**, 1-20.

2. J. D. Crowley, A.-L. Lee and K. J. Kilpin, *Aust. J. Chem.* , 2011, **64**, 1118-1132.

3. E. Peris and R. H. Crabtree, *C. R. Chim.* , 2003, **6**, 33–37.

4. F. E. Hahn and M. C. Jahnke, *Angew. Chem. Int. Ed.*, 2008, **47**, 3122-3172.

5. D. Bourissou, O. Guerret, F. P. Gabbaï and G. Bertrand, *Chem. Rev.*, 2000, **100**, 39-92.

6. A. J. Arduengo III, R. L. Harlow, M. Kline and . *J. Am. Chem. Soc.*, 1991, **113**, 361–363.

7. M. N. Hopkinson, C. Richter, M. Schedler and F. Glorius, *Nature*, 2014, **510**, 485-496.

8. W. A. Herrmann, *Angew. Chem. Int. Ed.*, 2002, **41**, 1290-1309.

9. J. Nasielski, N. Hadei, G. Achonduh, E. A. B. Kantchev, C. J. O'Brien, A. Lough and M. G. Organ, *Chem.–Eur. J.*, 2010, **16**, 10844–10853.

10. A. S. K. Hashmi, C. Lothschütz, K. Graf, T. Häffner, A. Schuster and F. Rominger, *Adv. Synth. Catal.*, 2011, **353**, 1407–1412.

11. M. Iglesias, D. J. Beetstra, J. C. Knight, L.-L. Ooi, A. Stasch, S. Coles, L. Male, M. B. Hursthouse, K. J. Cavell, A. Dervisi and I. A. Fallis, *Organometallics*, 2008, **27**, 3279–3289.

12. M. Iglesias, D. J. Beetstra, B. Kariuki, K. J. Cavell, A. Dervisi and I. A. Fallis, *Eur. J. Inorg. Chem.*, 2009, **2009**, 1913–1919.

13. C. D. Abernethy, A. H. Cowley, R. A. Jones and 5., *J. Organomet. Chem.*, 2000, **596**, 3-5.

14. U. Schuchardt, W.A. Carvalho and E.V. Spinace´, *Synlett*, 1993, **10**, 713.

15. R. A. Periana, G. Bhalla, W. J. Tenn III, K. J. H. Young, X. Y. Liu, O. Mironov, C. J. Jones and V. R. Ziatdinov, *J. Mol. Catal. A: Chem.* , 2004, **220**, 7–25.

16. D. Munz and T. Strassner, *Inorg. Chem.* , 2015, **54**, 5043–5052.

17. R. Lalrempuia, N. D. McDaniel, H. Mueller-Bunz, S. Bernhard and M. Albrecht, *Angew. Chem. Int. Ed.*, 2010, **49**, 9765–9768.

18. A. M. Kirillov, M. V. Kirillova, L. S. Shul'pina, P. J. Figiel, K. R. Gruenwald, M. F. C. Guedes da Silva, M. Haukka, A. J. L. Pombeiro and G. B. Shul'pin, *J. Mol. Catal. A: Chem.*, 2011, **250**, 26-34.

19.   A. J. Bailey, W. P. Griffith and P. D. Savage, *J. Chem. Soc., Dalton Trans.*, 1995, 3537-3542.

20.   D. Naicker, H. B. Friedrich and B. Omondi, *RSC Adv.*, 2015, **5**, 63123–63129.

21.   A. Sobkowiak, A. Qui, X. Liu, A. Llobet and D. T. Sawyer, *J. Am. Chem. Soc.* , 1993, **115**, 609–614.

22.   E. Kadwa, M.D. Bala and H. B. Friedrich, *Applied Clay Science*, 2014, **95**, 340–347.

23.   L. Soobramoney, M.D. Bala and H. B. Friedrich, *Dalton Trans.*, 2014, **43**, 15968–15978.

24.   S. G. Mncube and M. D. Bala, *J. Mol. Liq.*, 2016, **215**, 396–401.

25.   P. Li and L. Wang, *Lett. Org. Chem.*, 2007, **4**, 23-26.

26.   Z. Yacob, J. Shah, J. Leistner and J. Liebscher, *Synlett*, 2008, **15**, 2342–2344.

27.   Y. Wei, A. Petronilho, H. Mueller-Bunz and M. Albrecht, *Organometallics,* 2014, **33** 5834-5844.

28.   W. Buchowicz, W. Wojtczak, A. Pietrzykowski, A. Lupa, L. B. Jerzykiewicz, A. Makal and K. Wozıniak, *Eur. J. Inorg. Chem.*, 2010, **43**, 648–656.

29.   P. Mathew, A. Neels and M. Albrecht, *J. Am. Chem. Soc.*, 2008, **130**, 13534–13535.

30.   W. Buchowicz, A. Koziol, L. B. Jerzykiewicz, T. Lis, S. Pasynkiewicz, A. Pecherzewska and A. Pietrzykowski, *J. Mol. Catal. A: Chem.* , 2006, **257**, 118–123.

31.   A. Wada, S. Ogo, S. Nagatomo, T. Kitagawa, Y. Watanabe, K. Jitsukawa and H. Masuda, *Inorg. Chem.*, 2002, **41**, 616–618.

32.   K. Nikki, H. Inakura, N. Wu-Le and T. J. Suzuki, *Endo Chem. Soc. Perkin Trans.* , 2001, **2**, 2370–2373.

33.   G. B. Shul'pin, T. Sooknoi, V. B. Romakh, G. Suss-Fink and L. S. Shul'pina, *Tetrahedron Lett.* , 2006, **47**, 3071–3075.

34.   G. B. Shul'pin, G. Süss-Fink and L. S. Shul'pina, *J. Mol. Catal. A: Chem.* , 2001, **170**, 17–34.

35.   M.V. Kirillova, A.M. Kirillov, D. Mandelli, W. A. Carvalho, A.J.L. Pombeiro and G. B. Shul'pin, *J. Catal.*, 2010, **272**, 9–17.

36.   L. S. Shul'pina, M. V. Kirillova, A. J. L. Pombeiro and G. B. Shul'pin, *Tetrahedron*, 2009, **65**, 2424–2429.

37.   D. Mandelli, K. C. Chiacchio, Y. N. Kozlov and G. B. Shul'pin, *Tetrahedron Lett.* , 2008, **49**, 6693–6697.

38.   T.C.O. Mac Leod, M.V. Kirillova, A.J.L. Pombeiro, M.A. Schiavon and M. D. Assis, *Applied Catalysis A: General* 2010, **372** 191–198.

39.   V. B. Romakh, B. Therrien, G. Süss-Fink and G. B. Shul'pin, *Inorg. Chem.*, 2007, **46**, 1315–1321.

40.   S.M. Yiu, W.L. Man and T. C. Lau, *J. Am. Chem. Soc.* , **130**, 10821–10827.

41.   J. T. Fletchera and J. E. Reillya, *Tetrahedron Lett.* , 2011, **52**, 5512–5515.

42.   G. B. Shul'pin, *J. Mol. Catal. A: Chem.*, 2002, **189**, 39–66.

43.   G. B. Shul'pin, *Mini-Rev. Org.*, 2009, **6**, 95–104.

44.   G. M. Sheldrick, *Acta Crystallogr., Sect. A: Fundam. Crystallogr.* , 2008, **64**, 112–122.

45.   A. L. Spek, *J. Appl. Crystallogr.* , 2003, **36**, 7–13.

46.   L. J. Farrugia, *J. Appl. Crystallogr.*, 1997, **30**, 565-566.

CHAPTER 3

Synthesis, characterization and application of square-planar Ni(II) complexes

of mesoionic carbene ligands for catalytic oxidation reactions

3.1 General introduction

Catalytic oxidation of alkanes into value-added products is a issue of research interest owed to the potential applications of the oxidized organic products as building blocks for the pharmaceutical, petrochemical and fine chemicals industries.[1-8] However, direct, selective catalytic activation and oxidation of alkanes to alcohols has remained a challenge to researchers. Recently, considerable research has been directed towards the catalytic oxidation of alkanes in homogeneous solutions using earth-abundant first-row transition metals including Ti[9, 10], V[11], Mn[5], Fe[12-14], Co[15], Ni[16, 17] and Cu[7, 18] These metals have turn out to be much more attractive in comparison to late transition metals which until recently have dominated this sphere. Increased interest in 1st row transition metals in catalysis is due to their obvious advantages, which include high abundance, low toxicity, low price and unique or unusual catalytic characteristics.

Since the first isolation of a stable, free *N*-heterocyclic carbene (NHC), metal complexes with NHC ligands have increasingly found applications in homogeneous catalysis. The strong σ-donating effects of the NHC ligands towards metal centres make them good candidates for the stabilization of metal ions during catalysis. In this regards, non-toxic and easy to prepare Ni-NHC complexes are now widely used instead of the well-established but more expensive d^8 homologues Pt and Pd.[19-21]However, the use of Ni-NHC complexes as catalysts for alkane activation is still very limited. Hence, herein we present one of the first use of Ni-NHC pre-catalysts for the oxidation of a variety of substrates under mild reaction conditions.

3.2   Results and discussion

All the triazolium iodide ligand precursor salts (Scheme 3.1) were synthesized via standard "click" 2+3 cycloaddition reactions of organic azides and phenylacetylene followed by subsequent methylation using MeI. Their full characterization and synthesis details are presented in the literature.[13, 22-24] At the beginning of this project, we adopted the method of Albretch and co-workers for the synthesis of square-planar $X_2(NHC)_2Ni$ (X-halide) type of complexes.[25] But, we soon realized that the direct reaction of triazolium salts with nickelocene at high temperatures (Route A, Scheme 3.1) yielded a mixture of products of the monoNHC product(**3.2**), the intended product(**3.3**) and recoverable quantities of unreacted nickelocene.

Whilst such attempts proved to be successful, however only low yields (circa 10%) of the target complexes **3.3** were isolated after complicated workup procedures, and this makes this route synthetically inadequate for the preparation of pre-catalysts required in relatively large quantities for thorough catalytic studies. We then explored the metalation method (Scheme 3.1, Route B) also recently reported by Astakhov *et al*.,[26] whereby reaction of an *in situ* generated triazolium carbene ligand with anhydrous $NiCl_2$-DME in dry acetonitrile resulted in the exclusive formation of the bis(NHC) complexes **3.4a-e**. Because we are interested in extending our studies in Ni-NHC systems for catalytic oxidation of alkanes, all the triazolium salt derivatives (**3.1**) were conceptualized with the aim of controlling the strength of the interaction between the catalysts and the substrate (mainly alkanes), thus enhancing catalyst activity. In many cases, the electronic and steric electronic properties of the NHC ligand exerts profound effects on the reaction outcome.[13, 27] In this regard, introduction of hydrophobic alkyl chain groups as wingtip *N*-substituents in the catalyst structure is believed to positively influence the interaction between the hydrocarbon substrates and the catalyst for the preferential functionalization of the former.
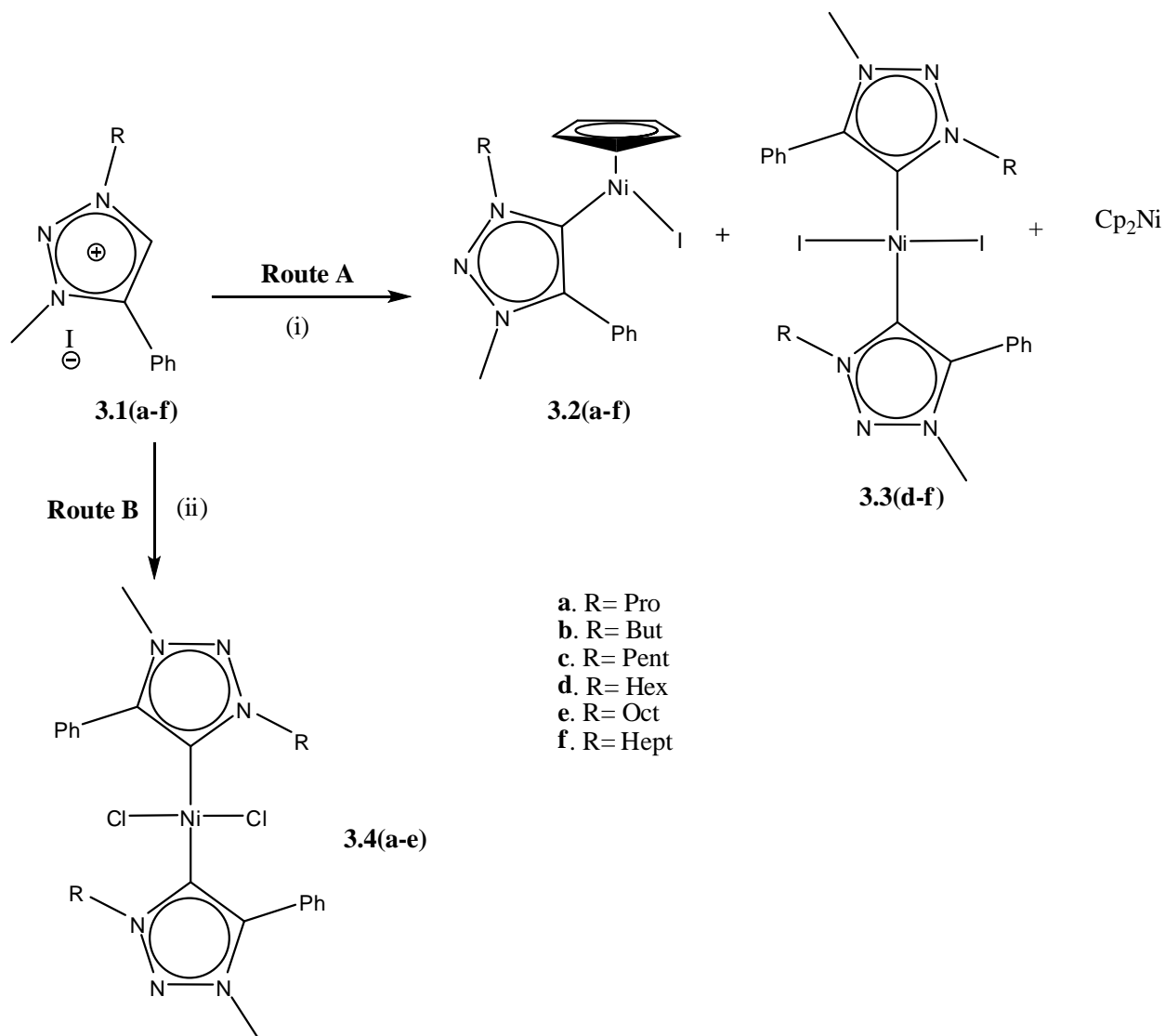
Scheme 0.1: Synthesis of Ni-NHC complexes. (i) NiCp₂,THF, 80 °C (ii) NiCl₂-DME, MeCN TEA, 80 °C.

All prepared Ni-NHC complexes were fully characterized by ^{1}H/^{13}C NMR, HRMS and EA. The spectral data indicate that the complexes were exclusively obtained as the *bis*NHC versions with no contamination of any side products as observed using the in previous method. Isolated yields are much improved to low to high (50-72%). In general, ^{1}H-NMR resonances for the *N*-alkyl substituents for all the complexes were observed as expected resonating as upfield multiplet peaks (0.5 to 4 ppm), while resonances integrating to 10H between 6.35 and 8.92 ppm assigned to the aromatic C4-substituents of the triazolium ligands, thus signifying a symmetric coordination of the ligand platform. In the ^{13}C NMR spectra of all the complexes (series **3.3d-f**

and **3.4a-e**), the expected characteristic resonances at δ 146-149 ppm represent the metal-carbene (Ni-C) C5 atoms which is a clear indication of NHC coordination to the Ni(II) centres.

Further confirmation of the structural integrity of the complexes was obtained from X-ray diffraction analysis of single crystals of compounds **3.3d-f** (Figures 3.1-3.3) single crystals suitable for XRD of the diiodido versions of the complexes were isolated.(**3.3d-f)**. All the structural data show that each complex contains a symmetric Ni(II) center within a square planar coordination of trans halide, trans NHC ligands. All the *N*-alkyl chains were oriented pointing away from each other to minimize steric interactions. All the key crystallographic parameters are standard and no major deviations were noted, for example, the Ni–I distances [2.50406(15) , 2.49400 and 2.4914(2) Å for **3.3d, 3.3e** and **3.3f** respectively] and the $C_{carbene}$-Ni(1)-$C_{carbene}$ angles [180.00] are consistent with those reported for similar compounds.[25, 28] For complex **3.3e**, the heptyl side chains of the NHC ligand showed strong anisotropic atomic displacements during refinement, suggesting a statistical positional disorder that was taken into account for the final model (Figure 3.2).
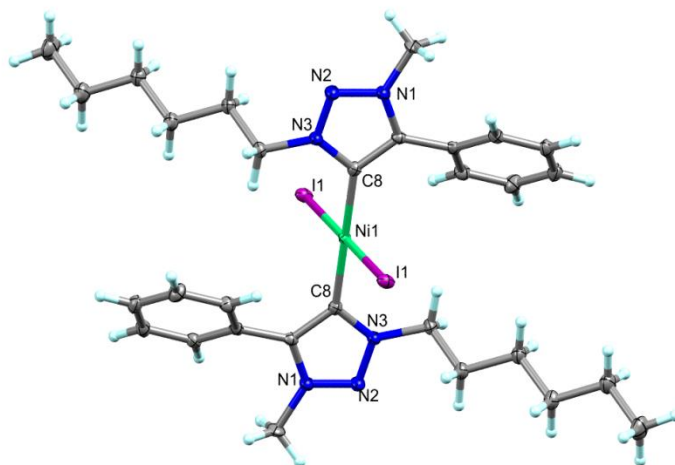
Figure 0.1: Molecular structure of complex **3.3d** with thermal ellipsoids drawn at the 50% probability level. Selected distances (Å) and angles (°): Ni(1)–C(8) 1.9094(16), Ni(1)–I(1) 2.50406(15), C(8)-Ni1-C(8) 180.00(8), I(1)-Ni1-I(1) 180.0, C(8)–Ni(1)–I(1) 88.65(5).
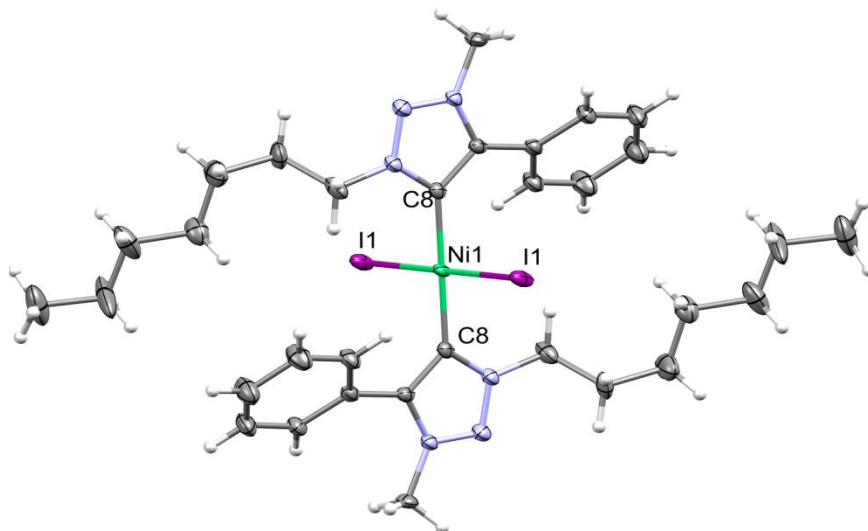
Figure 0.2: Molecular structure of complex **3.3e** with thermal ellipsoids drawn at the 50% probability level. Selected distances (Å) and angles (°): Ni(1)–C(8) 1.907(2), Ni(1)–I(1) 2.49400(17), C(8)-Ni1-C(8) 180.00, I(1)-Ni1-I(1) 180.0, C(8)–Ni(1)–I(1) 88.76(7).
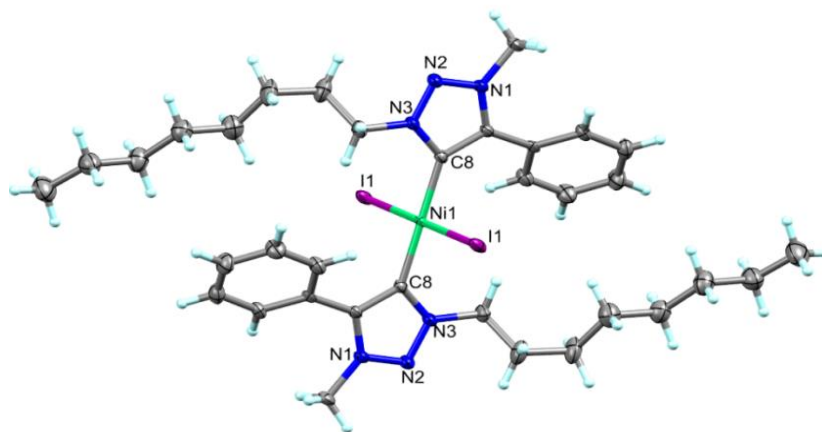
Figure 0.3: Molecular structure of complex **3.3f** with thermal ellipsoids drawn at the 50% level. Selected distances (Å) and angles (°): Ni(1)–C(8) 1.907(3), Ni(1)–I(1) 2.4914(2), C(8)–Ni(1)–I(1) 88.65(5).

3.2.1 DFT studies

To gain further insight into the influence of subtle changes in ligand structures (via increase in chain length of *N*-substituents) on the resulting metal bases catalysts. A series of DFT calculations were conducted. Electronic interactions involving relative energies and density mapping of HOMO and LUMO frontier orbitals are shown in Figure 3.4. The calculated/optimized geometric structures (and data) are in good agreement with crystallographic and NMR data of **3.3d** and **3.3f**.

LUMO   -5.04 eV   LUMO   -5.04 eV

0.35 eV   0.04 eV

               -5.08 eV

HOMO   -5.39 eV   HOMO

3.3d   **3.3f**
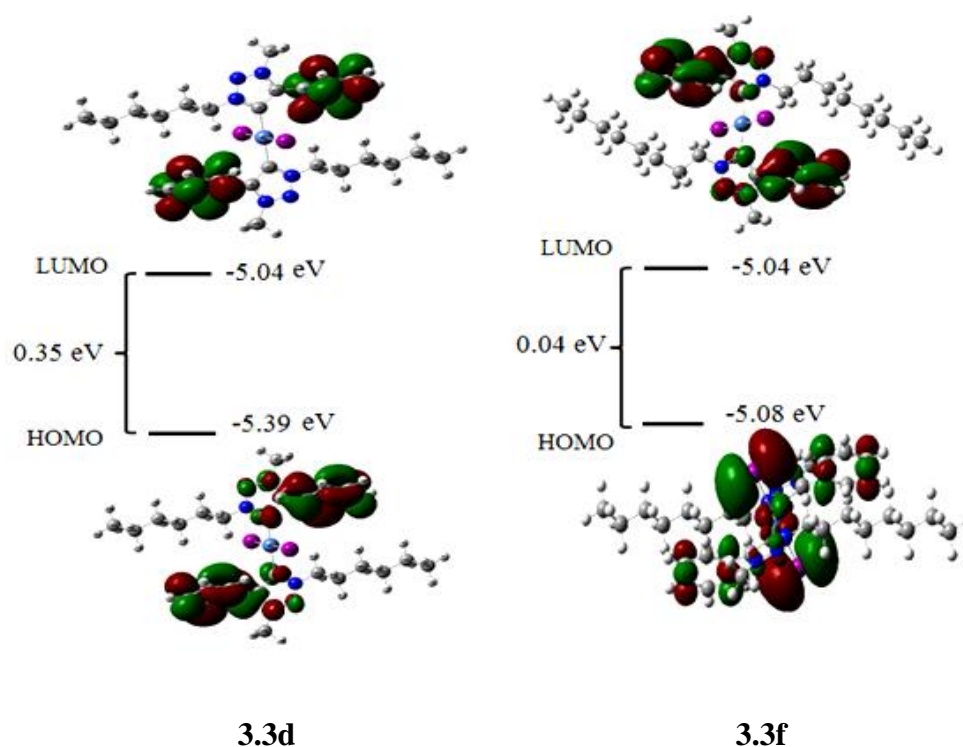
Figure 0.4: LUMO and HOMO representations and their relative energies for **3.3d**, and **3.3f** generated at the B3LYP/DGDZVP level of calculations.

The LUMO region of both complexes is mainly dominated by phenyl ring electron density. In both studied metal complexes, the *N*-alkyl chain of the ligands does not make significant contributions to the LUMO. Similar observations were made for the HOMO electron density distributions. The **3.3d** HOMO region is highly dominated by NHC fragment with phenyl ring moiety prevailing. Interestingly, redistribution of electron density is observed in **3.3f** HOMO

with metal center Ni(II) d orbital dominating, thereby decreasing the HOMO density around the NHC phenyl rings. The energy separation (ΔE) between the HOMO & LUMO for **3.3d** and **3.3f** are 0.35 and 0.04 eV respectively (Figure 3.4). A molecule with a large energy gap is generally associated with higher stability and lower chemical reactivity, which implies that theoretically **3.3d** is more stable than **3.3f**. Interestingly catalytic results supporting this phenomenon with **3.3f** showing better catalytic yield (11%) compared with **3.3d** (*vide infra*).

3.2.2   Electrochemistry

The continued success of NHCs as ancillary ligands in organometallic chemistry is largely due to the capability to fine-tune the steric and electronic properties of complexes via azolium ring and wingtip variations which routinely alter the topography around the metal center. In this regards, the electronic properties of organometallic catalysts usually have greater influence in catalytic activity and thus may be probed using cyclic voltammograms (CV) since it is a very convenient technique to observe the impact of changes in electronic properties around a metal center due to changes in ligand architecture. Hence the CV of compounds **3.4a-e** were recorded in MeCN to compare relative electrochemical response (Figure 3.5).
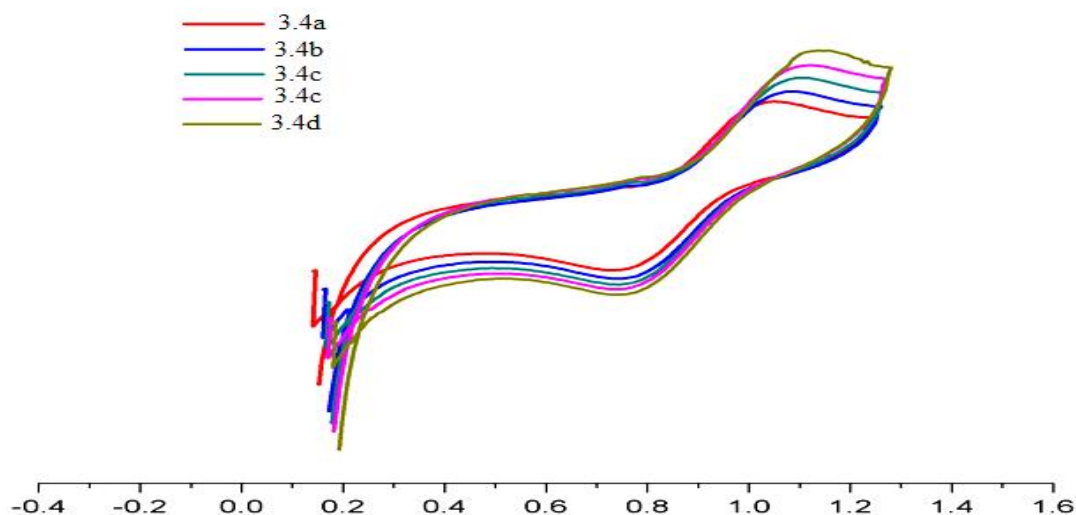
Figure 0.5: Comparison of the electrochemical response of for **3.4a-e** probed by CV.

All the compounds showed reversible oxidation responses that correlate with findings in the literature corresponding to the $Ni^{II/III}$ oxidation wave.[29-30] The influence of the wingtip alkyl N-substituents on the triazolium moiety is conveniently evaluated by comparing half wave potentials ($E_{1/2}$) of **3.4a-e**. Noteworthy, is the fact that increasing the length of the alkyl substituent showed a corresponding increase of the $E_{1/2}$ value to more positive potentials. This is due to increase in positive inductive effects as the alkyl chain length increased from **3.4a-e** which is believed to be beneficial to catalytic activity especially in the activation and functionalization of electrochemically stable and highly non-polar hydrocarbon containing substrates such as paraffins.

3.2.3   Oxidation of *n*-octane

n-octane is arguably the most studied straight chain alkane due to the fact that is it mid-range alkane with properties that are intermediate between those of light alkanes (gases and difficult to handle, requiring specialised reactors) and heavy alkanes (waxes that are difficult to oxidise under mild conditions). Hence, the catalytic activities of the synthesised complexes were explored in the oxidation of *n*-octane and the results are presented in Table 3.1. Control experiments in the absence of a catalyst and/or oxidant, results of which showed no conversion in the absence of either. Reactions utilising precursor $NiCl_2$ salt as catalyst showed circa 6% conversion of *n*-octane to mainly the ketone products only. screening of complexes **3.3d-f**, the diiodido compounds showed lower catalytic activities (8, 9 and 11% respectively) under similar reaction conditions, suggesting probably increased steric hindrance and restricted access to the Ni(II) centre during the course of catalysis due to the bulkier iodido ligands.

Catalytic results using **3.4a-e** produced up to 19% total yield to a mixture of C-8 products (isomeric alcohols and ketones, Table 3.1). The improved substrate conversion is indicative of the influence of the NHC ligands coordination to Ni(II). Statistically, the influence of changes in the electronic nature of the wingtip *N*-substituents on the catalytic results is minimal but noticeable with total yield showing slightly increase (16% for **3.4a** vs 19% for **3.4d** and **3.4f**) as the length of the substituent was increased. Also, the pattern of product distribution follows this

trend with an increase in alcohol production as the *N*-alkyl chain length increased (31% total alcohol for **3.4a** vs **3.4f**). Furthermore, in all sets of catalysts, C(2) products (mainly 2-one) dominated while the terminal C(1) position is the least reactive (Table 3.1). This indicates that the catalysts are selective to the internal carbons more readily than the terminal ones. In comparison, it is also obvious that the regioselectivity parameters for the oxidation of *n*-octane with TBHP catalyzed by these catalysts are comparable to those reported previously.[15, 22]

Table 0.1: Ni(II) complexes promoted catalytic oxidation of *n*-octane.[a]

Catalyst	Conversion (%)	Product distribution (%)				
		ketones (4-;3-;2-)	alcohols (4-;3-;2-;1-)	aldehyde	Acid	C1: C2: C3: C4[b]
3.3d	8	43 (5;15;23)	46 (4;15;20;7)	7	4	1.0: 5.3: 3.5: 1.1
3.3e	9	41 (6;14;21)	53 (7;17;21;8)	6	0	1.0: 4.5: 3.3: 1.3
3.3f	11	39 (7;14;18)	57 (5;19;23;10)	4	0	1.0: 4.7: 3.5: 1.3
3.4a	16	59 (8;18;33)	31 (4;10;15;2)	4	6	1.0: 6.0: 3.5: 1.5
3.4b	16	57 (8;17;32)	34 (4;11;15;4)	4	5	1.0: 5.4: 3.2: 1.4
3.4c	17	52 (6;18;28)	40 (3;11;21;5)	4	4	1.0: 5.7: 3.4: 1.1
3.4d	19	48 (7;16;25)	45 (5;12;21;7)	5	2	1.0: 4.9: 3.0: 1.3
3.4e	19	44 (4;16;24)	48 (6;15;22;5)	5	3	1.0: 5.3: 3.6: 1.2

[a]Conditions for all reactions: solvent (MeCN) = total vol. 5 mL; *n*-octane = 1 M; oxidant (TBHP) =14 M equivalent; catalyst = 1 mM ; 80 °C; 12 h. [b] Total yield based on product formed = [products]/[initial conc. of substrate]$_o$ x100. Selectivity (%) = (alcohol/ketone)/total products x 100. Selectivity ; C1:C2:C3:C4 is the normalized reactivity at carbon positions 1, 2, 3 and 4 respectively of the octane backbone with the reactivity at C(1) set to 1.

3.2.4 Oxidation of cyclohexane

In the application of complexes **3.4a-e** as catalysts for oxidation catalysis, the oxidation of cyclohexane was tested due to the importance of the cyclohexane oxygenation product (K-A oil) to the polymer industry.[31, 32] The oxidation of cyclohexane in the presence of TBHP and **3.4a-e** as catalysts was conducted under previously described optimum reaction conditions.[22] with TBHP used instead of H_2O_2 because we have earlier noticed decomposition of the catalyst when the more the aggressive H_2O_2 was used.

An optimum alkane to oxidant ratio of 1:14 and 12hr reaction time were used for all the studies reported in Table 2. As expected the K-A oil was the main product mixture with varying composition of the ketone and alcohol.

Table 0.2: Catalytic oxidation of cyclohexane based on catalysts **3.4a-e**.[a]

Cyclohexane → (3.4a-e, CH$_3$CN, 70 °C, TBHP) → Cyclohexanone (K) + cyclohexanol (A)
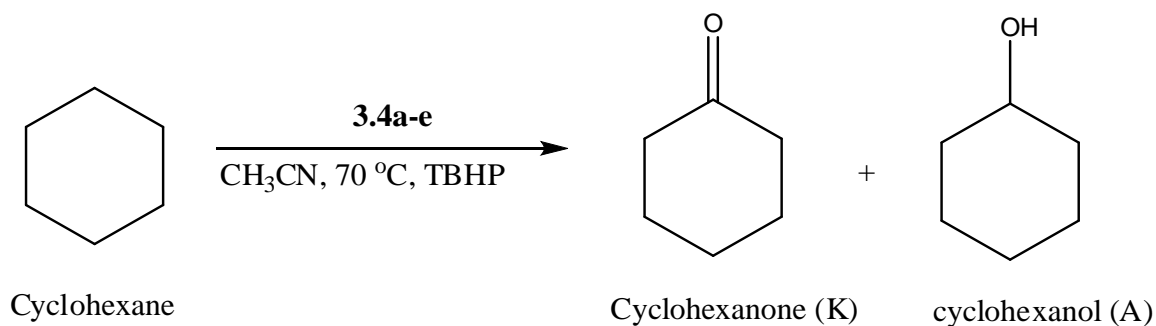
	Catalyst system	Conversion (mol %)[*]	K (mol %)	A (mol %)	K/A
1	**3.4a**	15	78	22	3.5
2	**3.4b**	15	69	31	2.2
3	**3.4c**	14	71	29	2.4
4	**3.4d**	14	61	39	1.6
5	**3.4e**	12	59	41	1.4

[a]Conditions for all reactions: Conditions for all catalytic reactions: same as in Table 1. Total yield based on product formed = [products]/[initial conc. of substrate]$_o$ x100. Selectivity (%) = (alcohol/ketone)/total products x 100.

The results suggest that the catalysis is insensitive to variations in the catalyst structure with total conversion of circa 15% for all catalysts studied. Theoretically, this is expected considering the cyclic structure of the substrate which essentially was unaffected by the variation in size of the wingtip alkyl substituents. Hence, the total conversion of the substrate and the relative ketone/alcohol (K/A) ratio remained essentially constant up to **3.4d**. However, as the chain length increased for **3.4e** the conversion slightly decreased indicating a probable onset of steric hindrance by the much longer wingtip N-substituents limiting access to the Ni(II) center, thus resulting in reduced interactions between the active centre and the substrate. In addition, cyclohexanone is the more dominant product in all the systems tested with K/A values decreasing as the wingtip alkyl chain size increased. Furthermore, generally the Ni-NHC catalytic systems are slightly more active on *n*-octane, up to (19%) in comparison to the cyclohexanone.

3.2.5   Oxidation of alcohols

Previous reports[13, 18] have proposed that alcohols are the primary products of alkane oxidation and that it is the over-oxidation of the alcohol products that led to the production of ketones as the dominant products often observed in many of homogenous alkane oxidation reactions
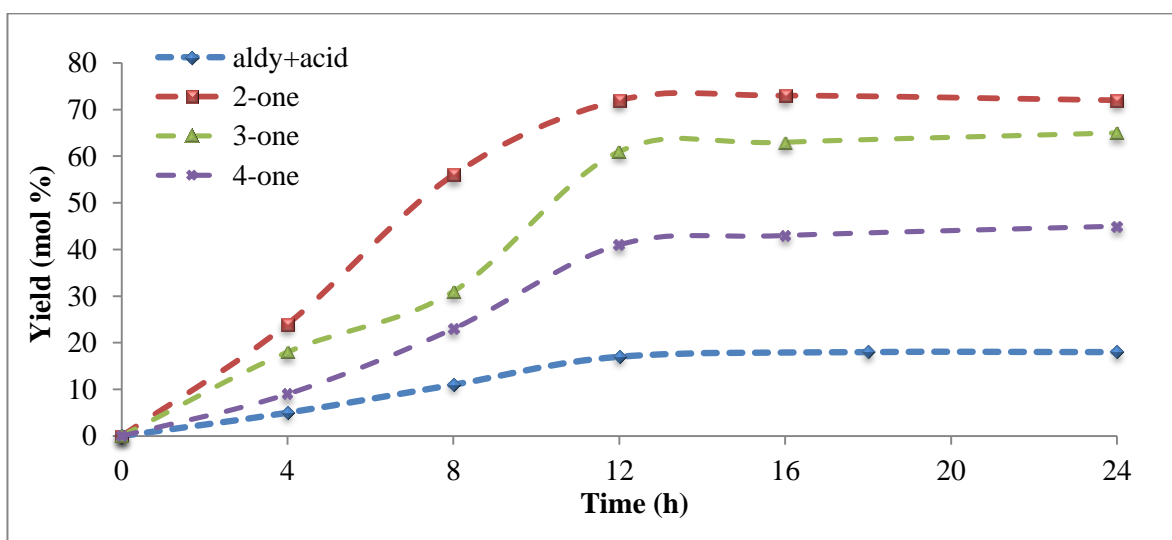
Figure 0.6: Peroxide promoted catalytic oxidation of alcohols (1-, 2-, 3- and 4- octanol) based on catalysts **3.4a**. Conditions for all catalytic reactions: same as in Table 1.

In our effort to further understand over-oxidation of alcohols to ketones products, a set of experiments were conducted under similar conditions (as used for the octane oxidation). We tested a number of alcohols (1-, 2- , 3- and 4- octanol) that were expected in the oxidation of *n*-octane towards further oxidation. Complex **3.4a** was used as a representative catalyst as it was the most effective in octanones production in the earlier *n*-octane oxidation study (Table 2). The obtained results show that oxidation of alcohols is time dependent (Fig. 6); however after 12 hr there was no significant change. In general, the 2- and 3- octanols were the more readily converted to the 2- and 3-octanones with conversion rate of 72 and 63% respectively. This is in agreement with many reports that indicate the C(2) position as the most reactive site in n-octane oxidation.[15, 33-36]

3.3   Conclusion

In the present study, highly symmetric square planar Ni(II) NHC complexes were successfully synthesized and fully characterized. Application of the metal complexes as catalysts in alkane oxidation resulted in a mixture of isomeric oxidation products. Based on these results, it is concluded that catalyst systems with long electronic donating and hydrophobic alkyl chain substituents benefit from electronic stabilization of the Ni(II) catalytic center resulting in high substrate conversion up to 19 mol%. Furthermore, comparative study of the catalytic results and CV data showed a direct relationship between the observed changes in catalytic activities and measurable shifts of the $E_{1/2}$ values towards more positive potentials for **3.3a-e**. Lastly, **3.3a** was found to be very effective catalysts for the oxidation of alcohols to ketone products indicating that probably ketone production in alkane oxidation is the result of secondary oxidation of alcohols which are often more reactive than the original alkane.

3.4   Experimental

All solvents were dried before used. All triazolium salts **3.1a-f** were synthesized as previously described in published literature and their corresponding characterization data were consistent

with reported literature.[13, 22-24] The following abbreviations are used to describe peak splitting patterns when appropriate: br = broad, s = singlet, d = doublet, t = triplet, q = quartet, m = multiplet. Infrared spectra (FTIR) were recorded on a Perkin Elmer FT-IR 1600 spectrophotometer.

3.4.1   General procedure for synthesis of diiodido nickel complexes (3.3)

The reported method[25] was modified. To a solution of triazolium salts **3.1d-f** in THF (15 mL) nickelocene (0.5 equiv.) was added. The mixture was stirred at 90 °C for 24 hr. The solvent was removed under vacuum and the residue was extracted with hot toluene (5 x 3 mL). Combined extracts were concentrated under reduced pressure and the residue obtained was chromatographed on with EtOAc/hexane (1:1). A red colored fraction was collected and evaporated to dryness to give **3.3**. Characterization data are:

(**3.3d**). Yield: 0.081 g (**10** %) of brown-red crystals. ^{1}H NMR (CDCl$_3$, 400 MHz): δ 0.95 (t, 6H, 2CH$_3$), 1.40 (m, 4H, 2CH$_2$), 1.91-2.00 (m, 8H, 4CH$_2$), 2.61 (m, 4H, 2CH$_2$), 4.26 (s, 6H, 2CH$_3$), 4.54 (m, 4H, 2CH$_2$), 7.39-7.79 (m, 10H, 2Ar). ^{13}C{^{1}H} NMR (CDCl$_3$, 400 MHz): δ 15.61, 25.92, 29.60, 35.52, 41.76, 43.43, 54.23, 119.54, 125.69, 126.94, 127.94, 128.06, 128.16, 128.54, 128.69, 128.80, 128.81, 128.98, 129.53, 129.53, 131.88, 148.14. . Anal. Calcd for C$_{30}$H$_{42}$I$_2$N$_6$Ni (799.19): C, 45.09; H, 5.31; N, 10.52. Found: C, 45.11; H, 5.41; N, 10.53.

(**3.3e**) Yield: 0.081 g (**10** %) of red crystals. ^{1}H NMR (CDCl$_3$, 400 MHz): δ 0.77 (t, 6H, 2CH$_3$), 0.11-1.39 (m, 8H, 4CH$_2$), 2.01 (m, 4H, 2CH$_2$), 3.79 (s, 6H, 2CH$_3$), 4.26 (m, 4H, 2CH$_2$), 7.48-7.68 (m, 10H, 2Ar). ^{13}C{^{1}H} NMR (CDCl$_3$, 400 MHz): δ 14.08, 22.62, 26.20, 28.89, 29.14, 29.26, 29.44, 31.77, 39.32, 54.63, 121.78, 129.71, 131.98, 142.95, 149.09. Anal. Calcd for C$_{32}$H$_{46}$I$_2$N$_6$Ni (826.12): C, 46.46; H, 5.60; N, 10.16. Found: C, 46.47; H, 5.66; N, 10.16.

(**3.3f**). Yield: 0.065 g (**9** %) of red crystals. ^{1}H NMR (CDCl$_3$, 400 MHz): δ 0.97-1.03 (t, 6H, 2CH$_3$), 1.40-1.56 (m, 10H, 5CH$_2$), 193 (m, 4H, 2CH$_2$), 4.07 (s, 6H, 2CH$_3$), 4.36 (t, 4H, 2CH$_2$), 7.42-7.83 (m, 10H, 2Ar). ^{13}C{^{1}H} NMR (CDCl$_3$, 400 MHz): δ 11.09, 11.18, 22.91, 23.76, 39.84, 52.03, 56.62, 119.81, 121.44, 152.27, 125.66, 158.52, 125.84, 128.89, 129.09, 129.13, 129.92,

13061, 143.57, 147.57. Anal. Calcd for $C_{34}H_{50}I_2N_6Ni$ (855.30): C, 47.75; H, 5.89; N, 9.83. Found: C, 47.75; H, 5.90; N, 9.85.

3.4.2   General procedure for synthesis of dichlorido nickel complexes (3.4)

The reported method[26] was also modified. To a solution of triazolium salts **3.1a-f** in THF (15 mL) was added anhydrous $NiCl_2$ (0.5 eq), and Et_3N (4 eq) in dry acetonitrile (20 mL) and heated under reflux for 6 h. The solvent was removed under reduced pressure, and the residue obtained was passed through a silica gel column, with neat $CHCl_3$ as eluent to give **3.4**. Characterization data are:

(**3.4a**). Yield: 0.451 g (56 %) of brown crystals. ^1H NMR ($CDCl_3$, 400 MHz): δ 0.94 (m, 6H, $2CH_3$), 2.01-2.03 (m, 4H, $2CH_2$), 4.13 (s, 6H, $2CH_3$), 4.38 (t, 4H, $2CH_2$), 7.46-7.56 (m, 10H, 2Ar). $^{13}C\{^1H\}$ NMR ($CDCl_3$, 400 MHz): δ 1.67, 14.86, 25.39, 43.85, 5.95, 121.97, 131.27, 132.75, 142.60, 148.41. Anal. Calcd for $C_{24}H_{30}Cl_2N_6Ni$ (532.13): C, 54.17; H, 5.68; N, 15.81. Found: C, 54.18; H, 5.67; N, 15.81. HR-MS: m/z calculated for $C_{24}H_{30}N_6Ni^+$ $[M+Na]^+$: 484.218; found 484.299.

(**3.4b**). Yield: 0.532 g (68 %) of yellow-brown powder. ^1H NMR ($CDCl_3$, 400 MHz): δ 0.01-0.06 (m, 6H, $2CH_3$), 1.49-1.55 (m, 4H, $2CH_2$), 2.09-2.12 (m, 4H, $2CH_2$), 4.33 (s, 6H, $2CH_3$), 4.70-4.76 (t, 4H, $2CH_2$), 7.66-7.80 (m, 10H, 2Ar). $^{13}C\{^1H\}$ NMR ($CDCl_3$, 400 MHz): δ 14.05, 28.98, 29.04, 31.70, 50.45, 119.35, 125.69, 128.07, 128.28, 128.48, 128.82, 130.64, 130.75, 147.3. Anal. Calcd for $C_{26}H_{34}Cl_2N_6Ni$ (560.18): C, 55.75; H, 6.12; N, 15.00. Found: C, 55.81; H, 6.14; N, 15.04. HR-MS: m/z calculated for $C_{26}H_{34}N_6Ni^{+.}$ 488.220; found 488.227.

(**3.4c**). Yield: 0.602 g (72 %) of brown powder. ^1H NMR ($CDCl_3$, 400 MHz): δ 0.82-0.83 (t, 6H, $2CH_3$), 1.26-1.36 (m, 12H, $6CH_2$), 2.03 (m, 4H, $2CH_2$), 4.25 (s, 6H, $2CH_3$), 4.74 (t, 4H, $2CH_2$), 7.52-7.69 (m, 10H, 2Ar). $^{13}C\{^1H\}$ NMR ($CDCl_3$, 400 MHz): δ 14.08, 22.62, 26.66, 28.81, 29.10, 31.77, 39.12, 44.64, 127.52, 127.71, 128.01, 128.85, 129.06, 148.54. Anal. Calcd for $C_{28}H_{38}Cl_2N_6Ni$ (588.24): C, 57.17; H, 6.51; N, 14.29. Found: C, 57.18; H, 6.52; N, 14.30. HR-MS: m/z calculated for $C_{28}H_{38}N_6ClNi^+$ $[M-Cl]^+$: 551.220; found 551.221.

(**3.4d**). Yield: 0.582 g (61 %) of brown powder. ^{1}H NMR (CDCl$_3$, 400 MHz): δ 0.95-0.97 (t, 6H, 2CH$_3$), 1.42 (m, 12H, 6CH$_2$), 2.14 (m, 4H, 2CH$_2$), 4.35 (s, 6H, 2CH$_3$), 4.70 (t, 4H, 2CH$_2$), 7.66-7.84 (m, 10H, 2Ar). ^{13}C{^{1}H} NMR (CDCl$_3$, 400 MHz): δ 22.62, 26.66, 28.81, 29.10, 31.77, 39.12, 44.64, 127.52, 127.71, 128.01, 128.85, 129.06, 148.54. Anal. Calcd for C$_{30}$H$_{40}$Cl$_2$N$_6$Ni (588.24): C, 58.47; H, 6.87; N, 13.64; . Found: C, 58.50; H, 6.88; N, 13.671. HR-MS: m/z calculated for C$_{30}$H$_{42}$N$_6$Ni$^+$ [M+Li]$^+$: 551.298; found 551.308.

(**3.4e**). Yield: 0.611 g (65 %) of brown powder. ^{1}H NMR (CDCl$_3$, 400 MHz): δ 0.78-0.81 (t, 6H, 2CH$_3$), 1.19-1.76 (m, 10H, 5CH$_2$), 1.78-1.82 (m, 4H, 2CH$_2$), 3.93-3.95 (s, 6H, 2CH$_3$), 4.01 (t, 4H, 2CH$_2$), 7.34-7.56 (m, 10H, 2Ar). ^{13}C{^{1}H} NMR (CDCl$_3$, 400 MHz): δ 1.87, 13.92, 22.32, 22.44, 25.83, 29.14, 30.96, 38.61, 54.37, 65.83, 127.67, 128.69, 128.84, 129.51, 129.68, 131.81, 143.25, 148.43. Anal. Calcd for C$_{34}$H$_{50}$Cl$_2$N$_6$Ni (670.28): C, 60.73; H, 7.50; N, 12.50. Found: C, 60.77; H, 7.53; N, 12.52. HR-MS: m/z calculated for C$_{34}$H$_{50}$N$_6$Ni [M+Li]$^+$: 607.36; found 607.30.

3.4.3   Typical procedure for the oxidation of substrates

Oxidation reaction was carried out under nitrogen atmosphere as follows: the reaction started by mixing 1.0 mL of a 10.0 mM stock solution of catalyst in MeCN and 1.0 mL of a stock solution of 1.0 M of substrate (n-octane, cyclohexane or alcohol). After stirring for 1 min, excess of aqueous solution of tert-butyl hydroperoxide (1.0 mL of 70% aq., 14 M) was added. Extra 2 mL MeCN was added to keep total volume constant at 5mL. The reaction mixture was stirred for the indicated time and temperature. The products were analyzed by GC (refer to chapter 2).

3.4.4   X-ray structure determination

Single crystals were selected and glued onto the tip of a glass fibre, mounted in a stream of cold nitrogen at 173 K and centred in the X-ray beam using a video camera. Intensity data were collected on a Bruker APEX II CCD area detector diffractometer with graphite monochromated

Mo Kα radiation (50 kV, 30 mA) using the APEX 2 data collection software. The collection method involved ω-scans of width 0.5° and 512 × 512 bit data frames. Data reduction was carried out using the program SAINT+ while face indexed and multi-scan absorption corrections were made using SADABS. The structures were solved by direct methods using SHELXS.[39] Non-hydrogen atoms were first refined isotropically followed by anisotropic refinement by full matrix least-squares calculations based on F^2 using SHELXS. Hydrogen atoms were first located in the difference map then positioned geometrically and allowed to ride on their respective parent atoms. Diagrams were generated using SHELXTL, PLATON[40] and ORTEP-3.[41] Crystallographic data for the structures in this article have been deposited with the Cambridge Crystallographic Data Centre, CCDC 1566136 (**3.3d**), 1571157 (**3.3e**) and 1566137 (**3.3f**). These data can be obtained free of charge at http://www.ccdc.cam.ac.uk/conts/retrieving.html (or from the Cambridge Crystallographic Data Centre, 12 Union Road Cambridge CB2 1EZ, UK; Fax: +44-1223/336-033; E-mail: deposit@ccdc.cam.ac.uk).

3.4.5 DFT studies

All electronic structure calculations were performed with the aid of Gaussian 09, revision B01. Gauss View 5.0.8 was utilized as a molecular builder and for visualization. The structure was fully optimized via mixed basis set at UB3LYP/GENECP level of theory with 6-31+G (d, p) for C, N, H, and landl2dz for Ni and I. Vibrational spectra of the compounds were calculated using optimized structures with the same basis set and computational methods. The ^{1}H and ^{13}C NMR shielding constants were predicted using the Gauge-Including atomic orbitals (GIAO) GIAO–DFT in gaseous medium. The 6-31++G (d, p) basis set was used since this was common standard used in Gaussian to compute isotropic shielding constants of ^{1}H and ^{13}C for TMS which is used as a reference molecule in Gaussian. Subsequently, isotropic shielding constants of carbon atoms in our complexes were computed using the GIAO method.

3.4.6 Electrochemistry

Cyclic voltammetry was performed using a standard three-electrode configuration: a platinum disk electrode was used as the working electrode, a platinum wire as the auxiliary electrode, and

a silver electrode as reference, separated from the test solution by a fine porosity frit. The electrochemical measurement of respective Ni-NHC complexes (2 mM) in MeCN and 0.1 M NBu4BF4 was used as the supporting electrolyte. Data workup was performed on OriginPro v8.0988.

3.5   References

1.   T.C.O. Mac Leod, M.N. Kopylovich, M.F.C. Guedes da Silva, K.T. Mahmudov and A. J. L. Pombeiro, *Appl. Catal., A*, 2012, 439– 440.

2.   J. A. Labinger and J. E. Bercaw, *Nature*, 2002, **417**, 507–514.

3.   E. Peris and R. H. Crabtree, *C. R. Chim.* , 2003, **6**, 33–37.

4.   A. J. Bonon, D. Mandelli, O. A. Kholdeeva, M. V. Barmatova, Y. N. Kozlov and G. B. Shul'pin, *Appl. Catal. A*, 2009, **365**, 96–104.

5.   G.B. Shul'pin, Y.N. Kozlov, G.V. Nizova, G. Süss-Fink, S. Stanislas, A. Kitaygorodskiy and V.S. Kulikova, *J. Chem. Soc. Perkin Trans.* , 2001, **2**, 1351–1371.

6.   M.V. Kirillova, A.M. Kirillov, D. Mandelli, W. A. Carvalho, A.J.L. Pombeiro and G. B. Shul'pin, *J. Catal.*, 2010, **272**, 9–17.

7.   M.V. Kirillova, Y.N. Kozlov, L.S. Shul'pina, O. Y. Lyakin, A.M. Kirillov, E.P. Talsi, A.J.L. Pombeiro and G. B. Shul'pin, *J. Catal.*, 2009, **268**, 26–38.

8.   A. Sen, *Acc. Chem. Res.*, 1998, **31**, 550–557.

9.   R.H.P.R. Poladi and C. C. Landry, *Microporous and Mesoporous Materials,* 2002, **52**, 11-18.

10.   B. Su, Z.C. Cao and Z. J. Shi, *Acc. Chem. Res.*, 2015 **48**, 886−896.

11.   L. S. Shul'pina, M. V. Kirillova, A. J. L. Pombeiro and G. B. Shul'pin, *Tetrahedron*, 2009, **65**, 2424–2429.

12.   E. Kadwa, M.D. Bala and H. B. Friedrich, *Appl Clay Sci.*, 2014, **95**, 340–347.

13.   S. G. Mncube and M. D. Bala, *J. Mol. Liq.*, 2016, **215**, 396–401.

14.   S.M. Yiu, W.L. Man and T. C. Lau, *J. Am. Chem. Soc.* , **130**, 10821–10827.

15.   L. Soobramoney, M.D. Bala and H. B. Friedrich, *Dalton Trans.*, 2014, **43**, 15968–15978.

16.   E. Tordin, M. List, U. Monkowius, S. Schindler and G. Knör, *Inorganica Chimica Acta*, 2013, **402,** 90–96.

17.   T. Nagataki, Y. Tachi and S. Itoh, *Chem. Commum.*, 2006, **22**, 4016-4018.

18.   T.C.O. Mac Leod, M.V. Kirillova, A.J.L. Pombeiro, M.A. Schiavon and M. D. Assis, *Appl. Catal., A,* 2010, **372,** 191–198.

19.   D. Schweinfurth, R. Pattacini, S. Strobel and B. Sarkar, *Dalton Trans.*, 2009, **42**, 9291–9297.

20.   D. Schweinfurth, S. Strobel and B. Sarkar, *Inorg. Chim. Acta.* , 2011, **374**, 253−260.

21.   K. J. Kilpin, E. L. Gavey, C. J. McAdam, C. B. Anderson, S. J. Lind, C. C. Keep, K. C. Gordon and J. D. Crowley, *Inorg. Chem.*, 2011, **50**, 6334-6346.

22.   S. G. Mncube and M. D. Bala, *Mol. Catal.*, 2017. dio: /10.1016/j.mcat.2017.03.005

23.   Z. Yacob, J. Shah, J. Leistner and J. Liebscher, *Synlett*, 2008, **15**, 2342–2344.

24.   P. Li and L. Wang, *Lett. Org. Chem.*, 2007, **4**, 23-26.

25.   Y. Wei, A. Petronilho, H. Mueller-Bunz and M. Albrecht, *Organometallics,* 2014, **33,** 5834−5844.

26.   A. V. Astakhov, O. V. Khazipov, E. S. Degtyareva, V. N. Khrustalev, V. M. Chernyshev and V. P. Ananikov, *Organometallics*, 2015, **34**, 5759-5766.

27.   H. Ibrahim and M. D. Bala, *New J. Chem.* , 2016, **40**, 6986-6997.

28.   K. Zhang, M. Conda-Sheridan, S. Cooke and J. Louie, *Organometallics*, 2011, **30**, 2546–2552.

29.   O. R. Luca, B. A. Thompson, M. K. Takase and R. H. Crabtree, *Journal of Organometallic Chemistry*, 2013, **730**, 79-83.

30.   T. P. Brewster, J. D. Blakemore, N. D. Schley, C. D. Incarvito, N. Hazari, G. W. Brudvig and R. H. Crabtree, *Organometallics*, 2011, **30**, 965-973.

31.   U. Schuchardt, W.A. Carvalho and E.V. Spinace´, *Synlett*, 1993, **10**, 713-718.

32.   U. Schuchardt, D. Cardoso, R. Sercheli, R. Pereira, R.S. da Cruz, M.C. Guerreiro, D. Mandelli, E.V. Spinace and E. L. Pires, *Appl. Catal. A*, 2001, **211**, 1-17.

33.   A. M. Kirillov, M. V. Kirillova, L. S. Shul'pina, P. J. Fig.iel, K. R. Gruenwald, M. F. C. Guedes da Silva, M. Haukka, A. J. L. Pombeiro and G. B. Shul'pin, *J. Mol. Catal. A: Chem.*, 2011, **250**, 26-34.

34.   L. J. R. Smith, Y. Iamamoto and F. S. Vinhado, *J. Mol. Catal. A: Chem.*, 2006, **252**, 23-30.

35.   A. J. Bailey, W. P. Griffith and P. D. Savage, *J. Chem. Soc., Dalton Trans.*, 1995, 3537-3542.

36.   D. Naicker, H. B. Friedrich and B. Omondi, *RSC Adv.*, 2015, **5**, 63123–63129.

37.   G. B. Shul'pin, *J. Mol. Catal. A: Chem.*, 2002, **189**, 39–66.

38.   G. B. Shul'pin, *Mini-Rev. Org.*, 2009, **6**, 95–104.

39.   G. M. Sheldrick, *Acta Crystallogr., Sect. A: Fundam. Crystallogr.* , 2008, **64**, 112–122.

40.   A. L. Spek, *J. Appl. Crystallogr.* , 2003, **36**, 7–13.

41.   L. J. Farrugia, *J. Appl. Crystallogr.*, 1997, **30**, 565-566.

CHAPTER 4

Homogeneous oxidation reactions catalyzed by

in situ generated Cu-mesoionic triazolylidene complexes

4.1   General introduction

Copper offers significant advantages compared to other transition metals typically used in catalysis: cupper is earth-abundant, inexpensive, nontoxic, and environmentally friendly. Inspired by the active centres of some Cu containing enzymes[1], copper complexes have been reported to potentially catalyse the functionalisation of many organic compounds under mild reaction conditions.[2-5] This is because copper can easily access Cu^0, Cu^I, Cu^{II}, and Cu^{III} oxidation states allowing it to act through one-electron or two-electron processes during catalytic cycles.[6]

Metal complexes containing mesoionic triazolylidene (*m*NHC) have been exploited as catalysts for a wide variety of organic transformations including alcohol oxidation,[7] intermolecular direct etherification of allylic alcohols,[8] Heck reaction,[9] etc. and for many of these, Cu‑*m*NHC catalysis has become an extremely popular area of research.[10] This is because the price of copper [11] and the benefit of *m*NHC as auxiliary ligands in catalysis have been strongly emphasised.

numerous synthetic methods have been reported for the preparation of Cu-*m*NHC, amongst which the earliest involves the preparation of "free" carbenes which are then reacted with Cu precursors. However, concerns over stability of isolated Cu-NHC complexes have resulted in the development of the *in situ* catalytic approach as an alternative method to circumvent the stability concerns. This method was first reported in 2001 by Woodward *et al*,[12] and a number of reports with the common theme being that Cu salts make better catalysts in the presence of NHC ligands.[13-18] Because of our interest in *m*NHC chemistry, herein we exploit the *in situ* generated (with steric and electronically tuned ligands) Cu-*m*NHC catalysts for the catalytic oxidation of a range of substrates.

4.2 Results and discussion

4.2.1 Synthesis of Cu-mesoionic triazolylidene complexes

Triazoles **4.1** and their corresponding triazolium salts **4.2** were prepared by reported methods and the characterisation data are matches with previous reports.[19-23]
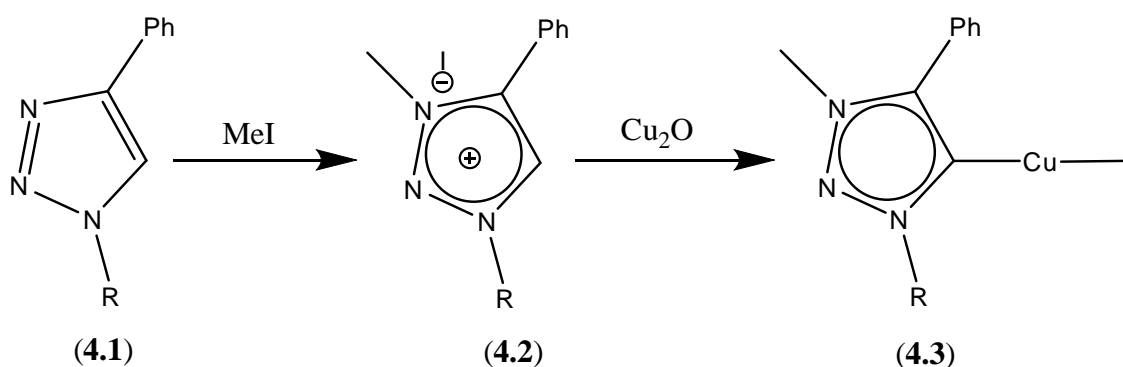
R = phenyl (**a**), mesitylene (**b**), propyl (**c**), hexyl (**d**).

Scheme 0.1: Direct synthesis of the Cu-*m*NHC complexes (4.3a-d) by reaction of triazoloium salts (**4.2a-d**) with Cu_2O.

For the synthesis of the Cu-*m*NHC complexes (**4.3**, Scheme 4.1), a method of Son and co-workers[24] was modified to suit the triazolium compounds reported herein. This methodology avoids the use of expensive and strong bases, tolerates the use of cheap starting materials and generates water as the only by-product whilst resulting in moderate conversions of the target products.[24, 25] Reaction of **4.2** with Cu_2O in dioxane led to the formation of analytically pure **4.3** complexes after workup. All complexes were isolated and characterized by ^1H and ^{13}C NMR spectroscopy, HRMS and EA, which all support formation of complexes of the type Cu-(*m*NHC)I. NMR spectroscopic analyses revealed the presence of only one triazolium moeity and complete loss of the low field triazolium proton resonance peaks and presence of low field resonance at 165-167 ppm strongly suggested the formation of copper(I)-*m*NHC complexes.[26] The high-resolution mass spectra were dominated by the Cu(*m*NHC)$^+$ molecular peaks and elemental analysis also strongly indicated the formation of targeted Cu(*m*NHC)I complexes in high bulk purity.

4.2.2 Stability studies

Although there is no doubt that *N*-heterocyclic carbenes (NHC) form strong bonds with transition metals, a number of reports have been published in the liturature describing decomposition/displacement of NHC ligands from the metal. In this work, attempts to crystallise **4.3** failed due to decomposition in solution to reform **4.2** and unidentified insoluble copper salts (*vide infra*). On this basis, a study of the stability and decomposition rate of **4.3** under different conditions was set up. Complex **4.3a** was used as representative for the study. In the solid state, complex **4.3a** was found to be air and moisture sensitive transforming completely into a green insoluble solid within a few minutes. Under a N_2 atmosphere however, no noticeable decomposition was observed, but, after 16 hr in the same atmosphere, slow demposition was perceived.
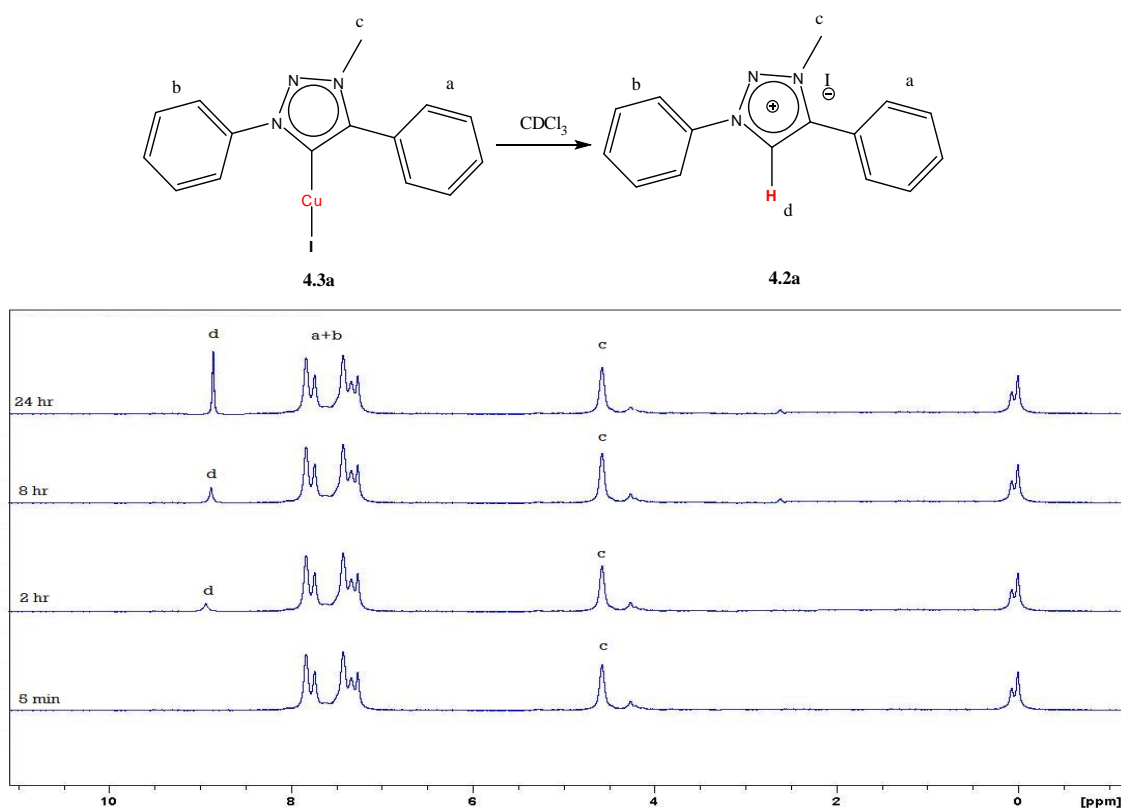

Figure 0.1: Time-dependent ^{1}H NMR spectral changes of **4.3a** in CDCl$_3$.
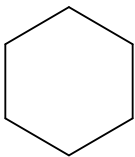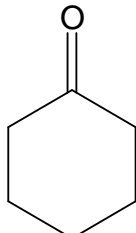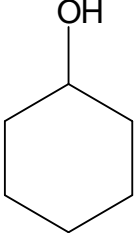
In solution, the decompotion of **4.3a** noticeably depends on the degree of solvent (CDCl$_3$) dryness and time in solution. A solution of compound **4.3a** in aqueous CDCl$_3$ discolored almost completely within a few minutes, indicating complete decomposition. Using pure and dry CDCl$_3$, a time-depedent study was set up, the result is shown in Figure 4.1. The progress of the decomposition was monitored by ^{1}H-NMR spectroscopy (by following the signal of the triazolium C-2 proton, marked *d* in Fig. 4.1). The data obtained showed strong-time dependence of the decomposition of **4.3a**, such that up to 2 hr in solution there was no much decomposition, however, after 8 hr, about 40% of **4.3a** was transformed back into **4.2a**, the starting triazolium salt. No signs of **4.3a** was observed after 24 hr, suggesting complete decomposition. This was also comfirmed by ^{13}C-NMR (loss of the low field resonance at 168 ppm).

4.2.3   Oxidation of cyclohexane

A preliminary attempt to isolate Cu-*m*NHC complexes and apply the molecular species as alkane oxidation catalysts was unsuccessful due to the decomposition of the complexes which led to the use of *in situ* catalytic methods. Hence, *in situ* generated Cu-*m*NHC complexes were evaluated as catalysts for oxidation catalysis. Initial trial studies were conducted with cyclohexane as the model substrate to optimise reaction conditions. Control experiments in the absence of Cu$_2$O (entry 1, Table 4.1), showed no signs of products observed and the use of Cu$_2$O revealed vigorous oxidation products (entry 2) within 4 hr suggesting the significance of the metal as the catalyst in the activation of cyclohexane. Reaction in the presence of both Cu$_2$O and **4.3a** (entry 3) under an inert atmosphere showed a colour change from colourless to bright yellow in solution and after the addition of the oxidant (H$_2$O$_2$) and the substrate, an instant change of the solution colour to light green was observed. Analysis of the crude solution showed formation of oxidation products at 27% substrate conversion which is much higher than for Cu$_2$O (12%) only. These results point to the direct influence of the triazolium ligand/Cu combination in the catalytic process. The extent of substrate conversion was slightly improved when the reaction temperature was increased to 80 °C, suggesting the positive effect of temperature in this catalytic reaction (entry 3). The study was limited to 80 °C due to

volatility of both the substrate and the solvent from the unpressurised reaction vessel. Increasing the amount of Cu$_2$O showed no positive effects to catalytic activity, however, a change in the overall ketone/alcohol (K/A) ratio with notable increase in ketone production was observed (entry 5). Similarly, increasing the amount of *m*NHC did positively impact the extent of catalytic activity.

Table 0.1: Oxidation of cyclohexane with *in situ* generated **4.3**.

Entry	Catalyst *m*NHC:Cu$_2$O	Temperature	Conversion (mol%)[b]	Selectivity (mol%)[c]	
				CyO	CyOH
1	1:0	50	-	-	-
2	0:1	50	12	85	15
3	1:1	50	27	39	61
4	1:1	80	31	32	68
5	1:2	80	34	48	52
6	2:1	80	31	28	72
7[d]	1:1.1	80	11	42	58
8[e]	1:1.1	80	14	39	61
9[f]	1:1.1	80	7	28	72
10[g]	1:1.1	80	21	47	53
11[h]	1:1.1	80	39	37	63
12[i]	1:1.1	80	38	39	61

[a]Reaction conditions (unless stated otherwise): Substrate (1.0 mol), **4.3a** (10 mmol, 1 mol % *vs.* substrate), H$_2$O$_2$ (10.0 mol), MeCN (5 mL)), indicated temperature, 12 hr; [b]Conversion = conc. products/ initial conc. of

cyclohexane x 100. [c]Selectivity = moles of CyO/(CyOH + CyO) x 100; [d]HCl added (1.0 mol); [e]Acetic acid added (1 mol); [f]TBHP used (instead of H_2O_2); [g]**4.3b**; [h]**4.3c** and [i]**4.3d**.

Based on the other *in situ* generated catalysts in the series (**4.3b-d,** entries 10-12 respectively), it was observed that due to steric reasons, complexes bearing bulky aromatic wingtip *N*-substituents **4.3a-b** afforded lower activities (31 and 21% conversions, entries 5 and 10 respectively) than those bearing aliphatic *N*-substituents respectively (39 and 38% conversions for **4.3c-d,** entries 11 and 12 respectively).

The addition of acids as promoters have been shown to improve substrate conversion in numerous oxidation reactions.[21, 27] However, in this study, addition of acids (entries 7 and 8) rather retarded the oxidation reaction with poor conversions. This may be due to catalyst decomposition in the acidic media. Only trace amounts of oxidation products were formed when t-BuOOH was used as the oxidant under the optimized conditions, an indication that it is not a suitable oxidant under the present catalytic reaction conditions.

To shed some light on the kinetic rates and mechanism of the oxidation reaction, a time-dependent study was conducted with the results presented in Figure 4.2. It is clear that the catalytic conversion of cyclohexane to products is time dependent with a significant induction period of 4-6 hr which is attributed to the *in situ* generation of active species.
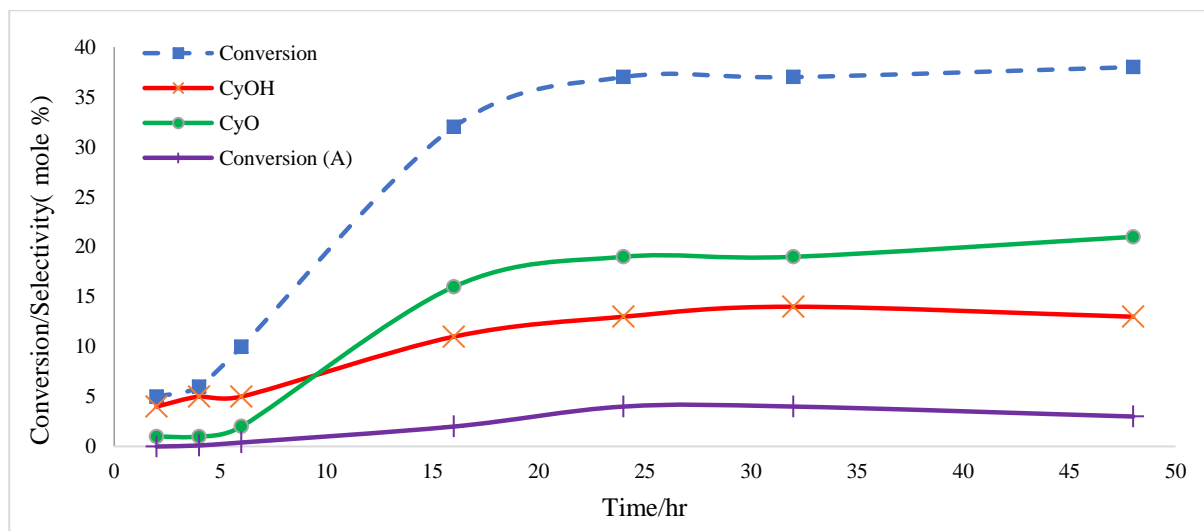
Figure 0.2: Effect of reaction time on cyclohexane oxidation with in situ generated **4.3a**. [■] Conversion; [●] selectivity to cyclohexanone; [×] selectivity to cyclohexanol; [+] conversion (A) when PH_2NH radical scavenger was added. Reaction conditions: Same as in Table 4.1.

The addition of a radical scavenger (diphenylamine, PH_2NH) in a stoichiometric amount relative to cyclohexane was observed to suppress the activity of the catalyst indicating the possible involvement of radical pathways in the mechanism of the oxidation reaction. On this basis coupled with NMR evidence of time dependent catalyst decomposition (Fig. 4.1), all the catalytic studies were conducted at 12 hr reaction time.

To put these results into context with closely related literature, comparative reports are summarized in Table 4.2. The group of Sawyer[22] reported good conversions up to 15% with $[Cu^I(bpy)_2]$/pyridine catalyst mixture which followed the very low conversions (up to 5%) obtained by Barton et al.[23] using combined Cu powder/pyridine/acetic acid catalyst mixture.

Table 0.2: Comparative representation of oxidation of cyclohexane by different [Cu] systems.[a]

Entry	Catalytic system	Conversion (mol %)	Reference
1[b]	$[Cu^I(bpy)_2]$/pyridine	15	[22]
2	Cu-powder/pyridine/Ac	5	[23]
3[c]	$([Cu_4(tea)\text{-}(BOH)_4(m\text{-}O)]^{2+})$	38	[28]
4[d]	Cu^I/TMPA	53	[29]
5[e]	Cu^I/(R,R)-BPBP	56	[29]
6	**4.3c**	39	This work

[a]All reactions were performed in MECN using H_2O_2 as an oxidant under mild reaction conditions. [b]bpy: 2,2'-bipyridine. [c]tea: trimethylamine. [d]TMPA: (tris(2-pyridylmethyl)amine). [e]BPBP: ((2R,2'R)-1,1'-bis(2-pyridylmethyl)-2,2'-bipyrrolidine).

Having observed steric influence of ancillary ligands in the oxidation of cyclohexane, Pombeiro and coworkers[28] reported efficient (conversions up to 38%) system using a tetranuclear Cu cluster (entry 3). Recently, Siegler et al.[29] reported a highly active and selective copper complex (entry 5) as catalysts for the mild peroxidative activation and functionalization of cyclohexane (conversions up to 56%) to the corresponding alcohol and ketone.

4.2.4 Oxidation of toluene

Toluene is a common aromatic hydrocarbon with multiple C-H bonds which may be activated and functionalised to variety of oxidation products. In many cases, benzaldehyde is the more desired product due to its importance to the fine chemicals and pharmaceutical industry as a building block. The oxidation of toluene is reported to suffer from low selectivity to the desired aldehyde due to the possibility for activation of both the methyl and/or aromatic C-H bonds depending on various reaction conditions (including type of catalyst, solvent, oxidant, etc.). The study with **4.3c** as catalyst for the catalytic oxidation of toluene resulted in a mixture of oxygenated products (total conversion up to 11 %) with benzaldehyde (PhCHO, 62 %) and benzyl alcohol (PhCH$_2$OH, 29%) as the main products and *o*/*m*/*p*-cresols as the minor products (Scheme 4.2). This selectivity pattern is in line with literature reports for similar studies.[30-32]
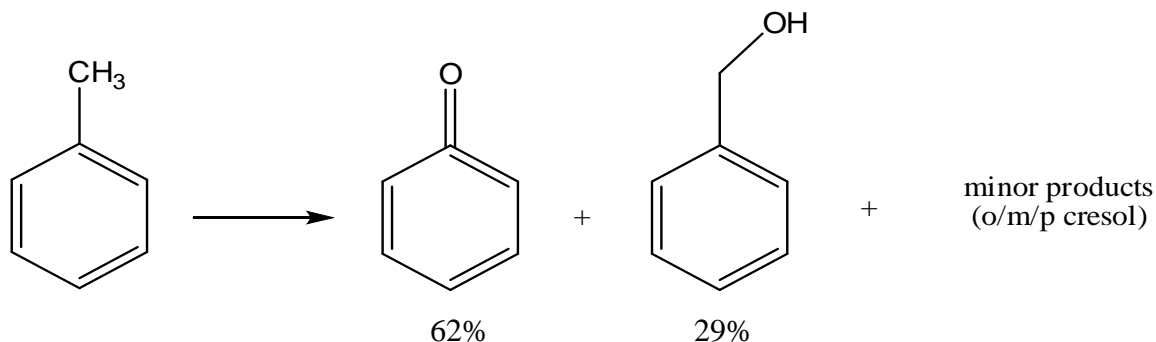
Scheme 0.2: Oxidation of toluene to oxygenated products with catalyst **4.3c**. Reaction conditions: same as in Table 4.1.

4.2.5 Oxidation of *n*-octane

Catalytic results based on **4.3c** as the catalyst produced circa 22% total conversion to a mixture C-8 products at position 1, 2, 3 and 4 of the *n*-octane chain (Figure 4.3). Regioselectivity indicated that internal carbons (especially C(2)) are more reactive than the terminal ones.

Similarly, the ketones dominated product distribution with 2-octanone (ca. 38%) as the most abundant. This is similar to observations in the literature indicating 2-octanone as the more probable product of *n*-octane oxidation.[33, 34]
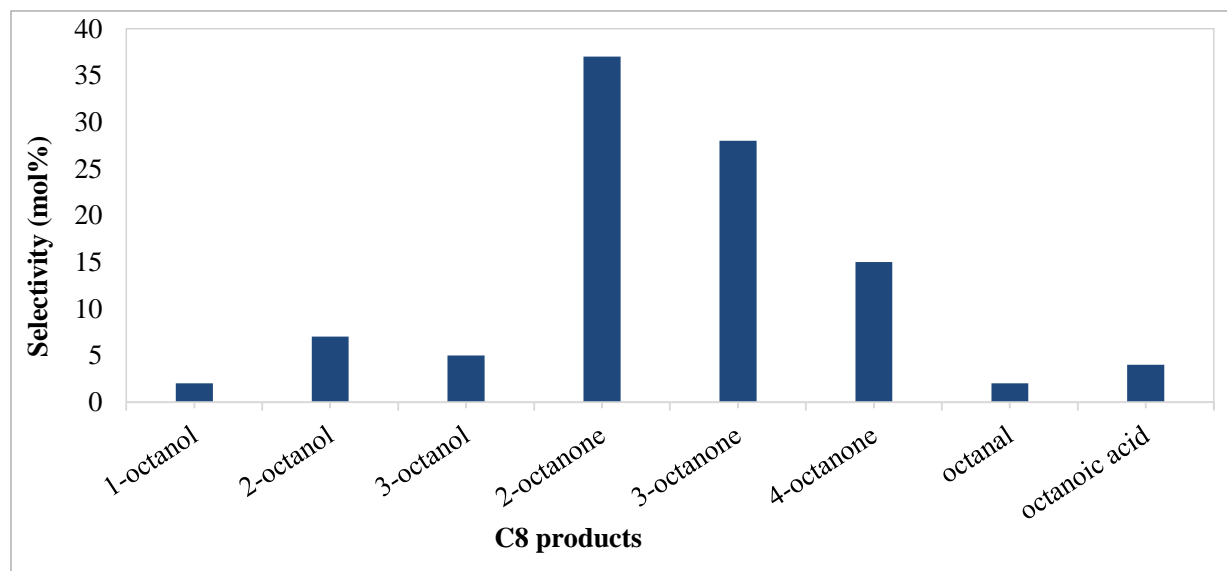
Figure 0.3: Product distribution in the oxidation with **4.3c**. Reaction conditions: same as in Table 4.1.

4.2.6   Mechanistic considerations

On the basis of all the experimental data presented herein, it is proposed that alkane oxidation reactions proceeded via the formation of alkyl hydroperoxo radicals. As was shown earlier, in the presence of diphenylamine as a radical scavenger, the rate of cyclohexane oxygenation was noticeably suppressed affirming that alkyl radicals may be involved in the oxidation process. This phenomenon has also been shown or demonstrated for related systems operating via the formation of hydroperoxo radicals.[35-38] Furthermore, in all the substrates tested, ketones/aldehyde(s) are the major products. This is consistent with reported observations, which concluded that over-oxidation of alcohol products led to the production of ketones/aldehydes as the final dominant products. This is due to the fact that the primary products (alcohols) are more susceptible to oxidation at a higher rate than the parent alkanes,

which normally leads to formation of the over-oxidised secondary products (ketones/aldehydes).[33]

4.3   Conclusion

In the present study, Cu-*m*NHC complexes were successfully synthesized and characterized using different methods including ^{1}H/^{13}C NMR, EA and HRMS. The catalytic properties of all the synthesized complexes were tested in the homogeneous oxidation of alkanes with low concentrations of *in situ* generated catalysts. The results showed that the Cu-*m*NHC complexes are capable of initiating the oxidation reactions. In all substrates tested, ketones/aldehyde were the dominant product groups with conversions depending on substrate and reaction conditions. The achieved selectivity parameters are comparable to those reported for other oxidation catalyst systems that proceeded via the formation hydroperoxyl radicals. The oxidation of toluene resulted in the preferential activation of the methyl group yielding benzaldehyde as the main product.

4.4   Experimental Section

Triazoles **4.1(a-d)** and their corresponding salts **4.2(a-d)** were synthesised as described in published literature and characterisation data consistent with the reported literature.[19-23]

4.4.1   General procedure for synthesis of 4.3(a-d)

Procedure for the synthesis of Cu-*m*NHC complexes[24]: triazolium salt (0.3 mmol) and Cu_2O (0.35 mmol) in 4 mL of dioxane were heated at 80 °C for 16 h. Then the reaction mixture was cooled to room temperature. The unreacted Cu_2O was removed by filtration, and the remaining solvent was evaporated to yield precipitates of the complex. Characterisation data are:

(**4.3a**) White solid product (0.41 g, 59%). ^{1}H-NMR (CDCl$_3$, 400 MHz): δ 7.19-7.65 (bm, 10H, Ar), 4.75 (s, 3H, N-CH$_3$), ^{13}C-NMR (CDCl$_3$, 400 MHz): δ 168.41, 148.54, 129.94, 129.77, 129.10, 128.76, 128.32, 126.89, 125.06, 121.06, 120.51, 117.63, 37.91. HRMS (ESI) m/z for

$C_{15}H_{13}CuN_3$ [M$^+$]: calculated: 298.040, found: 298.041. EA calculated ($C_{15}H_{13}CuIN_3$, 425.734): C, 42.32; H, 30.08; N, 9.87. Found: C, 42.33; H, 3.08; N, 9.88.

(**4.3b**) Greenish solid product (0.38 g, 48%). ^{1}H-NMR (CDCl$_3$, 400 MHz): δ 7.37-7.57 (m, 5H, Ar), 4.34 (s, 3H, N-CH$_3$), 2.47(bs, 9H, 3CH$_3$). ^{13}C-NMR (CDCl$_3$, 400 MHz): δ 166.55, 142.74, 131.94, 131.57, 130.58, 129.80, 129.66, 129.62, 129.37, 128.00, 121.93, 38.00, 22.36. HRMS (ESI) m/z for $C_{18}H_{19}CuN_3$ [M$^+$]: calculated: 340.08, found: 340.08. EA calculated ($C_{18}H_{19}CuIN_3$, 466.99): C, 46.21; H, 4.09; N, 8.98. Found: C, 46.21; H, 4.10; N, 9.00

(**4.3c**) Greenish solid product (0.53 g, 68%). ^{1}H-NMR (CDCl$_3$ 400 MHz): δ 7.28-7.47 (m, 5H, Ar), 4.75 (m, 2H, CH$_2$), 4.27 (s, 3H, N-CH$_3$), 1.90 (m, 2H, CH$_2$), 0.91 (t, 3H, CH$_3$). ^{13}C-NMR (CDCl$_3$, 400 MHz): δ 165.06, 143.33, 131.92, 130.90, 129.74, 129.66, 129.44, 121.8, 5386, 38.79, 27.45, 13.98. HRMS (ESI) m/z for $C_{12}H_{15}CuN_3$ [M$^+$]: calculated: 264.05, found: 264.13. EA calculated ($C_{12}H_{15}CuIN_3$, 390.96): C, 36.79; H, 3.86; N, 10.73. Found: C, 36.79; H, 3.87; N, 10.73

(**4.3d**) Greenish solid product (0.51 g, 53%). ^{1}H-NMR (CDCl$_3$ 400 MHz): δ 7.66-7.82 (m, 5H, Ar), 4.76 (m, 2H, CH$_2$), 4.34 (s, 3H, N-CH$_3$), 2.13 (m, 2H, CH$_2$) 1.40-1.51 (m, 6H, 3CH$_2$), 0.95 (t, 3H, CH$_3$). ^{13}C-NMR (CDCl$_3$, 400 MHz): δ 166.78, 144.65, 132.90, 130.84, 130.73, 130.02, 124.03, 55.38, 39.73, 32.31, 30.35, 27.03, 23.53, 14.47. HRMS (ESI) m/z for $C_{15}H_{21}CuN_3$ [M+2Li]: calculated: 320.135, found: 320.201. EA calculated ($C_{15}H_{21}CuIN_3$+CH$_3$CN, 474.85): C, 41.53; H, 4.88; N, 9.69. Found: C, 44.22; H, 5.33; N, 11.45

4.4.2 General procedure for the catalytic reactions

For each experiment, the catalytic study was prepared as follows: an appropriate amount of precursor salt **4.2(a–d)** was treated with a stoichiometric amount of Cu$_2$O in CH$_3$CN (5 mL) under indicated temperature and time. The substrate and oxidant were then added and the mixture was heated at the indicated temperature for the required time. Then the mixture was cooled and using GC (refer to chapter 2).

4.5   References

1.   L. Jr. Que and W. B. Tolman, *Nature*, 2008, 333-340.

2.   L. M. D. R. S. Martins and A. J. L. Pombeiro, *Coord. Chem. Rev.* , 2014, **265**, 74-88.

3.   M. Sutradhar, E. C. B. A. Alegria, M. F. C. Guedes da Silva, L. M. D. R. S. Martins and A. J. L. Pombeiro, *Molecules, 2016, 21, 425; doi:*, 2016, **21**, 425-435.

4.   H. V. R. Dias, H. L. Lu, H. J. Kim, S. A. Polach, T. Goh, R. G. Browning and C. J. Lovely, *Organometallics*, 2002, **21**, 1466-1473.

5.   A. G. Jarvis, A. C. Whitwood and I. J. S. Fairlamb, *Dalton Trans.* , 2011, **40**, 3695-3702.

6.   S. E. Allen, R. R. Walvoord, R. Padilla-Salinas and M. C. Kozlowski, *Chem Rev.*, 2013, **113**, 6234-6458.

7.   M. Delgado-Rebollo, D. Canseco-Gonzalez, M. Hollering, H. Mueller-Bunz and M. Albrecht, *Dalton Trans.*, 2014, **43**, 4462–4473.

8.   J. R. Wright, P. C. Young, N. T. Lucas, A.-L. Lee and J. D. Crowley, *Organometallics* 2013, **32**, 7065−7076.

9.   B. Karimi and D. Enders, *Org. Lett.*, 2006, **8**, 1237-1240.

10.   X. L. Hu, I. Castro-Rodriguez and K. J. Meyer, *Am. Chem. Soc.*, 2003, **125**, 12237-12245.

11.   J. D. Egbert, C. S. J. Cazin and S. P. Nolan, *Catal. Sci. Technol.*, 2013, **3**, 912-926.

12.   P. K. Fraser and S. Woodward, *Tetrahedron Lett.*, 2001, **42**, 2747–2749.

13.   F. Guillen, C. L. Winn and A. Alexakis, *Tetrahedron: Asymmetry*, 2001, **12**, 2083–2086.

14.   J. Pytkowicz, S. Roland and P. Mangeney, *Tetrahedron: Asymmetry*, 2001, **12**, 2087–2089.

15.   F. Gao, K. P. McGrath, Y. Lee and A. H. Hoveyda, *J. Am. Chem. Soc.*, 2010, **132**, 14315-14320.

16.   A. Guzman-Martinez and A. H. Hoveyda, *J. Am. Chem. Soc.*, 2010, **132**, 10634-10637.

17.   R. Shintani, K. Takatsu, M. Takeda and T. Hayashi, *Angew. Chem., Int. Ed.*, 2011, **50**.

18.   K.-S. Lee and A. H. Hoveyda, *J. Am. Chem. Soc.*, 2010, **132**.

19.   P. Li and L. Wang, *Lett. Org. Chem.*, 2007, **4**, 23-26.

20.   Z. Yacob, J. Shah, J. Leistner and J. Liebscher, *Synlett*, 2008, **15**, 2342–2344.

21.   D. Munz and T. Strassner, *Inorg. Chem.* , 2015, **54**, 5043–5052.

22.   A. Sobkowiak, A. Qui, X. Liu, A. Llobet and D. T. Sawyer, *J. Am. Chem. Soc.* , 1993, **115**, 609–614.

23.   D. H. R. Barton, D. Doller and Y. V. Geletii, *Mendeleev Commun.*, 1991, 115–116.

24.   J. Chun, H. S. Lee, G. Jung, S. W. Lee, H. J. Kim and S. U. Son, *Organometallics*, 2010, **29** 1518–1521.

25.   M. R. L. Furst and C. S. J. Cazin, *Chem. Commun.*, 2010, **46**, 6924–6925.

26.   J. Chun, H. S. Lee, I. G. Jung, S. W. Lee, H. J. Kim and S. U. Son, *Organometallics*, 2010, **29**, 1518.

27.   A. V. Astakhov, O. V. Khazipov, E. S. Degtyareva, V. N. Khrustalev, V. M. Chernyshev and V. P. Ananikov, *Organometallics*, 2015, **34**, 5759−5766.

28.   A. M. Kirillov, M. N. Kopylovich, M. V. Kirillova, E. Y. Karabach, M. Haukka, M. F. C. G. da Silva and A. J. L. Pombeiro, *Adv. Synth. Catal.* , 2006, **348**, 159–174.

29.   I. Garcia-Bosch and M. A. Siegler, *Angew. Chem.*, 2016, **128**, 13065 −13068.

30.   S. Saravanamurugan, M. Palanichamy and V. Murugesan, *Appl. Catal., A*, 2004, **273**, 143-149.

31.   G. Huang, J. Luo, C. Cai, Y. Guo and G. Luo, *Catal. Commun.*, 2008, **9**, 1882-1885.

32.   T.C.O. Mac Leod, M.V. Kirillova, A.J.L. Pombeiro, M.A. Schiavon and M. D. Assis, *Appl. Catal.,* 2010, **372** 191–198.

33.   S. G. Mncube and M. D. Bala, *J. Mol. Liq.*, 2016, **215**, 396–401.

34.   L. Soobramoney, M.D. Bala and H. B. Friedrich, *Dalton Trans.*, 2014, **43**, 15968–15978.

35.   Q. Zhu, Y. Lian, S. Thyagarajan, S. E. Rokita, K. D. Karlin and N. V. Blough, *J. Am. Chem. Soc.* , 2008, **130**, 6304–6305.

36.   K. L. Ciesienski, K. L. Haas, M. G. Dickens, Y. T. Tesema and K. J. Franz, *J. Am. Chem. Soc.*, 2008, **130**, 12246–12247.

37.   G. B. Shul'pin, R. S. Drago and M. Gonzalez, *Russ. Chem. Bull.*, 1996, **45**, 2386–2388.

38.   Y. N. Kozlov, G. V. Nizova and G. B. Shul'pin, *J. Mol. Catal. A: Chem.* , 2005, **227**, 247–253.

39.   G. B. Shul'pin, *J. Mol. Catal. A: Chem.*, 2002, **189**, 39–66.

CHAPTER 5

Selective alkane oxidation catalyzed by piano-stool iron-triazolylidene complexes

5.1 General introduction

The catalytic efficiency of first row transition metals is well studied and documented.[1-4] Among those, Fe-based catalyst systems have attracted attention due to the fact that they are readily available, cheap, non-toxic and possess exceptional synthetic flexibility compared to other transition metal catalytic systems.[5] Oxidation chemistry is undoubtedly one of the most significant areas to benefit from iron-based catalysis because Fe has been reported to show to be productive for C−H bond activation under mild reaction conditions.[6-9] The earliest example of Fe-based complex as a catalyst for C-H activation was reported a century back.[6] Although C-H activation is currently dominated by late transition metals (Rh, Ru, Pd), the number of encouraging examples using iron is growing.[10, 11]

N-heterocyclic carbenes (NHC) as auxiliary ligands have advanced significantly in organometallic chemistry and catalysis. The first example of an NHC containing piano-stool iron complex was reported by Lappert and Pye in 1977.[12] Since then, a number of synthetic routes towards this sub-class of iron complexes have been reported. Regardless of recent remarkable progresses of iron piano-stool NHC complexes in homogeneous catalysis,[13] these complexes are still under reported and rare. It is important to note that some of the catalytic applications of NHC piano-stool Fe complexes that include dehydration of primary amides[14], transfer hydrogenation[15] and hydrosilylation[16]. Hence, in this chapter, the chemistry and catalytic application of a series of piano-stool iron-triazolylidene complexes for oxidation reactions is presented.

5.2 Results and discussion

5.2.1 Synthesis of triazolylidenes iron complexes

In this work, the method reported by Guerchais and co-workers was followed for the synthesis of triazolylidenes iron piano-stool complexes.[17] The *in situ* reaction of the ligand precursor salts **5.1** (Scheme 5.1), with two equivalents of a base KOtBu at a low temperature (-50 °C), followed by the addition of CpFe(CO)$_2$I afforded the target complexes (**5.2**) in high yields after workup. All the complexes are stable in the solid state and may be handled in air without decomposition.

a : R= Phenyl   c : R= Propyl

b : R= Benzyl   d : R= Hexyl
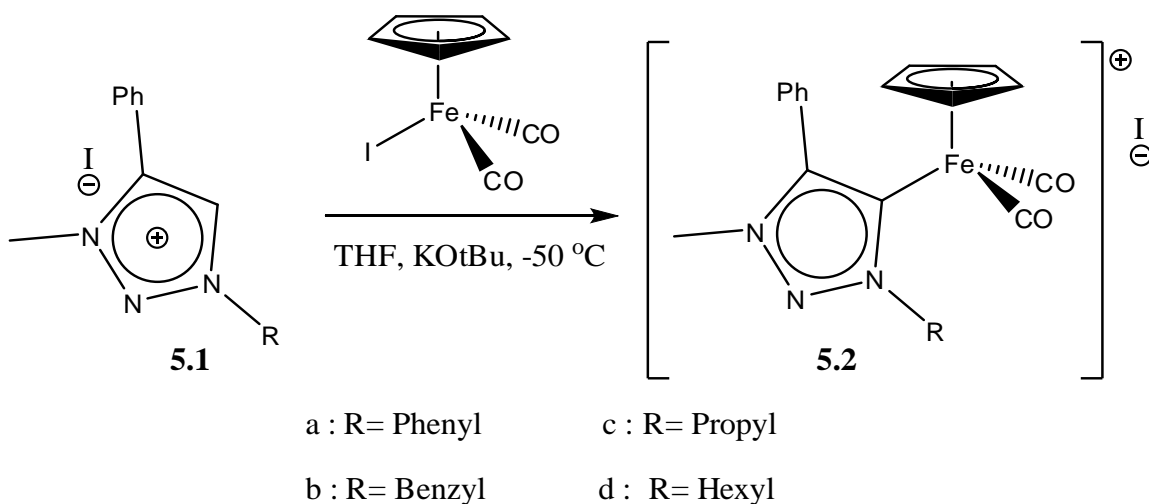
Scheme 5.1: Synthesis of complexes **5.2** using the free carbene route.

Full characterization using ^{1}H,^{13}C NMR, MS and EA all supported formation of the complexes as proposed (**5.1**, Scheme 5.1). In the ^{1}H-NMR data, the disappearance of the characteristic low field triazolium C-2 proton resonance at δ_H 8.8±0.5 ppm, in combination with appearance of low field resonance at δ_C 173±2 ppm in the ^{13}C-NMR data confirmed coordination of the triazolylidene ligand moiety to the metal center. The appearance of Cp protons which resonate at δ_H 4.7±1.5 ppm as a singlet in the ^{1}H-NMR spectra of all the complexes as supported by the resonances at δ_C 88.5 ±2 ppm corresponding to the Cp carbon atoms confirm the formation of

complexes **5.2**. These resonances appeared in the same range as for reported related iron piano-stool NHC complexes.[16, 19].

5.2.2 Oxidation of cyclohexane with varying amounts of catalyst 5.2a.

The catalytic activity of **5.2(a-d)** was evaluated for the oxidation of alkanes with H_2O_2 as oxidant in acetonitrile solutions. For the optimization study, cyclohexane and **5.2a** were used as model substrate and catalyst respectively. The influence of various reaction conditions including the relative amounts of catalyst, oxidant, reaction temperature and reaction time on the catalytic activity were all investigated in a systematic way.

The influence of catalyst concentration on the oxidation of cyclohexane was first investigated and the results are presented in Figure 5.1. The blank experiments confirmed that no products were obtained unless the catalyst **5.2a** was added, indicating that H_2O_2 autoxidation of the substrate in the absence of the catalyst was not possible.
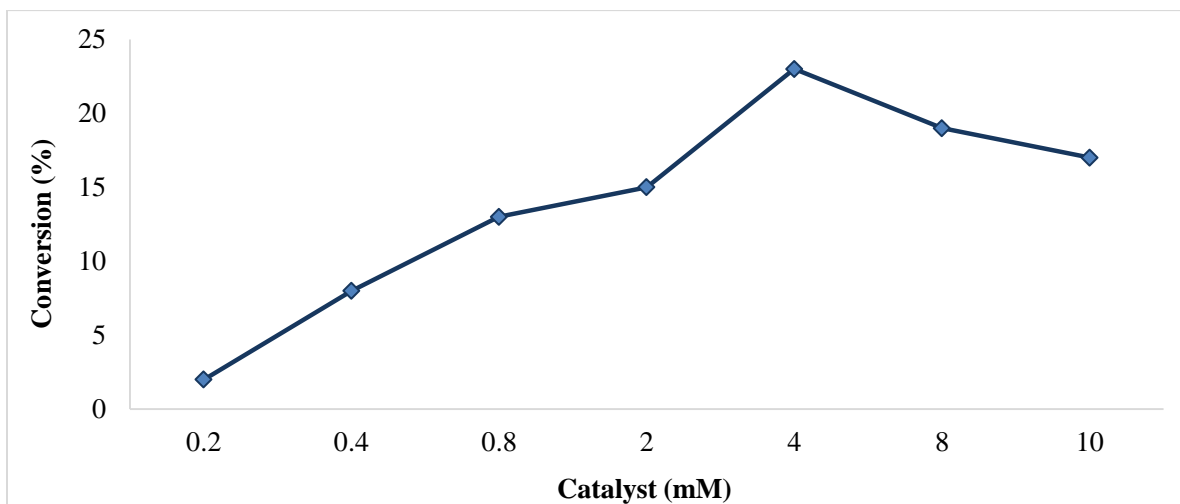

Figure 5.1: Influence of catalyst concentration on the oxidation of cyclohexane with complex **5.2a**. Conditions for all reactions: solvent (MeCN) = total vol. 5 mL; cyclohexane = 0.38 M; oxidant (H_2O_2) =20 M equivalent; catalyst = indicated conc.; 80 °C; 24 hr.

A distinct increase in the conversion of cyclohexane was observed when the amount of catalyst was gradually increased to a maximum of 4 mM concentration. Thus, 4 mM was used as the optimum catalyst concentration for all the catalytic reactions.

5.2.3 Effect of reaction temperature

Reaction temperature has been found to be a key influencer of paraffin oxidation reactions. Hence, in this work, the influence of temperature was investigated and the results are summarized in Figure 5.2. The results showed increase in cyclohexane conversion with increase in reaction temperature up to 60 °C. Probably due to decomposition of H_2O_2 at higher temperatures the conversion was seen to decrease beyond 60 °C, consequently, it was adopted as the optimum temperature for this study.
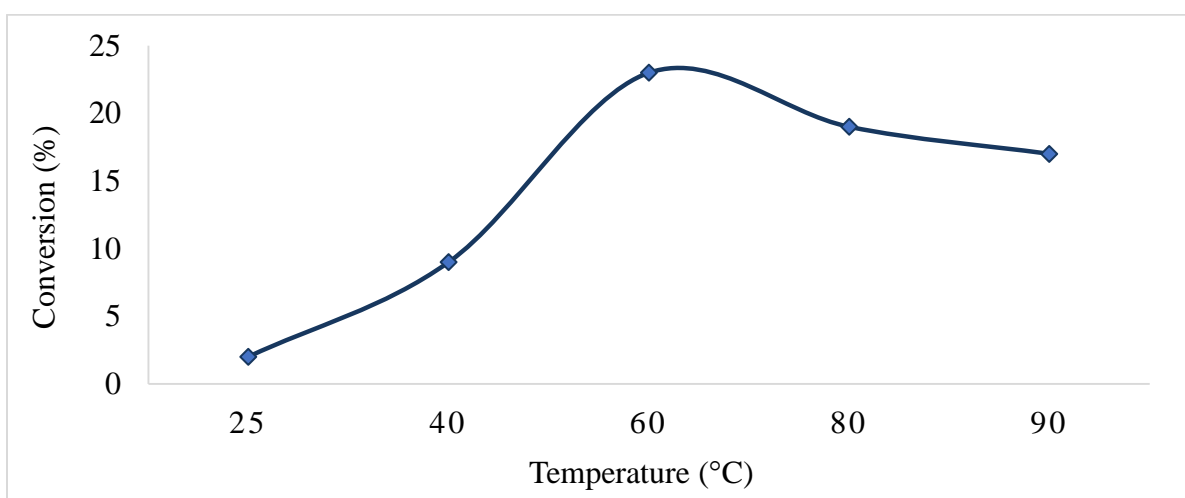

Figure 5.2: Influence of reaction temperature on the oxidation of cyclohexane with complex **5.2a**. Conditions for all reactions: solvent (MeCN) = total vol. 5 mL; cyclohexane = 0.38 M; oxidant (H_2O_2) =20 M equivalent; catalyst = 4 mM; indicated temperature; 24 hr.

5.2.4 Influence of reaction time

The reaction was carried out at different periods (2, 6, 18, 24 and 48 hr). The results followed an established trend of direct dependence of conversion on temperature up till a maxima at 18 hr. Beyond the 18hr reaction time, a slight decrease in the conversion of cyclohexane was observed. This trend is generally due to the activation period (during the first few hours) required for the formation of active catalytic species and intermediates which are later converted to the products. Product selectivity to the ketone product also increased with time, this is due to the further reaction of the alcohol products over time. Hence, 18 hr reaction time was adopted as the optimum for this study

5.2.5 Effect of oxidant concentration

Optimization of the substrate to oxidant ratio was investigated by varying the cyclohexane to H_2O_2 ratios of 1:5; 1:10, 1:15; 1:20 and 1:25. The results indicated an increase in substrate conversion as the ratio increased from 1:5 to 1:15, which was also accompanied by an increase in cyclohexanone production. This can be due to the fact that higher concentrations of the oxidant H_2O_2 led to over oxidation of the alcohol product yielding more ketone. Further increase in H_2O_2 concentration resulted in complete consumption of the cyclohexanol and appearance of unidentified side products.

5.2.6 Utilization of complexes 5.2a-d under the optimized conditions

The piano-stool Fe-NHC complexes were utilized for the catalytic oxidation of cyclohexane under the conditions and the results are presented in Table 5.1. Based on the various generated catalysts (**5.2a-d,** entries 1-4 respectively), it was observed that the complexes bearing aromatic wingtip *N*-substituents **5.2a-b** afforded higher conversions (23 and 20% respectively) and also higher selectivities (85 and 83%, entries 5 and 10 respectively) to the ketone when compared to 16 and 12% respectively for **5.2c-d** bearing aliphatic *N*-substituents.

Table 5.1: Oxidation of cyclohexane using catalysts **5.2a-d**.[a]

Entry	Catalyst	Conversion %	Selectivity %		
			Cyclohexanone	Cyclohexanol	K/A
1	**5.2a**	23	85	15	5.7
2	**5.2b**	20	83	17	4.9
3	**5.2c**	16	61	39	1.6
4	**5.2d**	12	75	25	3.0

[a]Conditions for all reactions: solvent (MeCN) = total vol. 5 mL; cyclohexane = 0.38 M; oxidant (H_2O_2) =15 M equivalent; catalyst = 4 mM ; 60 °C; 18 hr.

5.2.7 Oxidation of *n*-octane

The oxidation of *n*-octane with H_2O_2 as oxidant in the presence of the catalyst **5.2a** led to a mixture of isomeric C8 oxidation products oxidized at positions 2, 3 and 4 of the *n*-octane chain (Fig. 5.3). No terminal CH_3 oxidation products were detected under the reaction conditions. A total conversion of 23% was obtained with 4-octanone dominating the products distribution.
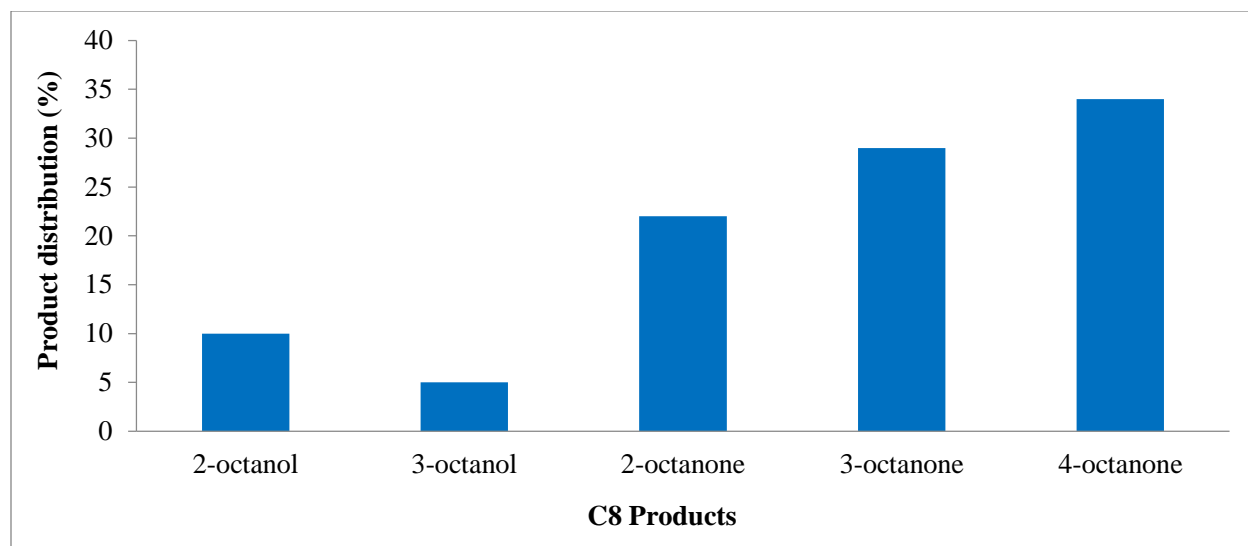

Figure 5.3: Product distribution in the oxidation of *n*-octane with complex 5.2a. Conditions for all reactions: solvent (MeCN) = total vol. 5 mL; cyclohexane = 0.38 M; oxidant (H_2O_2) =15 M equivalent; catalyst = 4 mM; 60 °C; 18 hr.

This is reflected by the regioselectivity parameter C(2):C(3):C(4)= 1.0:1.1:1.2. These values are different to those previously observed[20, 21] for the oxidation of *n*-octane, but a similar reactivity (with preferable oxidation at the position 4 on hydrocarbon chain) has also been observed in the literature as well.[22, 23] It is proposed that the linear hydrocarbon chain exists in varying conformations in solution; in this particular instance the position 4 of *n*-octane was found to be relatively more accessible for oxidation along the *n*-octane chain.

5.3   Conclusion

In the present study, piano-stool Fe-*m*NHC complexes were successfully synthesized and characterized by spectroscopic methods. The catalytic properties of all the synthesized complexes were tested in the homogeneous oxidation of cyclic and linear alkanes with low concentrations of catalysts **5.2a-d**. Amongst them, for the oxidation of cyclohexane, catalyst **5.2a** gave highest catalytic performance with overall conversion of 23% and high selectivity of 85% to the ketone under optimized reaction conditions. For the oxidation of a linear hydrocarbon (*n*-octane) by catalyst **5.2a**, hydrogens at the C-4 position 4 of the *n*-octane chain appeared to be the more accessible, thus preferably oxygenated. No products of terminal CH_3 activation were detected.

5.4   Experimental

5.4.1   General procedure for synthesis of 5.2a-d

The reported method[17] was modified. A mixture of **5.1** (1 mol) and t-BuOK (2 mol) in THF (20 mL) was stirred for 30 min at −50 °C. The mixture was gradually warmed to room temperature and a solution of [CpFe(CO)$_2$(I)] (1 mol in 5 ml THF) was added and the resulting solution was stirred overnight. The resulting solution was evaporated until dryness washed with hexane, then the residue was extracted with hot toluene (20 mL). The extract was evaporated under reduced pressure to afford **5.2**.

(**5.2a**) Yield: 0.63 g (**69**%) of light pink solid. ^{1}H-NMR (CDCl$_3$, 400 MHz): δ 7.36-7.66 (bm, 10H, 2Ar), 4.71 (s, 5H, Cp), 4.01 (s, 3H, N-CH$_3$), ^{13}C-NMR (CDCl$_3$, 400 MHz): δ 211.70, 176.20, 130.39, 129.64, 129.45, 129.11, 128.79, 128.55, 126.98. EA calculated for (C$_{22}$H$_{18}$FeIN$_3$O$_2$, 539.15): C, 49.01; H, 3.37; N, 7.79. Found: C, 49.12; H, 3.43; N, 7.88.

(**5.2b**) Yield: 0.59 g (**71** %) of red solid. ^{1}H-NMR (CDCl$_3$, 400 MHz): δ 7.52-7.12 (m, 10H, 2Ar), 5.85 (b, 2H, N-CH$_2$-), 4.89 (s, 5H, Cp), 4.1 (s, 3H, N-CH$_3$). ^{13}C-NMR (CDCl$_3$, 400 MHz): δ 213.73, 1776.20, 130.39, 129.64, 129.45, 129.11, 128.79, 128.55, 126.96, 88.56, 35.51. EA calculated for (C$_{23}$H$_{20}$FeIN$_3$O$_2$, 553.17): C, 49.94; H, 3.64; N, 7.60. Found: C, 50.03; H, 3.57; N, 7.71.

(**5.2c**) Yield: 0.72 g (**67**%) of red solid. ^{1}H-NMR (CDCl$_3$, 400 MHz): δ 7.52-7.69 (m, 5H, Ar), 4.72 (b, 2H, N-CH$_2$-), 4.42 (s, 5H, Cp), 3.95 (s, 3H, N-CH$_3$), 2.07 (b, 2H, -CH$_2$-), 1.60 (b, 3H, -CH$_3$). ^{13}C-NMR (CDCl$_3$, 400 MHz): δ 212.74, 173.76, 148.14, 138,08, 132.96, 128.06, 125.69, 88.56, 54.23, 43.43, 41.76, 35.52, 15.61. EA calculated for (C$_{19}$H$_{20}$FeIN$_3$O$_2$, 505.13): C, 45.183; H, 3.99; N, 8.32. Found: C, 45.12; H, 4.10; N, 8.35.

(**5.2d**) Yield: 0.72 g (**67**%) of red solid. ^{1}H-NMR (CDCl$_3$, 400 MHz): δ 7.41-7.79 (m, 5H, Ar), 5.05 (b, 2H, N-CH$_2$-), 4.78 (s, 5H, Cp), 4.08 (s, 3H, N-CH$_3$), 2.65-2.76 (b, 4H, 2(-CH$_2$-)), 1.82 (b, 2H, N-CH$_2$-), 1.48 (b, 3H, -CH$_3$). ^{13}C-NMR (CDCl$_3$, 400 MHz): δ 215.09, 172.42, 142.99, 132.00, 131.63, 129.99, 129.76, 129.31, 121.80, 87.02, 54.76, 39.30, 31.01, 29.45, 25.90, 22.36, 13.94. (C$_{22}$H$_{26}$FeIN$_3$O$_2$, 547.21): C, 48.29; H, 4.99; N, 7.68. Found: C, 48.37; H, 5.04; N, 7.77.

5.4.2 Oxidation reactions of alkanes with compounds 5.2a-d as catalysts

A typical procedure for oxidation of alkanes was carried as followed; under nitrogen atmosphere , the catalyst (as indicated) and substrate were added into dry MECN (15 mL) in a 3-neck round bottom flask fitted with an efficient reflux condenser and aqueous solution of H$_2$O$_2$ (as indicated) was added and stirred vigorously at the indicated temperature and duration time. The product was analysed by GC (refer to Chapter 2) after the required time period.

5.5   References

1.   T. W. Lyons and M. S. Sanford, *Chem. Rev.* , 2010, **110**, 1147–1169.

2.   I. A. I. M. Khalid, J. H. Barnard, T. B. Marder, J. M. Murphy and J. F. Hartwig, *Chem. Rev.* 2010, **110**, 890–931.

3.   D. A. Colby, R. G. Bergman and J. A. Ellman, *Chem. Rev.* 2009, **110**, 624–655.

4.   K. Godula and D. Samaes, *Science*, 2006, **312**, 67–72.

5.   J. Yamaguchi, K. Muto and K. Itami, *Eur. J. Org. Chem.*, 2013, 19–30.

6.   H. S. H. Fenton, *J. Chem. Soc.,Trans.*, 1894, **65**, 899-910.

7.   A. Fürstner, *ACS Cent. Sci.*, 2016, **2**, 778–789.

8.   A. Studer and D. Curran, *Angew. Chem., Int. Ed.* , 2016, **55**, 58−102.

9.   U. Jahn, *Top. Curr. Chem. Commum.*, 2011, **320**, 191−322.

10.   B. M. Monks, E. R. Fruchey and S. P. Cook, *Angew. Chem., Int. Ed.* , 2014, **53**, 11065−11069.

11.   G. Cera, T. Haven and L. Ackermann, *Angew. Chem., Int. Ed.* , 2016, **55**, 1484−1488.

12.   M. F. Lappert and P. L. Pye, *J. Chem. Soc., Dalton Trans.* , 1977, 2172–2180.

13.   C. Johnson and M. Albrecht, *Coord. Chem. Rev.*, 2017, **352**, 1–14.

14.   H. M. J. Wang and I. J. B. Lin, *Organometallics*, 1998, **17**, 972–975.

15.   D. Schweinfurth, S. Strobel and B. Sarkar, *Inorg. Chim. Acta.* , 2011, **374**, 253−260.

16.   W. A. Herrmann, M. Elison, J. Fischer, C. Köcher and G. R. J. Artus, *Angew. Chem., Int. Ed. Engl.*, 1995, **34**, 2371–2374.

17.   P. Buchgraber, L. Toupet and V. Guerchais, *Organometallics*, 2003, **2**, 5144–5147.

18.   T. M. Trnka, J. P. Morgan, M. S. Sanford, T. E. Wilhelm, M. Scholl, T.-L. Choi, S. Ding, M. W. Day and R. H. Grubbs, *J. Am. Chem. Soc.*, 2003, **125**, 2546-2558.

19.   C. Johnson and M. Albrecht, *Organometallics*, 2017, **36**, 2902–2913.

20.   S. G. Mncube and M. D. Bala, *J. Mol. Liq.*, 2016, **215**, 396–401.

21.   L. Soobramoney, M. D. Bala and H. B. Friedrich, *Dalton Trans.*, 2014, **43**, 15968–15978..

22.   T. C. O. Mac Leod, M. V. Kirillova, A. J. L. Pombeiro, M. A. Schiavon and M. D. Assis, *Applied Catalysis A: General* 2010, **372** 191–198.

23.   B. K. Keitz, J. Bouffard, G. Bertrand and R. H. Grubbs, *J. Am. Chem. Soc.*, 2011, **133**, 8498-8501.

CHAPTER 6

## Trihalide-based 1,2,3-triazolium ionic liquid:

Synthesis, X-ray crystallography and DFT studies

6.1   General introduction

The use of ionic liquids (IL) in catalysis required a great deal of consideration because of their excellent properties particularly for the stabilization of catalysts in the IL that takes into consideration reusing catalyst/solvent systems.[1, 2] Single-crystal X-ray diffraction studies,[3, 4] IR and fluorescence spectroscopic studies [5, 6] and computer simulation studies[7, 8] have been used with a view to understanding the structural and dynamic properties of room temperature ionic liquids (RTILs). In terms of applications of RTILs, we have detailed a first utilization of first row metal salts in triazolium IL systems as recyclable catalysts for the oxidation of alkanes with H_2O_2 as to yield oxygenated products in a biphasic system.[1] Studies of the interactions at molecular level between ions are important for the understanding of physical and chemical properties of RTILs. Hence, in this short chapter, SCXRD and DFT studies have been applied to a triazolium based RTIL.

6.2   Results and discussion

In an attempt to apply the free carbene route towards the synthesis of Cu-NHC complexes reported earlier (Chapter 4), compound **6.2** was isolated (Scheme 6.1). A similar compound has been reported in the literature obtained via the reaction of a chiral imidazolium carbene silver(I) complex with CuX_2 resulting in the formation of a haloimidazolium salt.[9, 10] Full characterization using NMR , Ms and EA supported formation of the proposed product (**6.2**). NMR spectroscopy displayed complete loss of the low field triazolium proton resonance and appearance of a low field resonance at 207.1 ppm for the C-Br bond which strongly supported formation of **6.2**. Furthermore, HRMS data confirmed formation of compound **6.2** as [**6.2**] – IBr_2^- ($C_{17}H_{25}BrN_3$) at m/z 350.147.
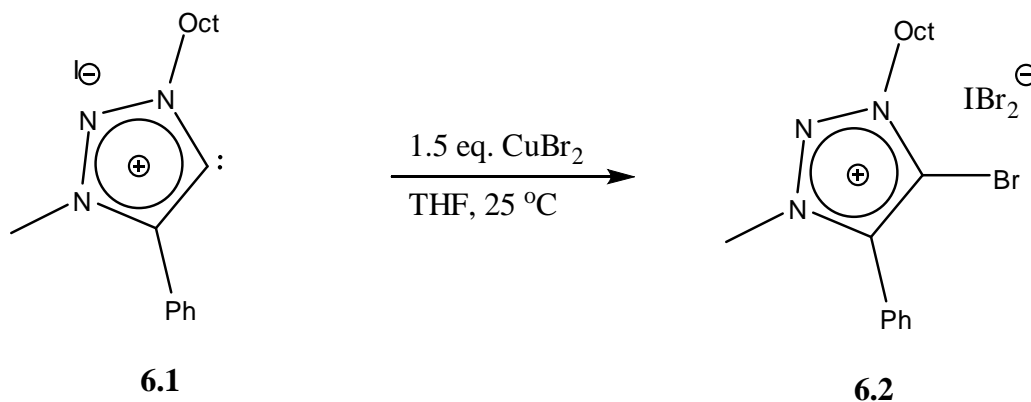
Scheme 0.1: Synthesis of **6.2**.

6.2.1 Crystal structure determination

The asymmetric unit of **6.2** consists of a cationic bromido-1,2,3-triazolium specie and a dibromoiodate anion as depicted in Figure 6.1. The five-membered triazolium ring and the phenyl ring are not co-planar as shown by a torsion angle of 1274(7)° for the adjoining C11-C12-C13-C14 carbon atoms.
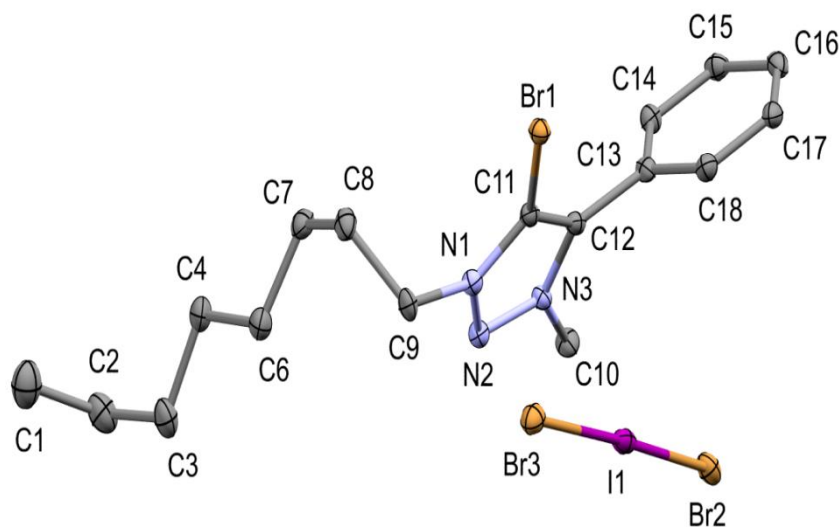

Figure 0.1: ORTEP diagram of the molecular structure of **6.1** drawn at the 50% thermal ellipsoid probability level. All hydrogen atoms were omitted for clarity.

Furthermore, the triazolium ring has equal N1-N2 and N2-N3 bond distances of 1.320 Å which suggests that π electrons are delocalized across the three nitrogen atoms. This feature appears to be typical for closely related halo-1,2,3-triazolium compounds.[11, 12] On the other hand, the dibromoiodate anion adopted a geometry that is almost linear with normal Br2-I1-Br3 bond angle of 177.74(1)° and I1-Br2 and I1-Br3 distances of 2.6855(4) Å and 2.7571(4) Å, respectively.[13-18]
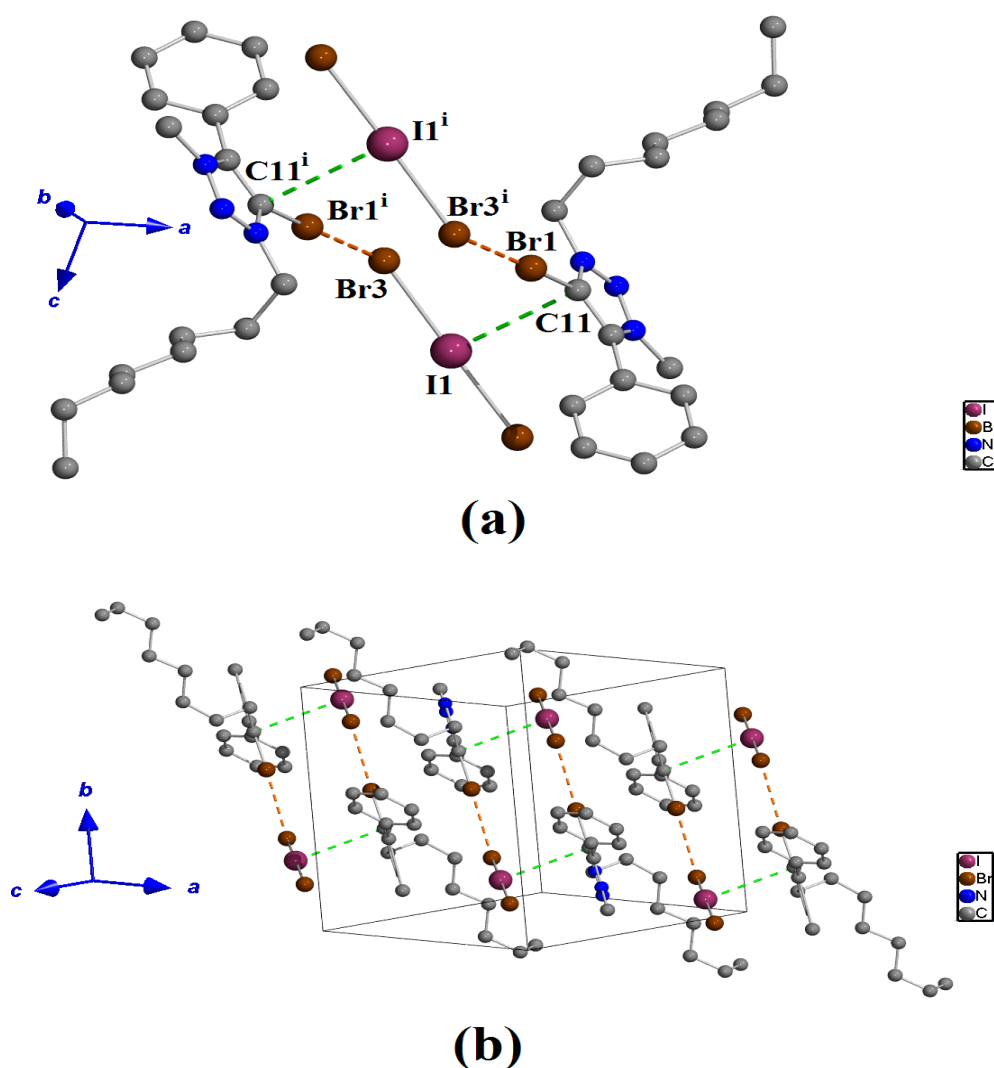

(a)

(b)

Figure 0.2: Intermolecular Br⋯Br (dashed orange lines) halogen bonding patterns and C⋯I interactions (dashed green lines) observed (a) between neighbouring molecular units and (b) in

the crystal packing of I (Symmetry code: (i) = 1-*x*, 1-*y*, 1-*z*). All hydrogen atoms were omitted for clarity.

Intermolecular Br…Br halogen bonds exist between the bromine atom of the triazolium moiety and the dibromoiodate counter anion (Figure 6.2a) with a Br…Br distance of 3.3181(5) Å which is shorter than the sum of their van der Vaal's radii of 3.70 Å.[19] and the C—Br1…Br3 angle is 176.3(1)°. The central iodine atom of the dibromoiodate anion appears to interact with C11 of the triazolium ring as shown in Figure 6.2a, with C11…I1 distance of 3.646(4) Å.[20] This C11…I interaction is almost orthogonal to the Br…Br halogen bond with a C11…I1—Br3 angle of 86.86(6)°. The Br…Br and C…I intermolecular interactions form ring-like patterns that link together four molecular units as shown in Figure 6.2b.

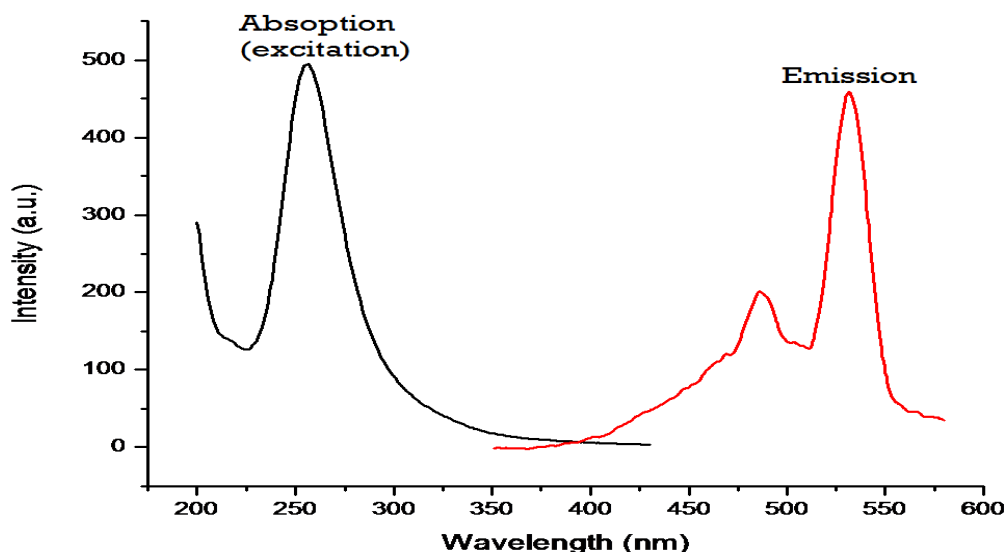### 6.2.2   Fluorescence behavior of compound 6.2

Figure 0.3: Normalised absorption and emission spectra of compound **6.2**.

Ultraviolet-visible spectroscopy was used to determine the normalised absorption and emission spectra of **6.2** in acetonitrile which is presented in Figure 6.3. It is characterised by an absorption

peak maxima at ~254 nm. An analysis of the molar absorption coefficient ($\log_\varepsilon$) indicates that a peak at about 254 nm may be attributed to the $\pi \rightarrow \pi*$ transition of the triazolium moiety. After the excitation of **6.2** at 254 nm, a two-shoulder emission spectrum was detected composed of a short-wavelength band around 485 nm and a long-wavelength band around 531 nm. The two shoulder emission spectrum is because of the presence of two energetically different however related species in solution. Although it is not very common, this kind of fluorescence behaviour has previously been observed for RTILs.[21]

6.2.3   DFT studies

Optimized geometric structures for **6.2** depicting graphical images of its HOMO-LUMO frontier orbitals is presented in Fig. 6.4. The calculated geometric structures (and data) were were observed to be in great concurrence with the determined crystallographic data. Similarly, the optimized geometric structures and NMR data are in fairly good agreement with experimental data. Interestingly, the dibromoiodate counter anion molecular orbital is the principal contributor (96.6%) to both the HOMO and LUMO electron density map. The alkyl chain does not make significant contributions to the HOMO and LUMO.
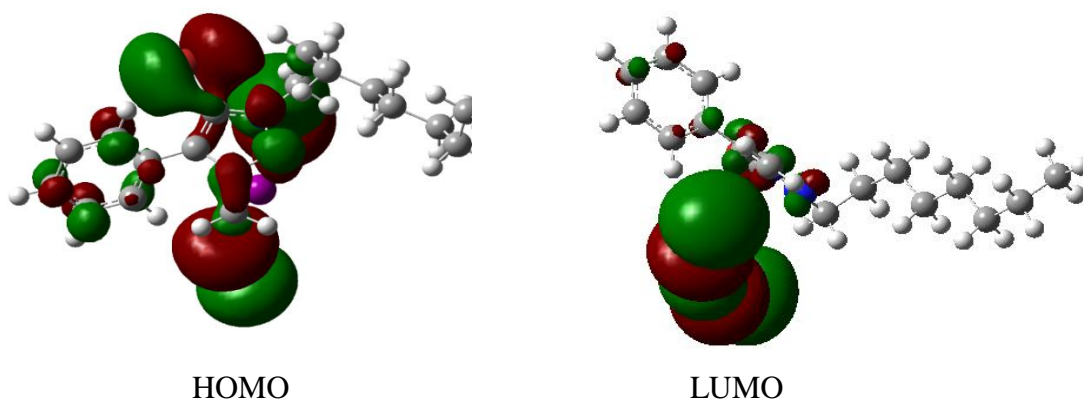

HOMO   LUMO

Figure 0.4: Graphical images of the frontier HOMO-LUMO orbitals and spin density electron distributions of **6.2**.

6.3   Conclusion

The synthesis of new 2-bromo-1,2,3-triazolium dibromoiodate ionic salt (**6.2**) is reported. It was isolated in an attempt to synthesize a copper *N*-heterocyclic carbene complex from the ligand (**6.1**). Full characterization of **6.2** using several procedures, including NMR spectroscopy, single crystal X-ray diffraction, MS, and EA is reported. The dibromoiodate anion adopted a "linear" geometry with intermolecular Br…Br halogen bonds between bromine atoms of the triazolium and dibromoiodate moieties. Furthermore, **6.2** showed interesting fluorescence behavior; $\pi \rightarrow \pi*$ transition from the triazolium moiety and the counter anion dominated the electron density map by DFT studies.

6.4   Experimental

6.4.1   Synthesis and crystallization of 6.2

To a solution of **6.1** (0.42 g, 1.55 mmol) in THF (10 mL) equipped with magnetic stirrer, $CuBr_2$ (0.520 g, 1.5 eq.) and TEA (0.21 mL, 1eq) was added. The mixture was stirred for 24 h. After the reaction, all volatile components were removed under reduced pressure and the crude was washed several times with Et_2O. Single crystals suitable for X-ray analysis were obtained from a dichloromethane/hexane solution (6 mL, 1:2). Yield: 0.102 g (**62** %) of red crystals. Mp: 89-91 °C. ^{1}H NMR ($CDCl_3$, 400 MHz): δ 0.89 (t, 3H, CH_3), 1.30-1.31 (m, 10H, $5CH_2$), 1.58 (m, 2H, CH_2), 4.36 (s, 3H, CH_3), 4.71 (m, 2H, CH_2), 7.66-7.73 (m, 5H, Ar). ^{13}C{^{1}H} NMR ($CDCl_3$, 400 MHz): δ 207.1, 142.9, 132.7, 130.1, 130.0, 120.7, 117.2, 54.4, 40.6, 31.6, 30.9, 28.9, 28.8, 28.4, 26.4, 22.6, 14.1. HRMS (ESI) m/z for $C_{17}H_{25}BrN_3$ [M^+]: calculated: 350.123, found: 350.147. Anal. Calcd for $C_{17}H_{25}Br_3IN_3$ (638.017): C, 32.00; H, 3.95; N, 6.59. Found: C, 32.01; H, 3.98; N, 6.61.

6.4.2 X-ray structural determination and refinement

Initially, non-hydrogen atoms were refined isotropically and then by anisotropic refinement with full-matrix least squares method based on F^2 using the *SHELXL*-2014 program2[3] and molecular graphics were done using *ORTEP*-3[24]. All hydrogen atoms were positioned geometrically, allowed to ride on their parent atoms and refined isotopically. The C-H$_{aromatic}$ and C-H$_{methyl}$ bond distances were restrained to 0.95 Å and 0.98 Å with $U_{iso}(H_{aromatic}) = 1.2U_{eq}$ and $U_{iso}(H_{methyl}) = 1.5U_{eq}$ of parent atom, respectively.

Table 0.1: Crystal data and structure refinement for 6.2**.**

Identification code	**6.2**	
Empirical formula	$C_{17} H_{25} Br_3 I N_3$	
Formula weight	638.03	
Temperature	100(2) K	
Wavelength	0.71073 Å	
Crystal system	Triclinic	
Space group	P -1	
Unit cell dimensions	a = 8.7178(2) Å	α= 102.704(2)°.
	b = 11.1993(2) Å	β= 104.5240(10)°.
	c = 12.3784(3) Å	γ = 104.225(3)°.
Volume	1081.80(4) Å^3	
Z	2	
Density (calculated)	1.959 Mg/m^3	
Absorption coefficient	7.025 mm^{-1}	
F(000)	612	
Crystal size	0.230 x 0.150 x 0.130 mm^3	
Theta range for data collection	1.967 to 27.567°.	
Index ranges	-10<=h<=11, -14<=k<=14, -16<=l<=16	
Reflections collected	25166	
Independent reflections	4921 [R(int) = 0.0295]	
Completeness to theta = 25.242°	99.2 %	
Absorption correction	Semi-empirical from equivalents	

Max. and min. transmission	0.471 and 0.284
Refinement method	Full-matrix least-squares on F^2
Data / restraints / parameters	4921 / 0 / 218
Goodness-of-fit on F^2	1.038
Final R indices [I>2sigma(I)]	R1 = 0.0247, wR2 = 0.0587
R indices (all data)	R1 = 0.0305, wR2 = 0.0607

6.4.3   Computational methods

All DFT calculations were performed with the aid of Gaussian 09, revision B01. Gauss View 5.0.8 was utilized as a molecular builder and for visualization. The structure was fully optimized via mixed basis set at UB3LYP/GENECP level of theory with 6-31+G (d, p) for C, N, H, and landl2dz for Ni and I. We predict the ^{1}H and ^{13}C NMR shielding constants using the Gauge-Including Atomic Orbitals (GIAO) GIAO–DFT[22] in gaseous medium. The 6-31++G (d, p) basis set was used since this was common standard used in Gaussian to compute isotropic shielding constants of ^{1}H and ^{13}C for TMS (tetramethylsilane) which is used as a reference molecule in Gaussian.[22]

6.5 References

1. S. G. Mncube and M. D. Bala, *J. Mol. Liq.*, 2016, **215**, 396-401.

2. J. Muzart, *Adv. Synth. Catal.* , 2006, **348**, 275-295.

3. J. D. Holbrey, W. M. Reichert, M. Nieuwenhuyzen, S. Johnson, K. R. Seddon and R. D. Rogers, *Chem. Commun.*, 2003, 1636-1637.

4. H. Katayanagi, S. Hayashi, H. Hamaguchi and K. Nishikawa, *Chem. Phys. Lett.* , 2004, **392**, 460-464.

5. J. H. Holbrey and K. R. J. Seddon, *Chem. Soc., Dalton Trans.*, 1999, 2133-2140.

6. P. A. Z. Suarez, J. E. L. Dullius, S. Einloft, R. F. De Souza and J. Dupont, *Polyhedron*, 1996, **15**, 1279-1219.

7. M. G. Del Popolo and G. A. Voth, *J. Phys. Chem. B.*, 2004, **108**, 1744-1752.

8. C. J. Margulis, H. A. Stern and B. J. Berne, *J. Phys. Chem. B*, 2002, **106**, 12017-12021.

9. D. Hirsch-Weil, D. R. Snead, S. Inagaki, H. Seo, K. A. Abboud and S. K. Hong, *Chem. Commun.*, 2009, 2475-2477.

10. E. L. Kolychev, V. V. Shuntikov, V. N. Khrustalev, A. A. Bush and M. S. Nechaev, *Dalton Trans.*, 2011, **40**, 3074-3076.

11. R. Tepper, B. Schulze, M. Jäger, C. Friebe, D. H. Scharf, H. Görls and U. S. Schubert, *J. Org. Chem.*, 2015, **80**, 3139-3150.

12. J. M. Mercurio, R. C. Knighton, J. Cookson and P. D. Beer, *Chem. Eur. J.*, 2014, **20**, 11740-11749.

13. M. Giese, M. Albrecht, C. Bohnen, T. Repenko, A. Valkonen and K. Rissanen, *Dalton Trans.*, 2014, **43**, 1873-1880.

14. A. R. Buist and A. R. Kennedy, *Cryst. Growth Des.*, 2014, **14**, 6508-6513.

15. M. S. Chernov'yants, I. V. Burykin, V. V. Kostrub, E. B. Tsupak, Z. A. Starikova and J. A. Kirsanova, *J. Mol. Struct*, 2012, **1010**, 98-103.

16. S. d'Agostino, D. Braga, F. Grepioni and P. Taddei, *Cryst. Growth Des.*, 2014, **14**, 821-829.

17. M. Giese, M. Albrecht, G. Ivanova, A. Valkonen and K. Rissanen, *Supramol. Chem.*, 2012, **24**, 48-55.

18. F. Cristiani, F. Demartin, F. A. Devillanova, F. Isaia, V. Lippolis and G. Verani, *Inorg. Chem.*, 1994, **33**, 6315-6324.

19. A. Bondi, *J. Phys. Chem.*, 1964, **68**, 441-451.

20. G. Cavallo, P. Metrangolo, R. Milani, T. Pilati, A. Priimagi, G. Resnati and G. Terraneo, *Chem. Rev.* , 2016, **116**, 2478–2601.

21. P. Aniruddha, K. M. Prasun and S. Anunay, *J. Phys. Chem., B* 2005, **109**, 9148-9153.

22. M. Frisch, G. Trucks, H. Schlegel, G. Scuseria, M. Robb, J. Cheeseman, G. Scalmani, V. Barone, B. Mennucci and G. Petersson, *Wallingford, CT, USA: Gaussian*, 2009.

23. A. L. Spek, *J. Appl. Crystallogr.* , 2003, **36**, 7–13.

24. L. J. Farrugia, *J. Appl. Crystallogr.*, 1997, **30**, 565-566.

CHAPTER 7

SUMMARY AND CONCLUSIONS

7.1   Project summary

This short chapter presents a summary on the outcomes of this project and proffer concluding remarks to tie the outcomes to the original objectives of the project. In addition, the chapter also offers some recommendations to future researchers. Various aspects of the chemistry of functionalized 1,2,3-traizolylidene metal (*m*NHC-M) complexes have been investigated. A chapter by chapter summary follows:

Chapter 2: Presented **half-sandwich nickel complexes (*m*NHC-Ni)** synthesized by the reaction of nickelocene and triazolium salts. The complexes were fully characterized by HRMS and multi-nuclear NMR, and representative ones further elucidated by single crystal X-ray diffraction analysis showed trigonal planar geometry of ligands around Ni(II) centers. All complexes showed activity for the catalytic oxidation of *n*-octane, yielding a range of oxygenated products. Under optimized reaction conditions, the catalyst with lighter substituents on the triazolium ring exhibited the highest catalytic activity of 15% total substrate conversion to products. With H_2O_2 as the more productive oxidant, the preferential activation of internal carbons led to the observed mixture of octanones as the dominant product stream of the oxidation reaction.

Chapter 3: Outlined the synthesis of related **square planar *trans*-Cl$_2$Ni(*m*NHC)$_2$ complexes** and their application as catalysts for the catalytic oxidation of alkanes under mild conditions in conjunction with tert-butyl hydroperoxide (TBHP) as an oxidant. Under optimized reaction conditions, results showed moderate to good catalytic activities of circa 15% and 19% for cyclohexane and *n*-octane respectively. Furthermore, the catalytic system proved to be very efficient for the oxidation of straight chain alcohols to the corresponding ketones which was interpreted as evidence that the oxidation of alcohols to ketones is a key mechanistic step.

Chapter 4: Presented the synthesis and characterisation of *in situ* generated *m*NHC-Cu complexes. The catalytic properties of all the synthesized complexes was tested in the homogeneous oxidation of alkanes with low concentrations of the *in situ* generated *m*NHC-Cu catalysts. Catalytic screening showed that the complexes are capable of catalysing oxidation

reactions. In all substrates tested, ketones/aldehyde were the dominant products with conversions depending on substrate and reaction conditions. The achieved selectivity parameters were found to be close to those reported for other oxidation catalyst system that proceeded via the formation alkyl hydroperoxyl radicals. The oxidation of toluene resulted in the preferential activation of the methyl group exclusively forming benzaldehyde as the major product.

Chapter 5: Described the synthesis of **triazolylidene iron(II) piano stool complexes** bearing a variety of aryl and alkyl substituents. The complexes were characterized by multi-nuclear NMR and elementary analysis. All complexes were active in the catalytic oxidation in the presence of H_2O_2 as an oxidant of which the catalyst bearing an aryl wingtip N-substituent gave the highest catalytic performance with an overall conversion of 23% accompanied by high ketone selectivity (85%) for the oxidation of cyclohexane. Whilst for the oxidation of a linear hydrocarbon (*n*-octane), interestingly, the C4 position was the more accessible, thus preferentially oxygenated and no products of terminal CH_3 activation were detected.

Chapter 6: Outlined the serendipitous isolation of a new **bromo-*m*NHC dibromoiodate salt**. Full characterization of the salt using a number of techniques, including NMR spectroscopy, MS, EA and single crystal X-ray diffraction was reported. From the single crystal X-ray results, the dibromoiodate anion adopted a "linear" geometry with intermolecular Br…Br halogen bonding between bromine atoms of the triazolium and dibromoiodate moieties. Furthermore, the salt showed interesting fluorescence behavior; a $\pi \rightarrow \pi*$ transition from the triazolium moiety and the counter anion dominated the electron density map by DFT studies.

7.2   Conclusions

The results obtained in this project indicated that non-precious metal *m*NHC complexes have great potentials in catalytic oxidation reactions of inert hydrocarbons and alcohols. All the complexes were active in the catalytic oxidation reactions in the presence of oxidants under mild reaction conditions. It is worth recapping that the *m*NHC-Cu complexes have overall shown the highest catalytic activity.

7.3   Future work that may be considered

Although the catalytic systems tested in this project have shown good catalytic activities in oxidation reactions, future research in this domain should consider growing the scope of the study along the following pathways:

- Study oxidation reactions using other sources of oxygen such as air and molecular O_2 as alternative and cheaper oxidants, this may result in procedures that are comparable to industrial processes.
- Exploring other variants of the complexes by introducing functional groups to act as wingtip *N*-tethers may strengthen the metal–NHC bond and lead to improved catalytic performance.
- Heterogenized versions of the complexes anchored to solid supports (silica, alumina and clays) for recyclability may lead to important catalytic innovations in the future.
- Expending more emphasis on the chemistry of Cu and related coinage metals (Ag and Au), their complexes with NHC ligands and applications in oxidation catalysis.